University of Stavanger

Faculty of Science and Technology

MASTER'S THESIS

Study program/ Specialization: Offshore Technology/ Subsea Technology	Spring semester, 20.11..... Open / ~~Restricted access~~
Writer: Adedayo Olalekan Adebayo	………………………………………… (Writer's signature)
Faculty supervisor: Dr. Daniel Karunakaran External supervisor(s): Dr. Daniel Karunakaran	
Title of thesis: Steel Catenary Risers supported by Subsurface Buoy	
Credits (ECTS): 30	
Key words: Steel Catenary Riser, Rectangular buoy, H-shaped buoy	Pages: ……166…………… + enclosure: ………… Stavanger, …June 15, 2011………….. Date/year

Frontpage for master thesis
Faculty of Science and Technology
Decision made by the Dean October 30th 2009

ABSTRACT

Oil and gas exploration and production activities in deep and ultra deep waters in hostile environments necessitates the need to develop innovative riser systems capable of ensuring transfer of fluids from the seabed to a floating vessel and vice versa, with little or no issues with respect to influences of environmental loads and vessel motions.

Over the years, studies have shown that the conventional flexible riser and steel catenary riser configurations cannot function effectively under such environmental and vessel motion influences as a result of issues such as collapse (predominant in flexible risers when used in deep waters), and fatigue (predominant in steel catenary risers). Nevertheless, a riser system known as the hybrid riser which is a combination of a vertical rigid riser and a flexible riser has been used effectively under these seeming adverse conditions and has been found effective. However, it is regarded as an expensive option considering the cost of its components, in addition to its limitation in terms of step-out distance between the floating vessel and a subsea well.

The limitations of the aforementioned riser systems are conveniently accommodated by a riser system presently undergoing development. It is known as "steel catenary risers supported by subsurface buoy". This riser solution combines the best properties of flexible risers (ability to uncouple a system from vessel motions) and steel catenary risers (usability in deep waters). In addition to this, it offers flexibility in terms of achievable step-out distance between a floater and a subsea well. This riser system is the thrust of this thesis.

This write-up begins with a review of the previously mentioned riser solutions, pros and cons related to their usage in harsh deep water environments, and some essential design code requirements to be fulfilled in a riser design activity. This is followed by design analysis of the thesis example riser system.

In-depth analysis is done with two different buoy types (rectangular buoy and H-shaped buoy) by conducting sensitivity studies to understand the contribution of factors such as the buoy size and submerged weight, flowline content density, riser anchor length, and so on, to the performance of the riser system in a typical North Sea environment. Observation was made that whilst both buoy shapes result in good flexible risers and steel catenary risers strength performance, the H-shaped buoy had line clashing issues when subjected to cross flow environmental loads. This was however eradicated through the use of another buoy shape referred to as the modified H-buoy.

The rectangular and H-shaped buoys were further studied for possibility of resonance with peak waves obtainable in the North Sea environment and were found to have satisfactory sway and heave periods.

In addition, a brief fatigue assessment was carried out with the rectangular buoy to show that the riser system helps in alleviating fatigue issues prominent in conventional steel catenary risers.

The study concludes by showing that while both the conventional buoy and the H-shaped buoy offer appreciable strength performance and stability to the riser system, the latter has better stability in comparison with the former while the former offers better strength performance to the steel catenary risers.

Keywords: Steel Catenary Riser, Rectangular buoy, H-shaped buoy

Acknowledgement

I would like to express my sincere appreciation to my supervisor, Dr. Daniel Karunakaran (Ph.D), whose guidance, encouragement and wealth of knowledge made every bit of time I spent on this work extremely meaningful.

My gratitude also goes to Subsea 7, Stavanger, Norway for granting me office space and all other necessities to facilitate the successful execution of this task. My profound gratitude goes to Markus Cederfeldt, Tommy Andresen, and Jørgen Reine for being there to provide answers to all questions I had during the course of this work.

I am exceedingly grateful for the contributions of my class mate and colleague, Iswan Herlianto, in making this work a success.

My heartfelt gratitude goes to all my African (Chukwunaru Ekwunu, Ekene Agbalakwe, Henry Ezeanaka, Rumi Achije, Justine Atarah, Oyewole Bamidele, and others too numerous to mention) and International friends who have made my M.Sc. study a most exciting experience.

I would like also like to say a very special thank you to my wonderful neighbours, Elsa M.N. and Taiwo Mesagan, for their wonderful contributions and unflinching support in the execution of this work.

Finally, with a heart issuing immeasurable gratitude, I express my endless thanks to the pillars of support I have had from the cradle- my parents and my brothers, for always being there in spite of the distance between us.

Adedayo Olalekan Adebayo

Stavanger, June 15, 2011.

Contents

List of Figures

List of Tables

Nomenclature

Greek Characters

α_{fab}	Manufacturing process reduction factor
σ_a	Basic allowable combined stress
σ_s	Load effect
σ_y	Material minimum yield strength
ρ_i	Density of the internal fluid
ϑ	Poisson ratio
γ_F	Functional Load effect factor
γ_E	Environmental Load effect factor
γ_A	Accidental Load effect factor

Symbol

C_a	Added mass coefficient
C_d	Drag coefficient
C_m	Inertia coefficient
f_n	Force per unit length in normal direction
f_0	Initial ovality of pipe
f_u	Tensile strength of pipe
f_y	Yield strength of pipe
H_s	Significant Wave Height
M_d	Design bending moment
M_k	Plastic bending moment resistance
T_p	Wave peak period

Abbreviations

ALS	Accidental Limit State
API	American Petroleum Institute
BHRT	Bundled Hybrid Riser Tower
DNV	Det Norske Veritas
FLS	Fatigue Limit state
FSHR	Free Standing Hybrid Riser
FPSO	Floating Production, Storage, and Offloading Unit
FPU	Floating Production Unit
GoM	Gulf of Mexico
JONSWAP	JOint North Sea WAve Project
LRFD	Load Resistance Factor Design
MBR	Minimum Bend Radius
OSCR	Offset Steel Catenary Riser
RAO	Response Amplitude Operator
ULS	Ultimate Limit State
WSD	Working Stress Design

Chapter 1: INTRODUCTION

1.0   Background

As the oil and gas industry moves farther into deep and ultra deep waters, recovery of hydrocarbon resources from reservoirs located at such water depths requires the identification of suitable gathering and transportation systems able to provide the fluid communication system necessary to dispatch production stream to surface treatment facilities. In recent times, there has been a number of exploits in the application of subsea tie-backs in conveying oil and gas from remote offshore locations to onshore facilities (e.g. Snøhvit and Ormen Lange fields in the North Sea). Nevertheless, these are still limited by issues such as the need for extensive sea bed preparation in routing pipelines from such remote locations to the shore (e.g. the Storrega slide at Ormen Lange field). However, this issue has minimal impact on the usage of floating platforms or vessels at such locations since fluid transport from the reservoir to the water surface facility is achieved in a vertical (or almost vertical) manner, thereby eradicating the need for extensive sea bed preparation. This exemplifies the importance of floating platforms and vessels in the recovery of oil and gas resources from deepwater locations.

Regardless of the floating platform concept adopted for any offshore field development activity, there is always a need for what is known as a riser system. This enables fluid transportation between the reservoir and the floating platform. Risers are part of the very complex aspects of deepwater developments. Over the years, it has become evident that riser systems play a very big role as part of offshore infrastructures. The riser system cost is particularly sensitive to any increase in water depth, and this also true for riser installation costs (Lim F., 2006). Also, hydrostatic collapse resistance becomes a great challenge for flexible riser systems as water depth increases.

While deepwater in itself presents challenges to riser manufacturers and design teams, these challenges are further compounded when environmental conditions are harsh. Harsh environments influence motions of the floating platform, which in turn influence the dynamic behavior of the riser system. For instance, the application of steel catenary risers (SCRs) with semi-submersibles or floating production, storage and offloading vessels (FPSOs) in harsh deepwater environments presents design challenges due to large wave-induced motions on the platform, and large vessel offsets caused by wind, currents, and slow-drift wave motions. The resulting large heave motions of the vessel cause buckling and fatigue related issues at the touchdown point (TDP) of the riser (Xia J., 2008).

These challenges posed by harsh deepwater environments are however being met by continuous advances in riser technology. One of such is the development of a riser system

known as **steel catenary risers supported by subsurface buoy**. This concept was developed with a view to combine the best qualities of flexible risers (i.e. ability to withstand vessel motions) and steel catenary risers (i.e. suitability for extreme water depths), thereby mitigating buckling and fatigue issues associated with steel catenary risers.

1.1 Purpose and Scope

Considering the challenges posed by influence of harsh deepwater environments and vessel motions on performance of riser systems, this thesis looks into performance enhancements offered by different buoy shapes to steel catenary risers supported by subsurface buoys in an area with extreme environmental conditions such as the North sea, in addition to comparing the influence of usage of the different buoy shapes on the performance of the riser system. The software utilized in this study is known as OrcaFlex. According to T.Andresen (2007), it is a marine dynamics program developed by Orcina for static and dynamic analysis of flexible pipelines and cable systems in an offshore/marine environment. OrcaFlex is widely used in the offshore industry for analysis of flexible risers from offshore production platforms and tanker loading buoys, cable lay, installation of subsea equipment, oceanographic moorings, pull-in analysis, and so on. OrcaFlex provides fast and accurate analysis of catenary systems such as flexible risers and umbilical cables under wave and current loads, and externally imposed loads.

The following are to be undertaken in this thesis work:

- Chapter 2 provides a review of some uncoupled riser systems used in deepwater applications, and some codes governing riser design.
- Chapter 3 gives an understanding of what the riser system (steel catenary risers supported by subsurface buoy) looks like, what makes it suitable for use in harsh deep water environments, and the advantages it offers.
- Chapter 4 supplies relevant design data, load case parameters, and design acceptance criteria on which subsequent analyses in this study are based.
- Chapter 5 looks into study of two subsurface buoy shapes (rectangular buoy and H-shaped buoy), and their influence on the strength performance and stability of the riser system under consideration. Sensitivity analysis is carried out to study influence of parameters such as buoy size, riser anchor length, buoy drag coefficient and added mass, buoy submerged weight, and flowline internal content on the performance of the riser system. In addition, modification of the H-shaped buoy is carried out in order to eradicate line clashing when the riser system is exposed to cross flow environmental loads.
- Chapter 6 demonstrates the usability of the rectangular buoy and H-shaped buoy in the North Sea environment with respect to issues with resonance with peak waves. This is achieved by computing the sway and heave periods of the buoys.

- Chapter 7 provides a brief fatigue analysis of the riser system.
- Chapter 8 provides conclusions drawn from the study and provides comparisons between the buoys (i.e. rectangular buoy versus H-shaped buoy, and H-shaped buoy versus modified H-buoy) in addition to recommendations for further study.

Chapter 2: REVIEW OF RISER SYSTEMS AND DESIGN CODES

2.0   Introduction

According to Mungall et al (1997), fluid transport from the reservoir to the water surface facility is achieved by a system commonly called a production riser or riser system which usually includes multiple conduits through which various produced fluids (oil, gas, water, etc) are transported between the marine bottom and the surface of the water body. These may also include conduits to be used for off-loading lines, fluid injection lines and service, electrical and hydraulic control lines.

Since the water surface facility is constantly exposed to surface and near surface conditions, it continuously undergoes a variety of movements and experiences a number of forces. For instance, in the "turbulence zone" (i.e. zone existing up to approximately 100 to 150 meters below the surface of an open body of water), a floating vessel may experience substantial heave, roll, pitch, drift, etc., caused by surface and near surface conditions (e.g. wave, wind, current, etc.). These motions are eventually transferred to the riser system connected to the water surface facility, thereby influencing the dynamic response and performance of the riser system. Some degree of sufficient compliance is therefore necessary in the configuration of such riser systems to isolate them from effects of vessel motions. The vessel motions, combined with the movement of the offshore industry into deep waters and harsh environments, places high premium on the effectiveness of riser systems used in such areas.

A review of some compliant riser systems is presented in subsequent sections of this write up.

2.1   Review of Riser Systems

Several types of riser systems have been designed to compensate for or reduce effects of vessel-riser motion interactions. There are essentially two kinds of risers, namely rigid risers and flexible risers, and the functions performed by these include (Bai and Bai, 2005):

- Production/injection
- Export/import or fluid circulation
- Drilling
- Completion and workover

Different riser systems originate from combination of the two, or modification of the configuration of each riser type. According to Shu et al (2011), deepwater riser systems can be categorized as follows:

- Free Hanging Risers

- Steel Catenary Risers (SCRs)
  - Simple Steel Catenary Risers
  - Wave Shape Risers
- Unbonded Flexible Risers
  - Metallic Unbonded Flexible Risers
  - Non-metallic Unbonded Flexible Risers
  - Metallic and Non-metallic Hybrid Unbonded Flexible Risers
- Offset Free Hanging Risers
  - Offset Steel Catenary Risers (OSCRs)
- Top Tensioned Risers (TTRs)
  - Top Tensioned Risers on Floating Production Platforms
    - Buoyancy Air Tank Tensioner
    - Hydro-pneumatic Tensioner, Pull Style
    - Hydro-pneumatic Tensioner, Ram Style
  - Free standing Hybrid Risers (FSHR)
    - Bundle Tower with Multiple Risers
    - Single Line Offset Riser (SLOR)
  - Bonded Non-metallic (Composite) Risers
    - On Floating Platforms or Free Standing

However, focus will be placed on riser systems with ability to uncouple vessel motions in this write-up.
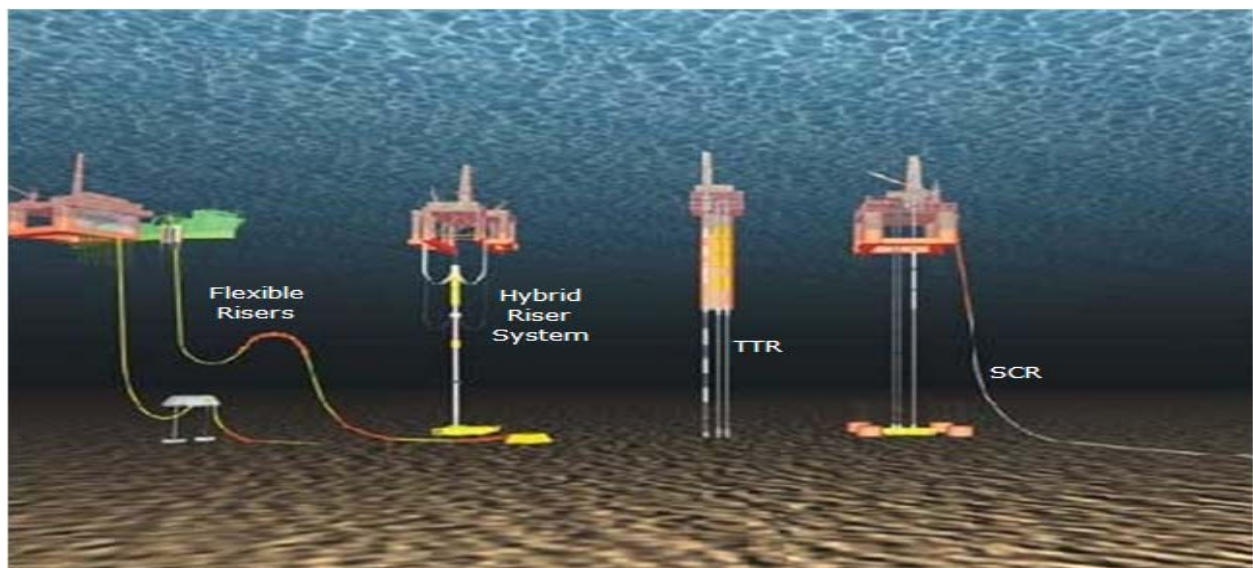
Figure 2 - 1: Examples of Riser Systems (Terje and D'Souza, 2001)

2.2 Uncoupled Riser Systems

Over the years, a number of riser systems with ability to decouple vessel motions have been developed and utilized by the offshore industry. They are mainly applied as production, export/import and injection risers. They range from derivatives of flexible risers to riser systems that combine attributes of flexible and rigid risers. These riser systems include the lazy wave and steep wave, lazy S and steep S, and pliant wave configurations of flexible risers (and also of steel catenary risers depending on the length of the riser); free standing hybrid risers which can be of bundled arrangement, single line offset riser arrangement (SLOR), or grouped single line offset riser arrangement (grouped SLOR); and the recently conceived steel catenary risers supported by subsurface buoy. Critical locations on these riser systems are typically the wave zone, hog and sag bends, touchdown area at seafloor and terminations to rigid structures e.g. I- or J- tubes.

Sub-sections of this section present discussion on these uncoupled riser systems.

2.2.1 Flexible Riser Systems

According to Hoffman et al (1991), a flexible pipe is defined as a composite of layered materials which form a pressure containing conduit. The pipe structure allows large deflection (especially in storm conditions) without a significant increase in bending stresses. The pipe is therefore designed so that it has a low bending stiffness, high axial stiffness and can accommodate high internal and external pressures. These risers accommodate floating platform motion and hydrodynamic loading by being flexible. However, they approach hydrostatic collapse and axial tension design limits as floating production systems move into deeper water applications, which limits them to relatively small internal diameters (Mungall et al, 1997). The pipe construction is either of a bonded type (whereby layers are bonded together using adhesive and are then vulcanized in an oven to form a homogeneous structure) or non-bonded (whereby individual layers remain separated allowing internal relative movements). Typical materials used for construction include polymers, textile, steel and fabrics.

Different flexible riser configurations were discussed by Bai and Bai (2005). Flexible risers can be installed in a number of different configurations. Riser configuration design shall be performed according to the production requirement and site-specific environmental conditions. Configuration design drivers include factors such as water depth, host vessel access/hang-off location, field layout such as number and type of risers and mooring layout, and in particular environmental data and the host vessel motion characteristics.
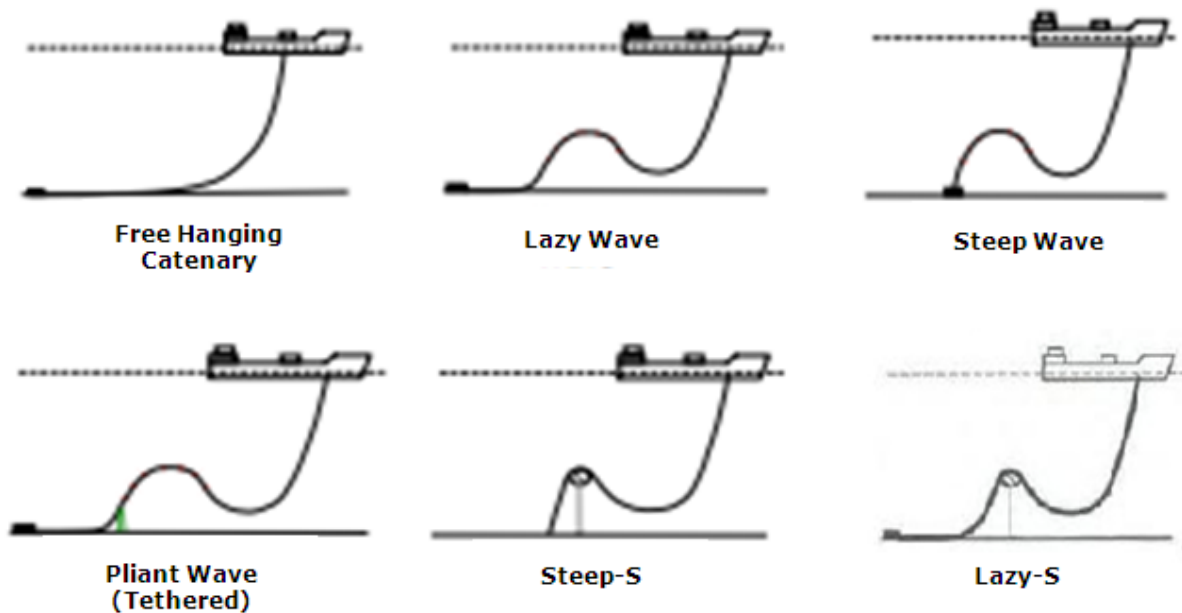
Figure 2 - 2: Flexible Riser Configurations (Bai and Bai, 2005)

2.2.1.1 Free Hanging Catenary

This is the simplest configuration for a flexible riser. It is also the cheapest to install due to its minimal subsea infrastructure requirement, and ease of installation. However, when exposed to severe loading due to high vessel motions, compression buckling at the riser touchdown point (TDP) might result as it is lifted off or lowered down on the seabed. In deeper water, the top tension is large due to the long riser length supported.

2.2.1.2 Lazy wave and steep wave

For these configurations, buoyancy and weight are added along some length of the riser to decouple the vessel motions from the touchdown point of the riser. Lazy waves are preferred to steep waves because they require minimal subsea infrastructure. However, while lazy waves are prone to configuration alterations if pipe content density changes during the riser's lifetime, steep wave risers are able to maintain their configuration even if the riser content density changes.

2.2.1.3 Lazy S and Steep S

In these configurations, there is a subsea buoy which is either a fixed buoy (fixed to a structure at the seabed) or a buoyant buoy. The addition of the buoy removes the problem associated with the touchdown point (described in section **2.2.1.1**). The subsea buoy absorbs the tension variation induced by the floater, and the touchdown point eventually experiences only little or

no tension variations. In case of large vessel motions, a lazy-S might still result in compression problems at the riser touchdown, leaving the steep-S as a possible alternative.

Due to the complex installation procedure of 'S' configurations, they are considered only if catenary and wave configurations are not suitable for a particular field. A lazy-S configuration requires a mid-water arch, tether and tether base, while a steep-S requires a buoy and subsea bend stiffener.

2.2.1.4 Pliant Wave

This configuration is almost like the steep wave configuration where a subsea anchor controls the touchdown point i.e. the tension in the riser is transferred to the anchor and not to the touchdown point. This configuration is able to accommodate a wide range of bore content densities and vessel motions without causing any significant change in configuration and inducing high stress in the pipe structure. However, due to complex subsea installation that is required, it would be required only if a simple catenary, lazy wave or steep wave is not viable.

2.2.2 Steel Catenary Risers (SCRs)

In ultra-deep water (beyond 2000m), riser systems become increasingly technically challenging and comprise a major part of the overall field development costs. Large external pressures and high production temperatures in these great depths cause traditional flexible solutions to run into weight, temperature and cost problems. However, steel pipes do not have these temperature limits (SBM Atlantia, 2011).

A steel catenary riser is a substantially rigid pipe, with or without insulation and casing, suspended from surface facilities to the seabed in a catenary contour. It is connected to the floating facility by a flexible joint or a tapered stress joint of steel or titanium to absorb the dynamic moment generated by the floater (Terje and D'Souza, 2001; Bell et al, 2005). Steel catenary risers are "flexible" in a long length, and so can be deployed in any of the flexible riser configurations shown in **Figure 2 - 2** (Lim F., 2006).

From the time the first steel catenary risers were installed on Shell's Auger Tension Leg Platform (TLP) in the Gulf of Mexico in a water depth of 872 m (2860 ft) in 1994 (Phifer et al., 1994; Bai and Bai, 2005), the number of steel catenary risers around the world has continued to increase owing to the continuing push of the offshore oil and gas industry into deep and ultra deep water. Among the different riser systems itemized in **section 2.1**, the steel catenary riser has been enjoying widespread acceptability for deep and ultra-deepwater oil and gas production in recent years due to its cost effectiveness, conceptual simplicity, significant structural simplicity, ease of fabrication and offshore installation. By the end of 2006, more than 100 deepwater and ultra-deepwater steel catenary risers have been installed worldwide,

mainly in the Gulf of Mexico (GoM), West of Africa (WoA), and offshore Brazil (Song and Staton, 2007).

In spite of the advantages of the steel catenary riser system over the other riser systems, critical issues with respect to its design are sensitivity to floater motion, and fatigue damage. The dynamic motion of the floater introduced at the upper end of the catenary riser generates dynamic loads which are transferred directly to the seabed with little dissipation, leading to compression, large bending moments and potential buckling at the touchdown region which result in difficulty in meeting strength and fatigue design criteria at the region and at the riser hang-off location (O'Brien and O'Sullivan, 1996; Xia J., 2008). Further, the steel pipelines when connected directly to the floater impose loads thereon which can be substantially greater than the loads imposed by the other riser systems. In addition, if the catenary portion of the pipeline undergoes fatigue or becomes damaged to the point of failure or possible failure, a large section of the submerged pipeline has to be replaced which is both expensive and difficult to accomplish (Mungall et al., 1997).

2.2.3 Free Standing Hybrid Risers

As field developments target deeper and deeper water, hybrid riser towers (HRTs) have become one of the solutions investigated systematically at bid stage. This is due to the capability of hybrid riser towers to accommodate the requirements for large diameter risers, reduced load on FPSO, demanding flow assurance requirements, and robust layout for later development phases (Legras and Saint-Marcoux, 2011).

A hybrid riser comprises a lower vertical steel section (hybrid tower) under tension, and an upper catenary section of flexible pipe (jumper). A buoyancy tank is located below the main wave zone at the upper end of the tower section, and the jumper is connected from the top of the tower or buoyancy tank to the floater. The tower section not only serves as a conduit for the reservoir fluid, but also as tendons to the buoyancy tank.

The hybrid riser combines the best qualities of vertical steel and flexible risers into one system. Using vertical steel through most of the water depth keeps cost per unit length to a minimum, while using flexible riser on the upper section enables the system to be compliant and cater for large vessel motions. This helps to reduce dynamic motions over a large part of the riser, meaning the tower section as well as the buoyancy tank will see little dynamics, with most of the motions taken in the jumper (O'Brien and O'Sullivan, 1996; Bell et al., 2005).

Free standing hybrid risers can be deployed both in bundle and single line arrangements. The hybrid bundle (otherwise known as bundled hybrid riser tower - BHRT) consists of a bundle of several rigid pipes which serve as production, export, water injection and service lines,

anchored to the seabed and tensioned by means of a buoyancy tank. It is connected to the floating production unit (FPU) by means of flexible jumpers and to flowlines and pipelines by means of spools (rigid jumpers). This arrangement has been used in fields including Green Canyon 29 and Garden Banks 388 in the Gulf of Mexico, and Girassol, Rosa and Great Plutonio in West Africa. Some of the major components of a bundled hybrid riser tower are as follows (Legras and Saint-Marcoux, 2011; Saint-Marcoux and Legras, 2011):

- Foundation: This is preferably a suction pile similar to those of the mooring system of floating production units. The bottom connection between the lower riser assembly and the foundation may be rigid or flexible.
- Lower Riser Termination Assembly (LRTA): This is the location of the interface between the production risers, gas lift risers, and production spool.
- Bundle: The design of the bundle is based on arranging the buoyancy foam (half-shells attached to the core pipe of the bundle) and the rigid pipes, so that flow assurance requirements are met, the buoy is neutrally buoyant, and there is no adverse hydrodynamic effect such as galloping. The bundle arrangement is done such that there is sufficient gap between the buoyancy foam blocks and risers to allow water circulation which helps to protect the foam from deterioration due high temperature.
- Upper Riser Termination Assembly (URTA): This is the location of the interface between the jumpers and the bundle. Its major advantage is that it helps simplify the construction of the buoyancy tank.
- Buoyancy Tank: It is a steel cylinder comprising a number of compartments to minimize consequences of accidental flooding. It is connected to the URTA by means of a tether, a worthwhile configuration that helps eliminate use of a highly stressed taper joint.
- Flexible jumpers: These are attached to the URTA (or the top of the buoyancy tank) by flanges or connectors, and enhance fluid communication between the floating production unit and the risers in the bundle.
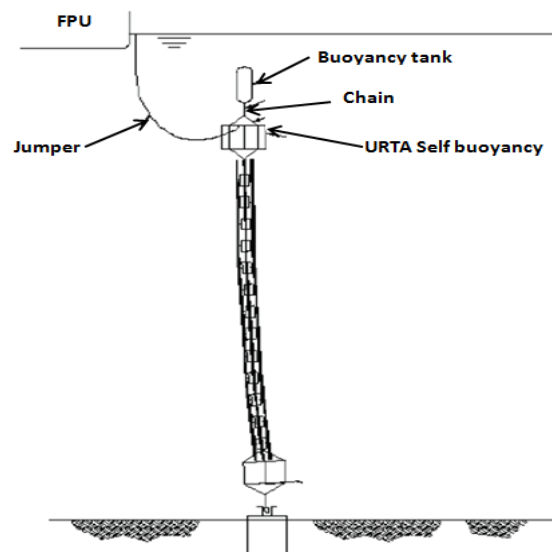
Figure 2 - 3: Bundled Hybrid Riser Tower (BHRT) Architecture (Legras et al, 2011)
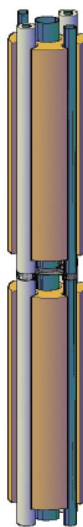
Figure 2 - 4: Bundle Configuration (Legras et al, 2011)

On the other hand, the single line arrangement is also known as the single line offset riser (SLOR). This employs a single vertical steel riser section that is linked to the host vessel via a flexible pipe jumper, and has been used in a number of fields including Exxon's Kizomba A and B and BP's block 31 NE in West Africa, Petrobras' P-52 in Brazil, and Cascade/Chinook in the Gulf of Mexico (Lim F., 2006; Shu et al., 2011).
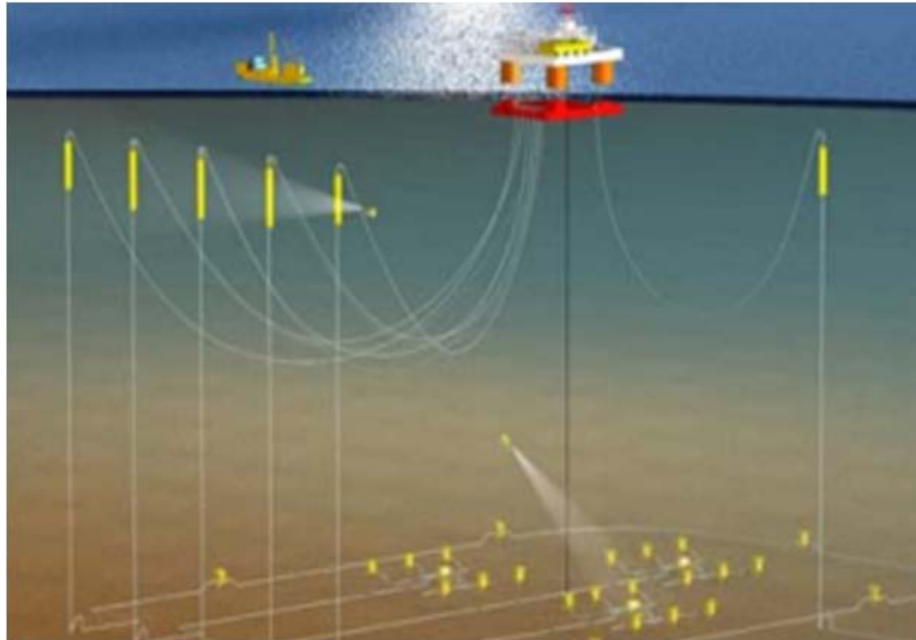
Figure 2 - 5: Single Line Offset Riser – SLOR (Lim F., 2006)

Both concepts are used in deepwater applications due to their excellent fatigue performance, decoupling of floater motions via jumpers, and the ability to pre-install them (before arrival of the floating platform), thus taking the installation activity off the critical path. However, both concepts have field layout problems. The bundled hybrid riser, whilst being able to efficiently incorporate 10-12 lines in a single structure, poses practical problems at the bottom and top ends where connections need to be made to flowline and jumpers respectively. Due to large number of lines terminating in a small envelope, there arises the problem of how to acceptably route flowlines and their associated jumpers, whilst accommodating pipe expansions, movements and installation tolerances. Similarly at the top end, the off take of dynamic flexible jumpers to the vessel can be challenging to achieve an acceptable arrangement that facilitates installation and prevents clashing during operation. The field layout challenge presented by the single line offset riser is primarily as a result of its large deflections due to current loading. This requires each single line offset riser to have a large spatial clearance with the adjacent single line offset riser, mooring line or umbilical. Hence, while the single line offset riser facilitates easy access at its top and bottom ends, its maximum number within a given field layout is often limited and insufficient to meet initial and future project requirements. The performance of both concepts with respect to field layout challenges however has been improved through the development of the Grouped Single Line Offset Riser (Grouped SLOR),a riser solution that uses a buoyant frame to constrain all risers to move collectively, thereby effectively eliminating the risk of clashing (Dale and Karunakaran, 2007).
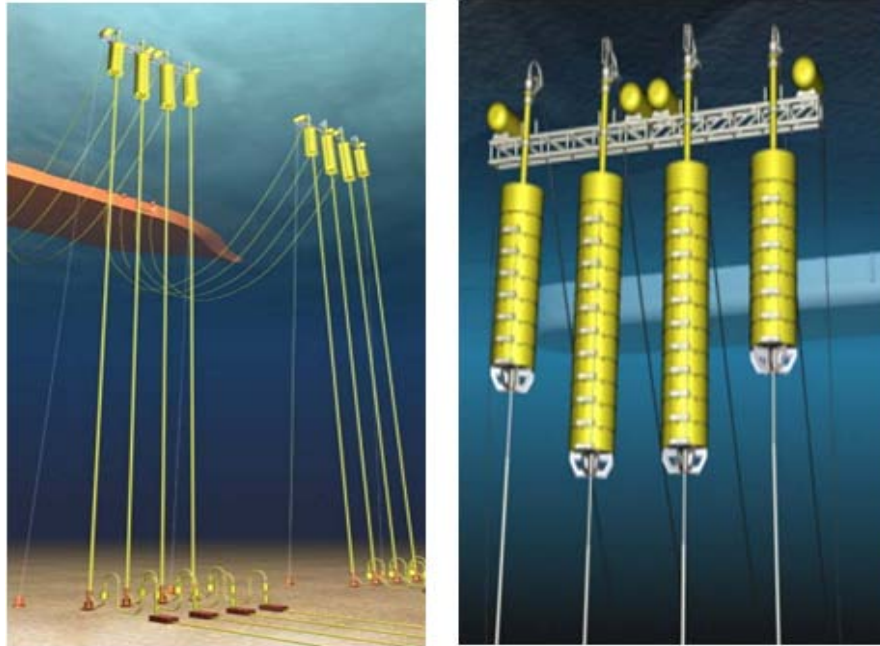
Figure 2 - 6: Grouped SLOR (Karunakaran et al, 2009)

2.2.4 Steel Catenary Risers supported by Subsurface Buoy

This is the main thrust of this thesis work. In comparison with the previously discussed riser systems, this is a relatively new riser concept. It combines the best properties of flexible risers and steel catenary risers to achieve a riser system with excellent strength behaviour and fatigue performance. Details about this system can be found in **chapter 3**.

2.3 Riser Code-based Design

Riser design codes serve as reference documents to be adhered to for guidance on structural design and analysis of riser systems. Authorities and classification societies have developed riser design codes such as ISO, API, NPD, HSE, NS, BS, CSA, DNV and ABS (Bai and Bai, 2005). While some of these codes are tailor-made for risers, others are extensions of pipeline codes to address riser design. The codes include API RP 16Q for drilling risers, API RP 2RD for risers attached to floating systems, API RP 17B and 17J for flexible pipes, DNV RP-F201 and F-202 for titanium and composite risers respectively, ISO 13628-7 for completion/workover riser systems, DNV-OS-F201 for dynamic risers, DNV-OS-F101 for submarine pipeline systems, and so on. With respect to this write-up, only DNV-OS-F201 and API RP 2RD will be used as reference codes.

2.3.1 Limit State Design

According to DNV-OS-F201 (2010), the objective of riser design is to keep failure probability (i.e. probability of exceeding a limit state) below a certain value. The code requires the identification

of all relevant failure modes for the riser, and verification that no corresponding limit state is exceeded. The following limit states are of prime importance to riser design:

- **Ultimate Limit State (ULS)**: It relates to issues related with the strength of the riser. This limit state requires that the riser must remain intact and avoid rupture, but not necessarily be able to operate. As such, the riser must be designed to have a very low probability of reaching this limit state due to its severe consequences.
- **Accidental limit state (ALS)**: This is an ultimate limit state (ULS) due to accidental loads (i.e. infrequent loads).
- **Fatigue Limit State (FLS)**: This is an ultimate limit state which results from accumulated excessive fatigue crack growth or damage under cyclic loading. This limit state is an essential consideration in design of steel catenary risers (SCRs) due to their susceptibility to fatigue which results from vessel motions and soil-riser interactions.

Hence, an important consideration in any riser design is the identification of extreme loads that could lead to exceedance of any of the limit states.

2.3.2 Riser Design Methods

Approaches employed in riser design are as follows (DNV-OS-F201, 2010):

- Load and Resistance Factor Design (LRFD) method
- Working Stress Design (WSD) method
- Reliability analysis
- Design by testing

To ensure consistency in any design activity, it is pertinent to utilize just one of the design methods when undertaking any riser design or analysis. However, riser failure modes such as local buckling possess failure resistance which is independent of the riser material, and as such does not fall strictly under the WSD criterion but more under the LRFD criterion (Xia J., 2008). Thus, both the WSD and LRFD methods will be employed in this write-up.

2.3.2.1 Working Stress Design (WSD) Method

The working stress design method is a design format where the structural safety margin is expressed by one central safety factor or usage factor for each limit state. In other words, the possible uncertainties in load effects and resistance are accounted for by a single usage factor. This distinguishes it from the load resistance factor design (LRFD) format wherein uncertainties in the different load effects and resistance are represented by individual safety factors. Thus, the working stress design method is a more easy-to-use conservative approach. The general working stress design format can be expressed as follows (API RP 2RD, 2006):

$$\sigma_s < C_f \sigma_a$$

where:

$\sigma_a = C_a \sigma_y$ = Basic allowable combined stress (or resistance)

$C_a = {^2}/{_3}$ = Allowable stress factor

σ_y = Material minimum yield strength

C_f = Design case factor as given in **Table 2 - 1**

σ_s = Load effect

Note that the product of C_f and C_a gives the usage factor.

Limit State Category	C_f	Allowable stress = $C_f \sigma_a$
ULS	1.2	$0.8\sigma_y$
ALS	1.5	$1.0\sigma_y$

Table 2 - 1: Design Case Factors and Allowable Stress (API RP 2RD, 2006; DNV-OS-F201, 2010)

2.3.2.2 Load Resistance Factored Design (LRFD) Method

DNV-OS-F201 (2010) says the fundamental principle of the load resistance factored design method is to verify that factorised design load effects do not exceed factored design resistance for any of the considered limit states. Some of the failure modes associated with limit states include bursting, collapse, propagating buckling for ultimate limit state; fatigue failure for fatigue limit state; failure caused by accidental loads directly, or by normal loads after accidental events (damage conditions) for accidental limit state, and so on.

The DNV-OS-F201 (2010) code requirements for some of the failure modes are discussed in the next sections.

2.3.2.2.1 Ultimate Limit State

2.3.2.2.1.1 Bursting

This occurs due to membrane rupture of the pipe wall as a result of internal overpressure only. The most critical area for this to occur along a content-filled riser is the top end because the internal fluid pressure is usually higher than the external hydrostatic pressure at the location.

Pipe members subjected to internal overpressure are required to satisfy the following condition at all cross sections:

$$(p_{li} - p_e) \leq \frac{p_b(t_1)}{\gamma_m \gamma_{sc}}$$

where:

p_{li} = Local incidental pressure = $p_{inc} + \rho_i g h$

p_{inc} = Incidental pressure (surface pressure that is unlikely to be exceeded during the lifetime

of the riser

p_e = External pressure

h = height difference between the actual location and the internal pressure reference point

p_b = Burst resistance = $\frac{2}{\sqrt{3}} \cdot \frac{2 \cdot t}{D-t} \cdot min\left(f_y; \frac{f_u}{1.15}\right)$

ρ_i = Density of the internal fluid

γ_m = Material resistance factor

γ_{sc} = Safety class resistance factor

t_1 = Minimum required wall thickness for a straight pipe without allowances and tolerance

$$= \frac{D}{\frac{4}{\sqrt{3}} \cdot \frac{min\left(f_y; \frac{f_u}{1.15}\right)}{\gamma_m \gamma_{sc}(p_{li} - p_e)} + 1}$$

D = Nominal pipe outer diameter

f_y = Yield strength of pipe

f_u = Tensile strength of pipe

2.3.2.2.1.2 System Hoop Buckling (Collapse)

This refers to gross plastic deformation (crushing) and/or buckling (collapse) of the pipe cross section caused by external overpressure only. This is most likely to occur at the lower end of a riser because the external hydrostatic pressure is highest at this location.

Pipe members subjected to external overpressure are required to satisfy the following condition:

$$(p_e - p_{min}) \leq \frac{p_c(t_1)}{\gamma_m \gamma_{sc}}$$

where:

p_{min} = Local minimum internal pressure (the most unfavourable internal pressure plus static

      head of the internal fluid

$p_c(t)$ = Resistance for external pressure, given by:

$$p_c(t) - p_{el}(t) \cdot \left(p_c^2(t) - p_p^2(t)\right) = p_c(t) \cdot p_{el}(t) \cdot p_p(t) \cdot f_0 \cdot \frac{D}{t}$$

$p_{el}(t)$ = Pipe elastic collapse pressure

$$= \frac{2 \cdot E \cdot \left(\frac{t}{D}\right)^3}{1 - \vartheta^2}$$

$p_p(t)$ = Pipe plastic collapse pressure

$$= 2\frac{t}{D} \cdot f_y \cdot \alpha_{fab}$$

E = Young's modulus of pipe material

f_0 = Initial ovality of pipe

α_{fab} = Manufacturing process reduction factor

2.3.2.2.1.3 Combination Loading

In addition to design for burst and collapse resistance, pipe members subjected to combined effects of bending moment, effective tension, and net internal overpressure are required to satisfy the following equation:

$$\{\gamma_{sc} \cdot \gamma_m\} \left\{ \left(\frac{|M_d|}{M_k} \cdot \sqrt{1 - \left(\frac{p_{ld} - p_e}{p_b(t_2)}\right)^2}\right) + \left(\frac{T_{ed}}{T_k}\right)^2 \right\} + \left(\frac{p_{ld} - p_e}{p_b(t_2)}\right)^2 \leq 1$$

where:

M_d = Design bending moment = $\gamma_F \cdot M_F + \gamma_E \cdot M_E + \gamma_A \cdot M_A$

M_k = Plastic bending moment resistance

T_{ed} = Design effective tension = $\gamma_F \cdot T_{eF} + \gamma_E \cdot T_{eE} + \gamma_A \cdot T_{eA}$

T_k = Plastic axial force resistance

p_{ld} = Local internal design pressure = $p_d + \rho_i g h$

$\gamma_F, \gamma_E, \gamma_A$= Respective load effect factors for functional, environmental, and accidental loads

M_F, M_E, M_A= Respective bending moments for functional, environmental, and accidental loads

T_{eF}, T_{eE}, T_{eA}= Respective effective tensions for functional, environmental, and accidental loads

p_d = Design pressure (maximum surface pressure during normal operations)

For pipe members subjected to combined effects of bending moment, effective tension, and net external overpressure, the following equation must be satisfied:

$$\{\gamma_{sc} \cdot \gamma_m\}^2 \left\{ \left(\frac{|M_d|}{M_k} \right) + \left(\frac{T_{ed}}{T_k} \right)^2 \right\}^2 + \{\gamma_{sc} \cdot \gamma_m\}^2 \left(\frac{p_e - p_{min}}{p_c(t_2)} \right)^2 \leq 1$$

2.3.2.2.2   Accidental Limit State

According to DNV-OS-F201 (2010), a simplified design check with respect to accidental load may be performed based on **Table 2 - 2** below multiplied on appropriately selected load effect factors ($\gamma_F, \gamma_E, \gamma_A$) and resistance factors (γ_{sc}, γ_m). γ_c is known as condition factor.

Prob. of occurrence	Safety Class Low	Safety Class Normal	Safety Class High
>10^-2	Accidental loads may be regarded similar to environmental loads and may be evaluated similar to ULS design check		
10^-2 -10^-3	To be evaluated on a case by case basis		
10^-3 -10^-4	$\gamma_c = 1.0$	$\gamma_c = 1.0$	$\gamma_c = 1.0$
10^-4 -10^-5		$\gamma_c = 0.9$	$\gamma_c = 0.9$
10^-5 -10^-6	Accidental loads or events		$\gamma_c = 0.8$
<10^-6	may be disregarded		

Table 2 - 2: Simplified Design Check for Accident Loads (DNV-OS-F201, 2010)

2.3.2.2.3   Fatigue Limit State

It is required that a riser system has adequate safety against fatigue within the service life of the system. According to DNV-OS-F201 (2010), fatigue checks can be carried out via:

- Methods based on S-N curves
- Methods based on crack propagation

The former is utilized in this present study and more details are provided in **Chapter 7**.

2.3.3 Riser Design Loads

API RP 2RD (2006) and DNV-OS-F201 (2010) classify the loads to be considered in the design of riser systems as follows:

- **Functional and Pressure Loads**: Functional loads are loads that occur as a consequence of the physical existence of the system and by operating and handling the system, without environmental or accidental loads, while pressure loads are loads strictly due to combined effect of hydrostatic internal and external pressures. The functional and pressure loads included in the analysis in this write-up are:
  - Weight of riser, subsurface buoy, contents, and coating
  - Internal pressure due to contents, and external hydrostatic pressure
  - Nominal top tension
  - Buoyancy
  - Vessel constraints
  - Weight of marine growth
- **Environmental Loads**: These are loads imposed directly or indirectly by the ocean environment. These are:
  - Wave loads
  - Current loads
  - Vessel motions
  - Seismic loads
  - Ice loads
  - Wind loads

Only the first three types of environmental loads are included in the analysis in this write-up.

- **Accidental Loads**: These are loads to which the riser may be subjected in case of abnormal operations, incorrect operation or technical failure. They typically result from unplanned occurrences. These include:
  - Partial loss of station keeping capability
  - Small dropped objects
  - Tensioner failure
  - Fires and explosions
  - Flow-induced impact between risers
  - Vessel impact

Chapter 3: THESIS EXAMPLE RISER SYSTEM

3.0 Steel Catenary Risers Supported by Subsurface Buoy

This category of risers was referred to as Offset Steel Catenary Risers (OSCRs) by Shu et al (2011) and as Tension Leg Risers (TLRs) by Alexander et al (1999). The system was first developed in Deepstar Joint Industry Project (JIP) coordinated by Texaco in 1996/1997, and in subsequent years, several structural analyses have been conducted for H-shaped and rectangular ring-shaped buoys by Petrobras (Franciss R., 2005).

This concept is composed of a steel catenary riser(s) and flexible jumper(s) in conjunction with a submerged buoy located below the turbulence zone of the water body and moored to the seabed by tension leg tether lines. Basically, the steel catenary risers are curved upwards through the water body in a gentle catenary path and connected by means of separate flex joints or stress joints to a spool on the submerged buoy to enhance handling of the dynamic motions of the risers. The flexible jumpers are fluidly connected to the steel catenary risers by means of the same spool at the buoy and extend upward through the turbulence zone to the surface floating vessel (Mungall et al., 1997).

This riser system takes advantage of the best attributes of the steel catenary riser and the flexible pipe (as described in **sections 2.2.1** and **2.2.2**), while avoiding the limitations of both. The concept thus offers the following advantages (Franciss R., 2005; Serta et al., 2001):

- Uncouples the movements of the riser system, thereby providing freedom to choose the best production platform (FPSO or semi-submersible). The vessel motions are directly transferred to the jumpers and not to the main catenary (the steel catenary risers).
- Influence of riser top loads on the floating production unit design is substantially reduced.
- The installation schedule is improved, making it more flexible as it does not depend on the floating production unit's arrival at the field site.
- Increases significantly the technical feasibility window of the steel catenary risers in free hanging configuration (with respect to fatigue analysis) since the flexible jumpers will absorb the movements of the production vessel.
- Less exigency of the stiffness of the mooring system of the production vessel.
- Reduction in the complexity and capacity of the pull-in and pull-out systems for the flexible jumpers at the production vessel, thus reducing time and risks associated with the operations.
- The flexible jumpers can be installed or replaced using conventional vessels due to smaller loads.

- The system is composed of field proven technologies (steel catenary risers and flexible risers), which will help to improve its market competitiveness.
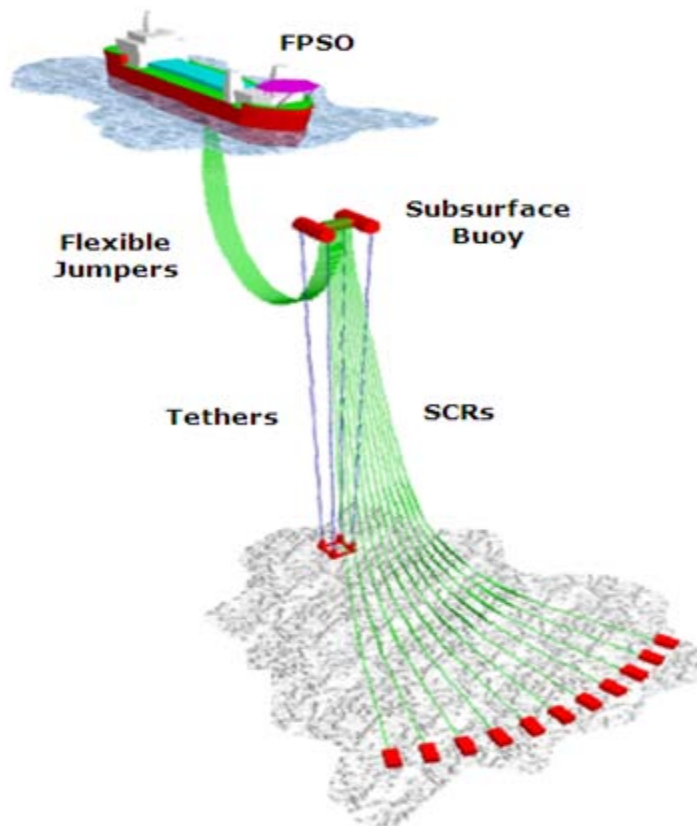
Figure 3 - 1: Steel Catenary Risers supported by Subsurface Buoy

To study the behaviour of this riser system, three different subsurface buoy shapes are considered in this write-up. These are:

- Rectangular Buoy (hitherto called the conventional buoy)
- H-shaped Buoy
- Modified H-Buoy

Details about these are presented in **section 4.1.3**.

Chapter 4: DESIGN DATA AND METHODOLOGY

4.0   Introduction

The properties of the components of a riser system, the behaviour of adjoining facilities such as the floating platform, and the environmental conditions of the area of deployment of the riser system determine the performance of the riser system. All these form the basic input parameters for a typical riser design and analysis operation. An accurate knowledge of these parameters is therefore important before commencing any riser system analysis.

In this chapter, the input parameters, coupled with the different load case parameters to be utilized in analyzing the performance of the riser system under consideration are presented. The validity of any riser design and analysis is based on a number of design acceptance criteria. The criteria to be satisfied by the riser system under consideration are presented in this chapter.

4.1   Design Parameters

As mentioned earlier, this study is based on a riser system called "steel catenary risers supported by subsurface buoy" which is connected to a Floating Production, Storage and Offloading (FPSO) vessel in deepwater areas of the North Sea. The basic design parameters for this study case are based on data obtained from a previous confidential project carried out by Subsea7, Norway.

4.1.1   Environmental Data

4.1.1.1 Water Depth

The water depth is 1500m and the subsurface buoy is located 200m below the sea surface. This is a typical water depth for deepwater areas of the North Sea.

4.1.1.2 Wave Data

The extreme sea state typical to the North Sea location is modelled by irregular waves. It is desirable to design a riser system such that it is able to withstand extreme sea states with a low probability of exceeding its 100-year response value. It is therefore common to design riser systems to be able to withstand different combinations of wind, waves and currents yielding the same return period of 100 years in conformity with standards such as NORSOK N-003, API RP 2RD, and DNV-OS-F201.

For this study, the following sea states are considered:

- 100-year sea state:

- Significant wave height, H_s 17 m
- Corresponding wave peak period, T_p 18.8 sec
- 10-year sea state:
  - Significant wave height, H_s 14.6 m
  - Corresponding wave peak period, T_p 17.5 sec

Each sea state is modelled as a wave spectrum with energy distributed over a range of frequencies. The spectrum that typifies the North Sea condition is the JONSWAP (Joint North Sea Wave project) spectrum and this will be deployed in this study. Analysis with irregular waves is otherwise known as the design storm approach, and a three-hour or six-hour design storm duration is usually considered (Andresen T., 2007). The former (i.e. three-hour duration) will be considered in this study.

4.1.1.3 Current Data

The 10-year and 100-year return period current profiles typical to the North Sea location are considered in this study. These are presented in **Table 4-1.**

Water Depth (m)	10-year Current (m/s)	100-year Current (m/s)
At surface	1.65	1.85
-50	1.26	1.40
-100	1.25	1.40
-200	1.09	1.20
-300	0.83	0.90
-400	0.74	0.80
-500	0.73	0.80
-600	0.60	0.65
-800	0.60	0.65
-1000	0.55	0.60
-1200	0.55	0.60
3 m above seabed	0.46	0.50

Table 4 - 1: Current Data

The current flow and wave directions are assumed to be in the same direction as the vessel offset as the most critical loading conditions generally occur when these actions are in the plane of the catenary (DNV-OS-F201, 2010).

4.1.1.4 Soil-Riser Interaction

According to Bai and Bai (2005), when the portion of a riser in contact with the seabed is subjected to oscillatory motion, there is complex interaction between the motion of the riser and the seabed. This forces the riser into the soil, thereby increasing the soil resistance. This makes a proper description of the soil-riser interaction an important consideration for accurate estimation of riser fatigue performance. Soil-riser interaction is commonly modelled by use of friction coefficients (sliding resistance) and linear springs (elastic soil stiffness).

The soil-riser interaction parameters used in this study are as follows:

- Lateral friction coefficient   0.5
- Axial friction coefficient   0.3
- Horizontal lateral/axial soil stiffness   200 kN/m^2
- Vertical soil stiffness   50 kN/m^2

4.1.2 Flowline Data

4.1.2.1 Riser Material

Commonly used riser pipe material grades are typically API 5L X60, X65 and X70 carbon steel. An important consideration in line pipe specification for a riser system is the property of the reservoir fluid as corrosive fluids such as CO_2 and H_2S influence the fatigue performance of a riser. As such, materials such as solid corrosion resistant alloy (CRA) have been utilized to obtain satisfactory fatigue life in some deepwater steel catenary risers.

For this study, the riser material is carbon steel, grade X65 with yield stress value (σ_y) of 448 MPa.

4.1.2.2 Riser Sizing

According to Bai and Bai (2005), the wall thickness of a steel catenary riser is typically sized to satisfy pressure containment (hoop and burst strength) and collapse requirements.

The minimum wall thickness used in this study was estimated in the confidential project mentioned in section 3.1 based on the burst, collapse and combined loading criteria discussed in **section 2.3.2.2.1**. The safety class is high and a corrosion allowance of 3mm is used for sizing. The riser size parameters and mechanical properties are presented in **Table 4-2.**

Parameter	Value	Unit
Internal diameter	254	mm
Wall thickness	26	mm
Coating thickness	76	mm
Young's Modulus	2.07E5	MPa
Riser material density	7.850	Mg/m^3
Length	2030	m
Design pressure	500	Bar
Mass in air	244	Kg/m
Mass in water	75	Kg/m
Diameter to weight ratio	0.622	m/(kN/m)
Bending stiffness	46800	kN.m^2
Axial stiffness	4734	MN
Torsional stiffness	36170	kN.m^2

Table 4 - 2: SCR Size Parameters and Mechanical Properties

4.1.2.3 Jumper Sizing and Marine Growths

The jumper sizing is based on internal diameter and limitation in minimum allowable tension. The outer diameter is influenced by the amount of marine growth anticipated in the North Sea location. According to NORSOK N-003 (2007) and DNV-OS-F201, 2010, marine growths may cause increased hydrodynamic actions, increased weight, increased hydrodynamic additional mass, and may influence hydrodynamic instability as a result of vortex shedding and possible corrosion effects. Site dependent data for marine growth are normally specified in terms of density, roughness, and depth variation of thickness. Based on NORSOK N-003 (2007), the following marine growth thicknesses are adopted for this study:

Water Depth (m)	Marine Growth Thickness (mm)
Above +2	0
+2 to -40	60
Below -40	30

Table 4 - 3: Thickness of Marine Growth (NORSOK N-003, 2007)

The density of the marine growth is set to 1325 kg/m^3.

Presented in **Table 4-4** are the structural properties of the flexible jumpers considered in this study and their size parameters with respect to influence of marine growths.

Parameter	Value	Unit
Structural properties		
Bending stiffness	87	kN.m^2
Axial stiffness	1900	MN
Torsional stiffness	400	kN.m^2
Design pressure	500	bar
Young's Modulus	2.07E5	MPa
Riser material density	7.850	Mg/m^3
Marine growth from +2 m to -40 m water depth		
Internal diameter	254	mm
Outer diameter including marine growth	544	mm
Jumper length	24	m
Mass in air	508	Kg/m
Mass in water	270	Kg/m
Diameter to weight ratio	0.206	m/(kN/m)
Marine growth below -40 m water depth		
Internal diameter	254	mm
Outer diameter including marine growth	484	mm
Mass in air	444	Kg/m
Jumper length	356	m
Mass in water	255	Kg/m
Diameter to weight ratio	0.193	m/(kN/m)

Table 4 - 4: Jumper Size Parameters and Mechanical Properties

Thus, the total length of each flexible jumper considered in this study is 380 m.

4.1.2.4 Flowline Hydrodynamic Coefficients

Waves and current should be considered when calculating hydrodynamic actions on structures. In combination with waves, the current velocity profile should be stretched to the local water surface. According to DNV-OS-F201 (2010), the hydrodynamic loading on slender structures (for instance, risers) can be expressed by the Morison equation in terms of the relative fluid-structure velocities and accelerations. The water particle velocity and acceleration vectors are found by considering relevant contributions from wave kinematics and current kinematics. The Morison equation for a uniform circular cross-section exposed to hydrodynamic loading in a direction normal to the structure's axis is given by:

$$f_n = \frac{1}{2}\rho C_d D_h |v_n - \dot{r}_n|(v_n - \dot{r}_n) + \rho \frac{\pi D_b^2}{4} C_m \dot{v}_n - \rho \frac{\pi D_b^2}{4}(C_m - 1)\ddot{r}_n \text{ .... (1)}$$

where:

f_n	Force per unit length in normal direction
ρ	Water density
D_h	Hydrodynamic diameter
D_b	Buoyancy diameter (i.e. equivalent diameter for description of resulting buoyancy on a general riser cross section)
$v_n, \dot{v}_n$	Fluid velocity and acceleration in normal direction
$\dot{r}_n, \ddot{r}_n$	Structural velocity and acceleration in normal direction
C_d, C_m	Drag and inertia coefficients in normal direction ($C_m = C_a + 1$)
C_a	Added mass coefficient in the normal direction

Equation (1) is utilized in OrcaFlex to compute the hydrodynamic loads on the risers considered in this study (the software automatically calculates the fluid and structural velocities and accelerations). The hydrodynamic and buoyancy diameters are equal to the outer diameters presented in **Tables 4-2** and **4-4** because there are no buoyancy attachments on the cross sections of the risers.

The hydrodynamic coefficients C_d and C_m depend on a number of parameters such as the Reynolds number of the flow past the riser's outer diameter, body shape of the riser and the riser's surface roughness. However, it can be difficult to decide the values of the coefficients

based on the above-mentioned parameters, for instance due to varying flow conditions. DNV-OS-F201 recommends the usage of values such as C_m = 2 and C_d = 0.7 and 1.0 as initial approximations.

Based on the project from which the data implemented in this study were obtained, the following hydrodynamic coefficients are used for this work:

- C_d, Jumpers   0.8
- C_d, SCRs   1.1
- C_a, Jumpers and SCRs   1.0

Drag and inertia forces in the axial direction of the risers are not considered in this study.

4.1.2.5 Flowline End Termination (Hang-Off System)

According to Song and Stanton (2007), terminating a steel catenary riser at a floater requires usage of a hang-off system. In general, three hang off systems have been used; they are flex joint, tapered stress joint (TSJ), and pull tube. Selection of any of these hang-off systems depends on its functional requirements in terms of required angular deflection, steel catenary riser size, and expected top tension. Some pros, cons and limitations of hang-off system are presented in **Table 4-5.**

Hang-off System	Pros	Cons	Limitations
Flex Joint	• Decouples the riser from the platform pitch and roll motions, thereby reducing the stresses in the upper region of the riser and the supporting porch structure. • Better accommodates variations in riser performance characteristics. • It is a reliable technical solution, particularly for fatigue design.	It is a relatively sophisticated component	Appropriate inspection procedures are needed under high temperature and pressure fluctuation environment.
Tapered Stress Joint (TSJ)	It is a one piece metallic component without any moving parts. Thus, it is less complicated than a flex joint.	As the riser size increases or the platform pitch and roll motions become more severe, the tapered stress joint design becomes more challenging.	Suitable in cases where the relative rotation between the platform and the riser is not excessive.
Pull Tube	Avoids the use of any subsea mechanical connections on the riser. It is thus simple and economical	• It has little room for flexibility. • There is potential for wear between the riser and the end of the pull tube. This implies good inspection procedures are required.	With larger diameter risers, there is increasing risk of the riser getting stuck in the pull tube due to the high bending stiffness.

Table 4 - 5: Pros, Cons, and Limitations of Various Riser Hang-off Systems (Xia J., 2008)

The most commonly used hang-off system is the flex joint due to its ability to better accommodate variations in riser performance characteristics. This is of extreme importance because of the tendency of the dynamic response of the riser to be both relieved and compounded by the dual influence of wave action and vessel motions. Differences between vessel and riser response can lead to high bending moments at the vessel attachment point. This can be relieved by use of flex joints at the vessel attachment point as it allows the riser to rotate with minimum bending moment.

For this study, the top and bottom ends of the flexible jumpers, and the top end of the steel catenary risers are assumed to be equipped with flex joints and are modelled as pinned connections (i.e. free to rotate) in the model subjected to global analysis.

Figure 4 - 1: Riser Hang-off Systems (Song and Stanton, 2007)

4.1.2.6 Internal Fluid Data

Three flowline internal fluid conditions will be considered in this study. These are presented in **Table 4-6.**

Internal Fluid	Density (kg/m^3)	Flowline Design Pressure (bar)
Oil	500	500
Water	1025	0
Empty	0	0

Table 4 - 6: Internal Fluid Data of Flowlines

The oil and water internal fluid conditions will subsequently in this write-up be referred to as content and flooded conditions respectively.

4.1.3 Subsurface Buoy Data

4.1.3.1 Buoy Shape

Three buoy shapes are considered in this study. These are the rectangular buoy (which will also be referred to as the conventional buoy in this write-up), the H-shaped buoy and the modified H-shaped buoy. The buoy shapes are as shown in **Figures 4-2, 4-3** and **4-4**. Brief descriptions of the buoys are presented below:

- Rectangular Buoy: It is built up in the analysis software (OrcaFlex) as being made up of parts such as the main spar, back spar and side spars, which are modelled to yield an overall buoy

submerged weight of -1800.6 tonnes, based on an assumed submerged weight to buoyancy ratio of 0.6. The base case dimension of the buoy is 15m width by 39m length. Variations will be made to the length of the buoy to study the effect of such on the stability of the buoy.

- H-shaped Buoy: This is 27m wide by 30m long buoy with an "H" shape. It is made up of building blocks such as the main spar and two side spars, each built based on an assumed submerged weight to buoyancy ratio of 0.6 to yield an overall buoy submerged weight of -1661 tonnes.

- Modified H-buoy: Whilst this also has an "H" shape, the distance between the arms of the "H" are widened to eradicate line clashing which could be present in the H-shaped buoy described above. It has a width of 47 m and length of 30 m, and its component parts have the same submerged weight to buoyancy ratio as the H-shaped buoy.

Buoy calculations can be found in **Appendix B**.
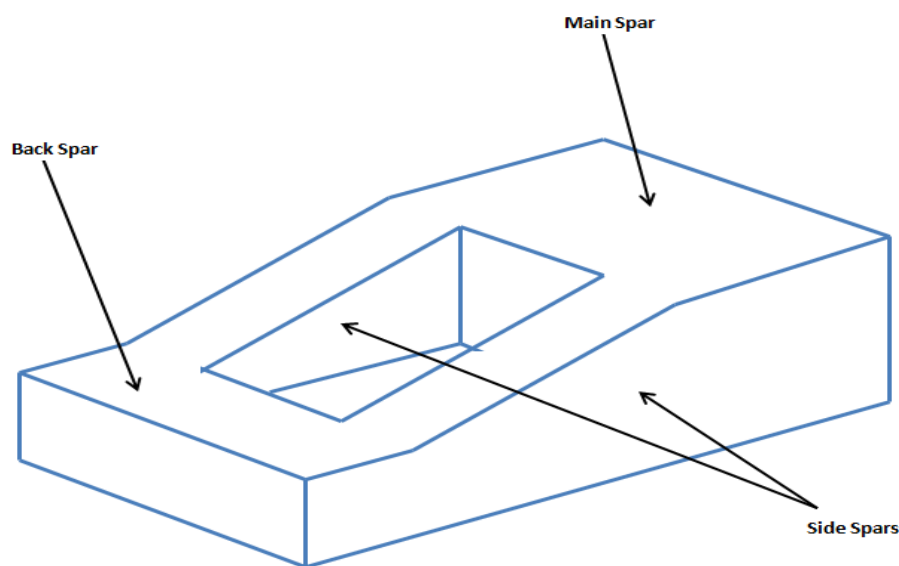
Figure 4 - 2: Rectangular Buoy
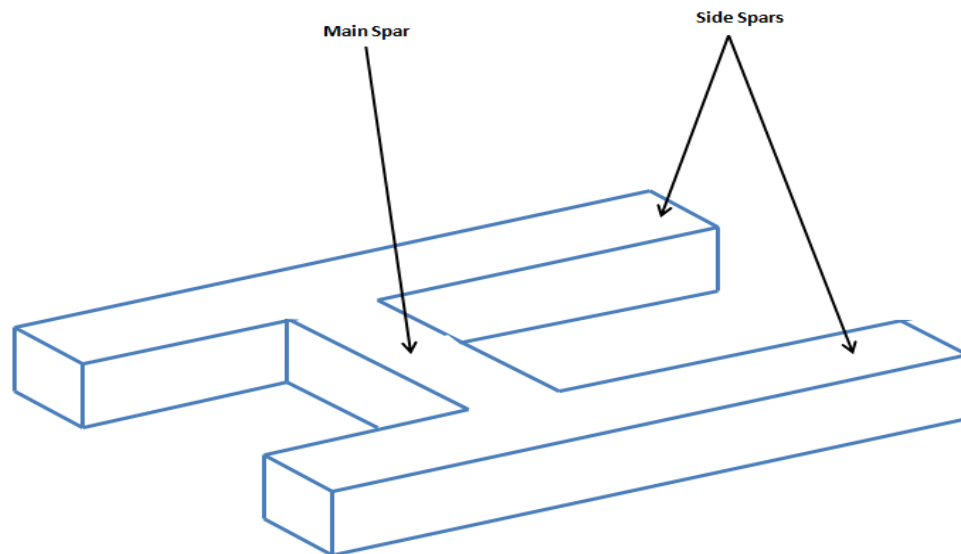
Figure 4 - 3: H-shaped Buoy
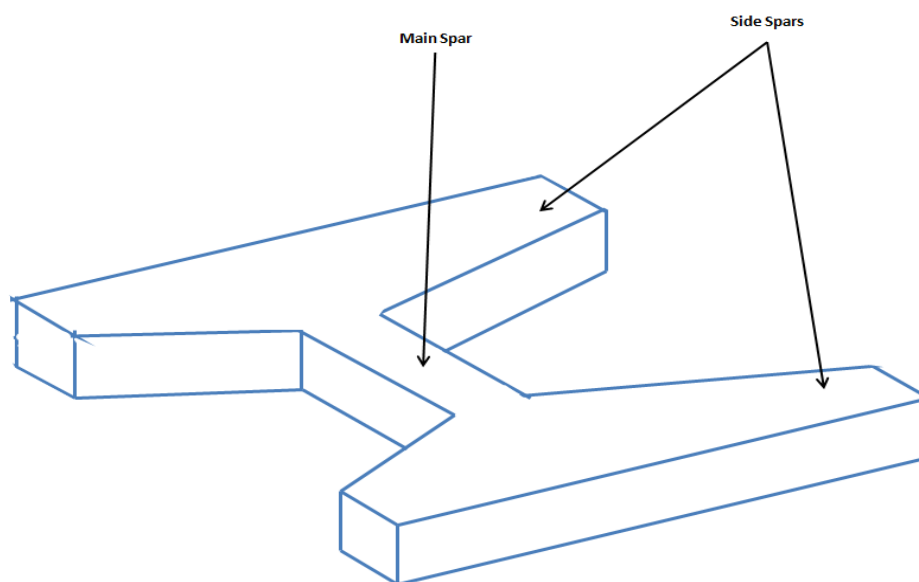
Figure 4 - 4: Modified H-buoy

4.1.3.2 Buoy Hydrodynamic Coefficients

Two important hydrodynamic coefficients that characterize the response of a submerged body to wave and current forces are drag coefficient (C_d) and added mass coefficient (C_a). Based on DNV-RP-H103 (2011), the drag coefficient on a submerged body depends on the projected area

of the body in the direction of the flow incident on the body and the Reynolds number (Re) of the flow past the body. **Tables 4-7** and **4-8** below present the shapes on which the calculated values of the drag coefficient and added mass coefficient of the components of each of the three buoys are based.
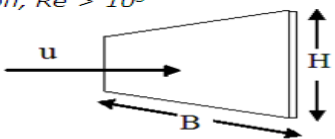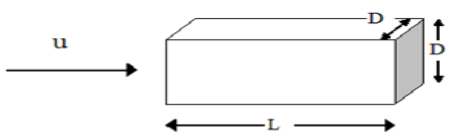
Geometry	Dimensions (B/H) and (L/D)	Drag Coefficient, C_d
Rectangular plate normal to flow direction, $Re > 10^3$	1	1.16
	5	1.20
	10	1.50
	∞	1.90
Square rod parallel to flow direction, $Re = 1.7 \times 10^5$	1.0	1.15
	1.5	0.97
	2.0	0.87
	2.5	0.90
	3.0	0.93
	4.0	0.95
	5.0	0.95

Table 4 - 7: Drag Coefficients of selected Three-dimensional Bodies (DNV-RP-H103, 2011)
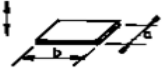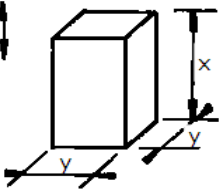
Body Shape	Direction of Motion	Dimensions (b/a) and Added Mass Coefficient (C_a)			
		b/a	C_a	b/a	C_a
Rectangular Plate	Vertical	1.00	0.579	3.17	0.840
		1.25	0.642	4.00	0.872
		1.50	0.690	5.00	0.897
		1.59	0.704	6.25	0.917
		2.00	0.757	8.00	0.934
		2.50	0.801	10.00	0.947
		3.00	0.830	∞	1.000
Square Prism	Vertical	x/y		C_a	
		1.00		0.68	
		2.00		0.36	
		3.00		0.24	
		4.00		0.19	
		5.00		0.15	
		6.00		0.13	
		7.00		0.11	
		10.00		0.08	

Table 4 - 8: Added Mass Coefficients of selected Three-dimensional Bodies (DNV-RP-H103, 2011)
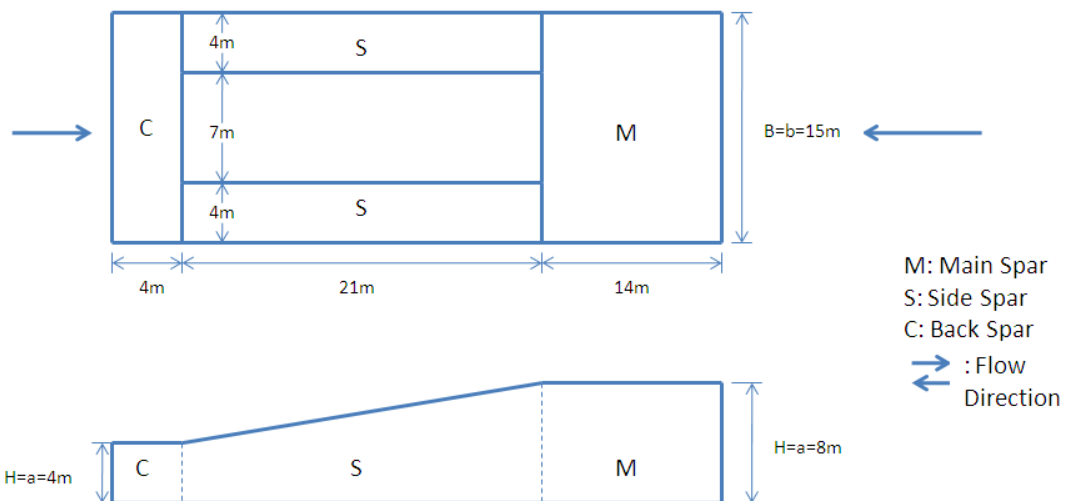
Figure 4 - 5: Plan and Side Views of Rectangular Buoy
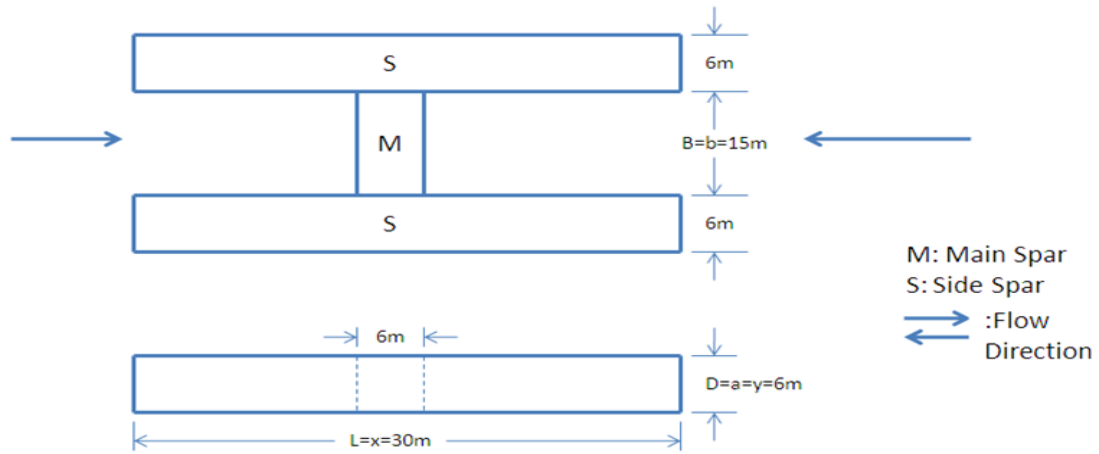
Figure 4 - 6: Plan and Side Views of H-shaped Buoy
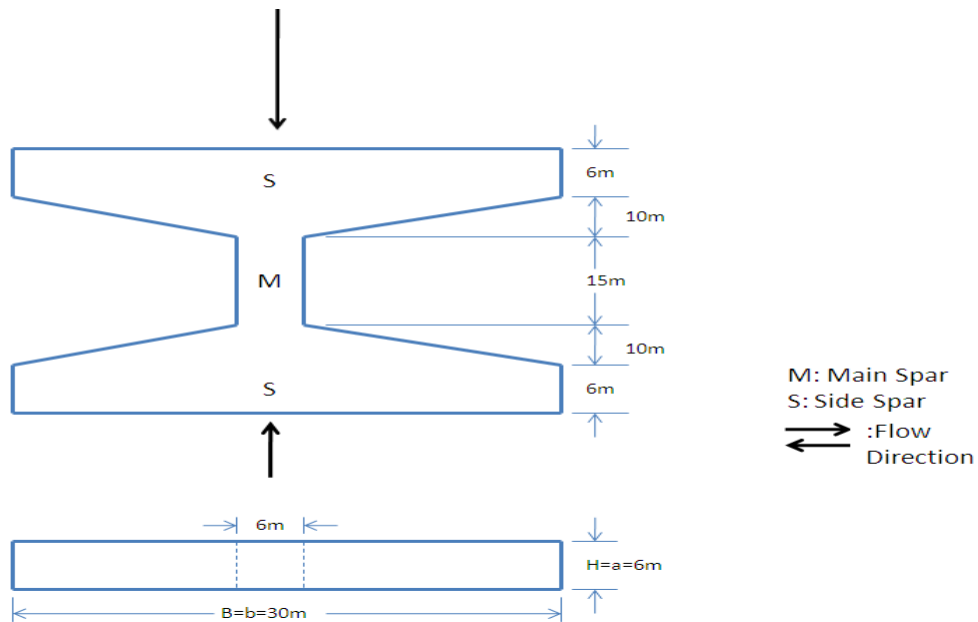
Figure 4 - 7: Plan and Side Views of Modified H-Buoy

With reference to **Tables 4-7** and **4-8** above, the following drag coefficient and added mass values were obtained for component parts of the three buoys based on the flow directions indicated in **Figures 4-5, 4-6** and **4-7** above.

Buoy Type	Buoy Part	Corresponding Geometry and Shape based on Figures …		Dimensions		Hydrodynamic Coefficients	
		For C_d	For C_a	For C_d	For C_a	C_d	C_a
Rectangular Buoy	Main Spar	Rectangular Plate normal to flow direction	Rectangular Plate	B/H = 1.875	b/a = 1.875	1.169	0.741
	Back Spar			B/H = 3.75	b/a = 3.75	1.188	0.862
H-shaped Buoy	Main Spar	Rectangular Plate normal to flow direction	Rectangular Plate	B/H = 2.5	b/a = 2.5	1.175	0.801
	Side Spar	Square Rod parallel to flow direction	Square Prism	L/D = 5.0	x/y = 5.0	0.95	0.15
Modified H-Buoy	Side Spar	Rectangular Plate normal to flow direction	Rectangular Plate	B/H = 5.0	b/a = 5.0	0.95	0.897

Table 4 - 9: Drag and Added Mass Coefficients of Rectangular Buoy, H-shaped Buoy, and Modified H-Buoy

However, it should be noted that the base case drag coefficient (C_d) value used for the buoys considered in this study is 1.4. This is because the shapes given in **Tables 4-7** and **4-8** above (especially the rectangular plates) will only give approximate drag coefficient values for the buoys since the geometry of the shapes and that of the component parts of the buoys are not exactly similar (this can be easily seen by comparing the rectangular plates with the main spars of the buoys). The value C_d = 1.4 was chosen based on data from another confidential project.

4.1.4 Buoy Mooring Line

4.1.4.1 Mooring Line Configuration

A total of eight (8) mooring lines are assumed to be used for the riser system under consideration, and they are connected in pairs on the sides of the buoy, close to the corners of the buoy. This is to minimize the rotation of the buoy due to horizontal forces. The seabed anchor points are spaced with the same distance as for the connection points at the buoy. This ensures that the ends of the mooring lines define a rectangle on the seabed.

The eight mooring lines are modelled by four mooring lines in the model used in this study, to ease the analysis operations. The implication of this is that each mooring line in the analysis model is modelled as having the properties of two mooring lines, and the mooring line construction type is taken as that of 6×19 Wire with Wire core in the analysis software. The size

and structural parameters of each mooring line used in the model is presented in **Table 4-10** below.

Parameter	Value	Unit
Outer diameter	120	mm
Inner diameter	0	mm
Length	1297	m
Mass in air	90	kg/m
Mass in water	78	kg/m
Diameter to weight ratio	0.157	m/(kN/m)
Bending stiffness	0	$kN.m^2$
Axial stiffness	909	MN
Torsional stiffness	80	$kN.m^2$

Table 4 - 10: Mooring Line Size and Structural Parameters

4.1.4.2 Mooring Line Hydrodynamic Coefficients

According to DNV-RP-H103 (2011), the drag coefficient of a spiral wire with sheathing ranges from 1.0-1.2. Based on the reference confidential project from which the data for this present study were obtained, a drag coefficient (C_d) value of 1.1 is adopted for each of the mooring lines in the model in this study. In addition, an added mass coefficient (C_a) value of 1.0 is used for the mooring lines based on assertions of DNV-RP-H103 (2011) that the added mass coefficient of a body with a circular cross section and that of an infinitely long cylinder is 1.0.

4.1.5 Vessel Motion

Xia J., (2008) says floating vessels experience first order short period motions in response to wave action. This first order short period motion is important for dynamic analysis of compliant risers and can be defined using Response Amplitude Operators (RAOs). The response amplitude operators define the first order motion of a vessel in response to waves with specified period and amplitude. In dynamic analysis, a vessel moves harmonically, in all six degrees of freedom (surge, sway, heave, roll, pitch, and yaw) about its primary position. These harmonic motions are specified by giving the RAO amplitudes and phases for the six degrees of freedom. The analysis software calculates the vessel motion using wave and RAO data, and applies the relevant motion to the riser system by means of special boundary conditions.

For this study, the response amplitude operators of a vessel from a previous project by Subsea 7 are used. A vessel heading of 270° is applied in this present study, and the flexible risers are modelled as being fixed to the vessel at a distance of 16m below its keel. The vessel will be considered in four positions known as the zero mean offset position (or nominal position), near offset position, far offset position, and cross offset position.

- Zero Mean Offset Position (Nominal Position): The vessel is in its initial position without displacement in any direction.
- Near Offset Position: The vessel is displaced in the plane of the SCR, moving away from the touchdown zone (TDZ) of the SCR, leading to a reduction in length of the SCR section on the seabed.
- Far Offset Position: The vessel is displaced in the plane of the SCR, moving towards the touchdown zone (TDZ) of the SCR, leading to an increase in the length of the SCR section on the seabed.
- Cross Offset Position: The vessel is displaced out of the plane of the SCR with the vessel being in the in-plane zero mean offset position. This offset position will only be considered in analyzing the modified H-buoy while the three aforementioned offset positions will be considered in analyzing the conventional buoy and the H-shaped buoy.
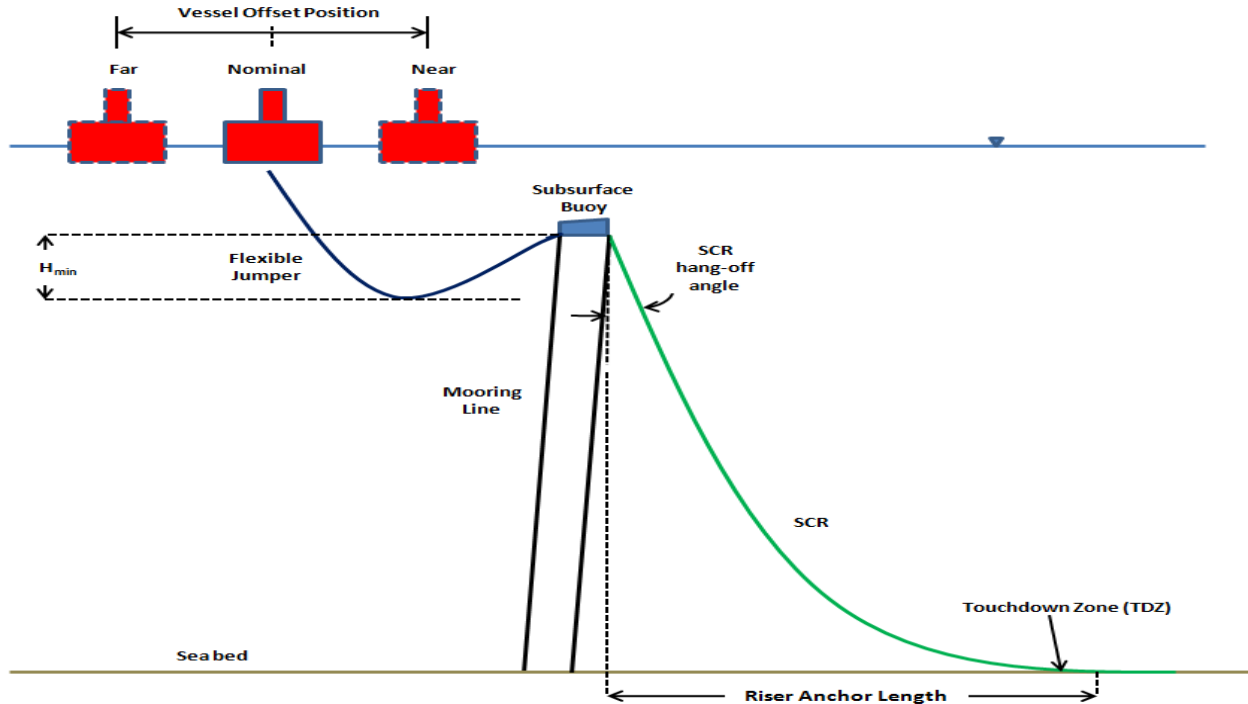
Figure 4 - 8: Thesis Example Riser System and Vessel Positions

4.1.6 Other Important Analysis Parameters

In addition to the design parameters discussed so far, other important input parameters to the design of dynamic risers are the dynamic simulation time duration, dynamic simulation time step, mesh length, and the structural damping coefficients. Sensitivity study is usually recommended in order to accurately capture the appropriate values of these parameters since they are of prime importance to the convergence of a simulation. However, values will be

chosen for these parameters based on previous similar projects such as Xie J., (2008) and the reference confidential project for this study. The selected values are as follows:

- Dynamic simulation time duration   10800 (3 hrs)
- Dynamic simulation time step   0.1 s
- Steel catenary riser mesh length (around hang-off and sagbend areas)   5 m
- Steel catenary riser mesh length (elsewhere)   10 m
- Flexible jumper mesh length   5 m
- Critical damping coefficient   0.5% at 10 secs

4.2 Model Description

The model consists of a subsurface buoy (conventional, H-shaped, or modified H-buoy) which is tethered to the seabed by four mooring lines connected to its corners. Four equispaced and equal length steel catenary risers (with a space of 3 m between successive risers on the buoy) run from one end of the buoy and are anchored to the seabed (and they are modelled as having a distance of 60 m between successive risers on the seabed). Also, four flexible jumpers connected in like manner as the steel catenary risers to the other end of the buoy run through the turbulence zone of the sea to the surface floating vessel, and are modelled as being equispaced at their connection point to the vessel, with a distance of 3 m between successive buoys. The model is presented in **Figure 4-9** below.
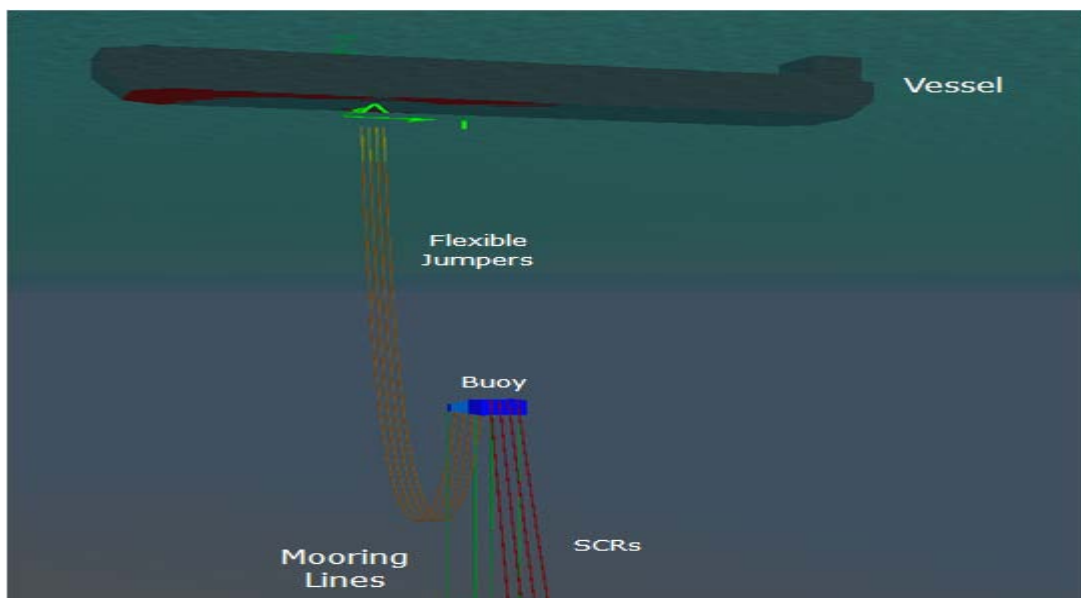
Figure 4 - 9: Typical Riser System Analysis Model

4.3   Load Case Parameters

A load case refers to critical combinations of parameters that should be checked in a design activity. The following parameters will form the bed rock of analyses in this study under ultimate limit state (ULS):

- Flowline internal fluid: Oil (i.e. content), water (i.e. flooded), or empty.
- Current return periods: 10 years, 100 years.
- Current directions: 0°, 180°.
- Wave return periods: 10 years, 100 years.
- Wave directions: 0°, 180°.
- Environmental load combinations (dynamic analysis): 10-year current + 100-year wave, 100-year current + 10-year wave.
- Vessel heading: 270°.
- Vessel offsets:
    - Near vessel position: -50 m and -30 m for 10-year and 100-year currents respectively.
    - Nominal vessel position: 0 m for both 10-year and 100-year currents.
    - Far vessel position: 50 m and 30 m for 10-year and 100-year currents respectively.

Necessary variations to any of these parameters in any analysis will be specified in such analysis.

4.4   Design Acceptance Criteria

Riser design is iterative in nature and there is need to fulfill a number of requirements before a design can be deemed acceptable. The following are the requirements to be satisfied by this study:

- Minimum bend radius (MBR) of flexible jumpers: The minimum bend radius of the flexible jumpers is given as 5 m. To ensure this value is not breached during analysis, a limiting value of 25 m is fixed for static analysis at any vessel offset, and H_{min} which is the distance between the lowest point along the catenary of a flexible jumper and its connection point to the subsurface buoy (see **Figure 4-8** in **section 4.1.5**) is also fixed as 30 m for static analysis.
- Minimum tension of flexible jumpers: No compression is permitted along the flexible jumpers. This implies negative tension values are not acceptable.
- Maximum Von Mises stress of steel catenary risers: This is set to be 358 MPa and 448 MPa in accordance with API RP 2RD (2006) requirements for ultimate limit state (ULS) and accidental limit state respectively as given in **Table 2-1** of **section 2.3.2.1**. Thus, Von Mises

utilization factors of less than 0.8 and 1.0 must govern the results for ultimate and accidental limit states respectively at any vessel offset. To achieve this, a limiting value of around 300MPa (which corresponds to a utilization factor of around 0.67) is utilized for static analysis (Note that Von Mises utilization factor is the ratio of the Von Mises stress at any point along a riser and the yield strength (σ_y) of the riser).

- Buckling utilization factor: A buckling utilization factor of less than 1.0 is used in this study in consonance with requirements of DNV-OS-F201 (2010).

In addition to the above criteria, the top angle of each steel catenary riser is desired to be 9° for static analysis at nominal vessel position with no current acting.

Chapter 5: DESIGN ANALYSIS

5.0   Introduction

In this chapter, the effects of various parameters on the behaviour of the different buoy types and on the structural performance of the steel catenary risers and flexible jumpers will be studied. The parameters to be studied here are as follows:

- Length of the conventional buoy
- Riser Anchor length
- Offset of the main spar of the H-shaped buoy relative to the mid-length of its side spars
- Internal content of the flowlines
- Drag coefficient (C_d) of the buoys
- Added mass coefficient (C_a) of the buoys
- Submerged weight of the conventional buoy

For each study case, all other parameter values are fixed while only the parameter being investigated is varied. The first five parameters will only be subjected to static analysis while the remaining two parameters will be subjected to dynamic analysis. The resulting riser system configuration (at the end of the static analysis of the first five parameters) with respect to the conventional buoy and the H-shaped buoy will also be subjected to dynamic analysis. Furthermore, all analyses shall be carried out with respect to **ultimate limit state** with the exception of the case of the submerged weight of the buoy which will be carried out with respect to **accidental limit state**.

In addition to the above parametric studies, the H-shaped buoy and the modified H-buoy will be studied for possibility of clashing of the flowlines and the mooring lines of the buoy.

The first set of parametric studies will be carried out with the conventional buoy used in the riser system under study, followed by the H-shaped buoy. The final set of studies will be about line clashing.

5.1   Design Analysis of Steel Catenary Risers supported by Conventional Buoy (Static Analysis)

5.1.1 Sensitivity to Length of the Conventional Buoy

The length of the buoy determines the trim angle (i.e. rotation) of the buoy and its eventual stability. For this study, the length variation of the conventional buoy is achieved by varying the length of the side spars of the buoy (the lengths of the side spars are equal in each variation). Changes in the side spar length leads to change in the overall submerged weight of the buoy (as

seen in **Figure 5-1** below) and calculations in respect of this for each buoy length are presented in **Appendix B.4**.
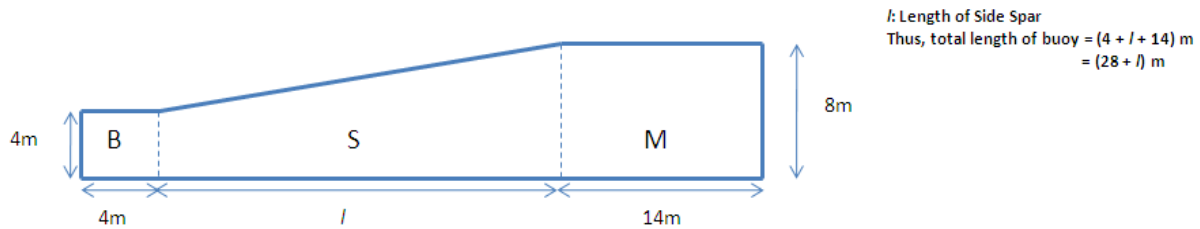
Figure 5 - 1: Illustration of Total Length of Conventional Buoy

The study is carried out for five different lengths of the side spar as follows:

Analysis Parameters

- Side spar lengths   11, 16, 21, 26, and 31 m
- Riser anchor length   1350 m
- Internal content of flowlines   Oil
- Drag coefficient of buoy (C_d)   1.4
- Added mass coefficient of buoy (C_a)
  - Main spar   0.741
  - Back spar   0.862
- Vessel offset   Nominal position (0 m)
- Current case   No current

The resulting buoy trim angle, minimum bend radius and H_{min} of the flexible jumpers, and the hang-off angle and maximum Von Mises stress values (top and sag bend areas) for the different spar lengths are presented in **Table 5-1** below (full results can be found in **Appendix C.1-1**).

Side Spar Length	Flexible Jumpers			Maximum Values for SCRs				
	Minimum Bend Radius (MBR)	H_{min}	Buoy Trim Angle	Hang-off Angle	Max. Von Mises Stress (Top)	Max. Von Mises Stress (Sagbend)	Von Mises Utilization (Top)	Von Mises Utilization (Sagbend)
(m)	(m)	(m)	(deg)	(deg)	(MPa)	(MPa)		
11	64	46	1.8	9	276	259	0.62	0.58
16	61	49	0.6	9	276	259	0.62	0.58
21	57	51	0.0	9	276	259	0.62	0.58
26	54	53	-0.3	9	276	258	0.62	0.58
31	51	55	-0.5	9	276	258	0.62	0.58

Table 5 - 1: Summary Static Analysis Results for Conventional Buoy Length Variation, at Zero Vessel Offset and No Current

The above table reveals that all the spar lengths considered satisfy the minimum bend radius and H_{min} criteria of the flexible jumpers, and the hang-off angle and Von Mises utilization criteria of the steel catenary risers as spelt out in **section 4.4**. It is observed that the hang-off angles of the steel catenary risers are fairly equal for all the side spar lengths considered, likewise the Von Mises utilizations at top and sagbend areas. However, the buoy trim angle values reveal that the most unstable buoy is obtained when the side spar length is 11 m, and the angle decreases as the side spar length increases, with the most stable buoy being that which gives a trim angle of 0.0° (and this is obtained when the side spar length is 21 m). Note that negative buoy trim angles imply counter-clockwise rotation of the buoy while positive buoy trim angles imply clockwise rotation of the buoy.

Plots of the results presented in **Table 5-1** above are given below.
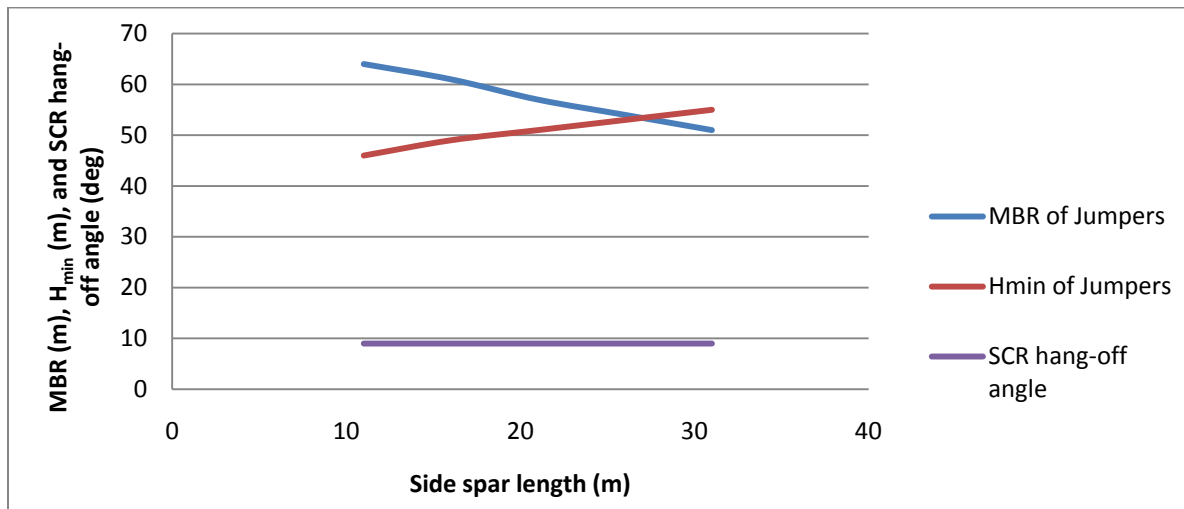
Figure 5 - 2: Sensitivity of H_{min} and MBR of Jumpers, and Hang-off angle of SCRs to Conventional Buoy Length Variation, with Zero Vessel Offset and No Current
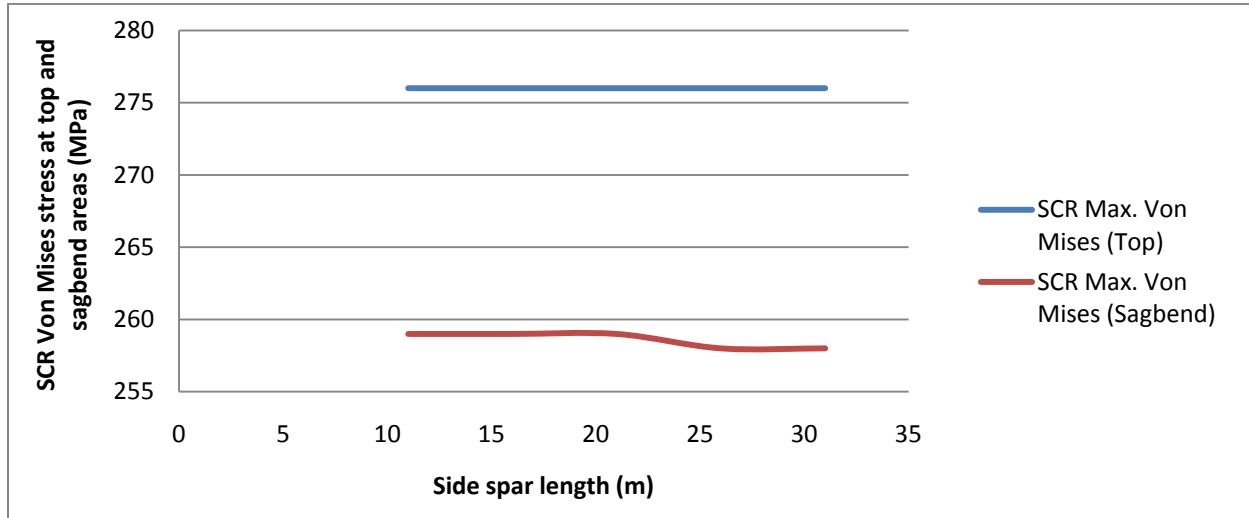
Figure 5 - 3: Sensitivity of Top and Sagbend region Von Mises Stresses of SCRs to Conventional Buoy Length Variation, with Zero Vessel Offset and No Current
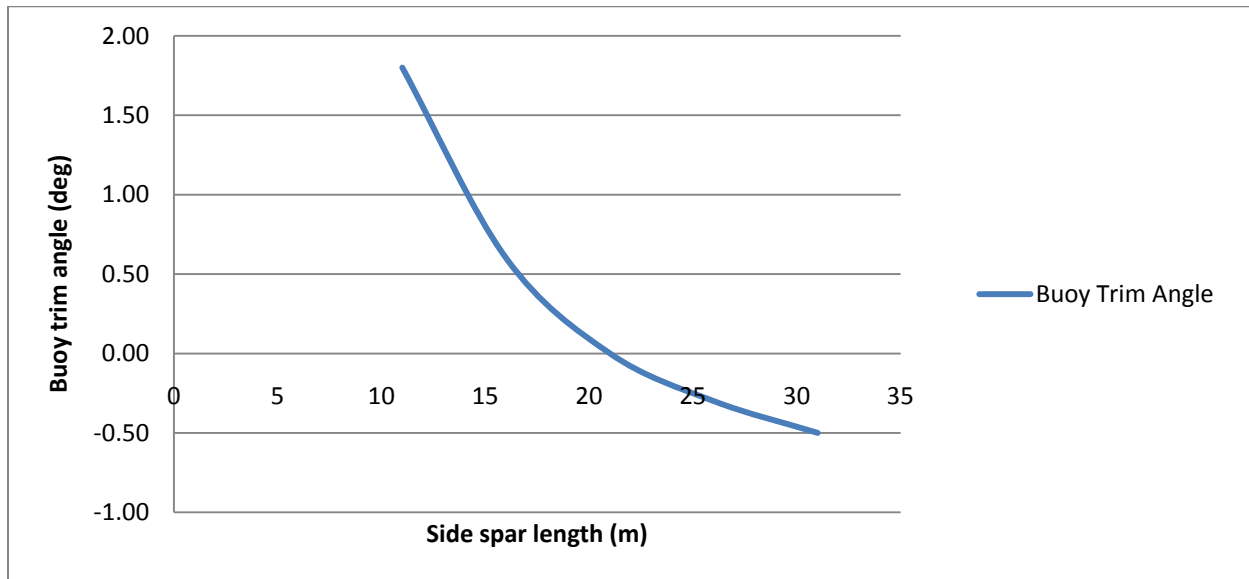
Figure 5 - 4: Sensitivity of Buoy Trim Angle to Conventional Buoy Length Variation, with Zero Vessel Offset and No Current

To further study the behaviour of the riser system for each length of the side spar, the above study was conducted for situations when the vessel is at its near and far offset positions, with the inclusion of the current conditions presented in **section 4.1.1.3**. Thus, in addition to the analysis parameters given at the beginning of this section, the following parameters are also employed to accurately model the vessel offset positions:

Analysis Parameters

Case 1:

- Vessel offset   Near position (-50 m)
- Current return period   10 years, No current (i.e. 0 years)
- Current direction   0°

Case 2:

- Vessel offset   Far position (50 m)
- Current return period   10 years, No current (i.e. 0 years)
- Current direction   180°

Case 3:

- Vessel offset   Near position (-30 m)
- Current return period   100 years, No current (i.e. 0 years)
- Current direction   0°

Case 4:

- Vessel offset   Far position (30 m)
- Current return period   100 years, No current (i.e. 0 years)
- Current direction   180°

Table 5-2 below presents the results obtained for cases 1 and 2 (full results can be found in **Appendices C.1-2** to **C.1-6**).

Side Spar Length	Case	Vessel Offset	Current Return Period	Current Direction	Flexible Jumpers		Buoy Trim Angle	Hang-off Angle	Maximum Values for SCRs			
					MBR	H_{min}			Max. Von Mises Stress (Top)	Max. Von Mises Stress (Sagbend)	Von Mises Utilization (Top)	Von Mises Utilization (Sagbend)
(m)		(m)	(yr)	(deg)	(m)	(m)	(deg)	(deg)	(MPa)	(MPa)		
11	1	-50	10	0	66	43	1.5	10	274	300	0.61	0.67
			0		48	57	1.6	8	275	264	0.61	0.59
	2	50	10	180	65	48	3.3	8	278	246	0.62	0.55
			0		85	36	2.0	10	276	255	0.62	0.57
16	1	-50	10	0	59	47	0.1	10	274	297	0.61	0.66
			0		44	59	0.4	8	276	263	0.62	0.59
	2	50	10	180	64	48	1.2	8	278	247	0.62	0.55
			0		81	38	0.8	10	276	255	0.62	0.57
21	1	-50	10	0	54	50	-0.5	10	275	294	0.61	0.66
			0		40	62	-0.1	8	276	262	0.62	0.58
	2	50	10	180	62	49	0.5	8	278	247	0.62	0.55
			0		78	39	0.1	10	276	255	0.62	0.57
26	1	-50	10	0	49	54	-0.7	10	275	291	0.61	0.65
			0		37	65	-0.4	8	276	261	0.62	0.58
	2	50	10	180	61	50	0.0	8	278	247	0.62	0.55
			0		75	41	-0.2	10	276	255	0.62	0.57
31	1	-50	10	0	44	57	-0.8	11	275	289	0.61	0.65
			0		34	67	-0.6	8	276	261	0.62	0.58
	2	50	10	180	59	52	-0.2	8	278	247	0.62	0.55
			0		71	43	-0.4	10	276	255	0.62	0.57

Table 5 - 2: Static Analysis Results for Conventional Buoy Length Variation at Near and Far Vessel Positions, and 0- and 10-year currents.

The above table reveals that the five spar lengths satisfy the minimum bed radius and H_{min} requirements of the jumpers, and the Von Mises utilization criteria of the steel catenary risers. The maximum Von Mises stress values show that the most critical region along the steel catenary risers when the vessel is at its near offset position with current acting is the sagbend region since the Von Mises stress value is highest at this region, while the most critical region when the vessel is at its far offset position is the top (or hang-off) region. The values also show that it is easier to breach the Von Mises stress condition given in **section 4.4** at the sagbend region than at the hang-off region since the values at the sagbend region approach 300MPa faster at the vessel's near offset position than those at the hang-off region at any vessel offset position. This shows that the governing maximum Von Mises stress value will be that at the sagbend region since analysis is usually done at a vessel's near and far offset positions. Furthermore, a look at the trim angles shows that the 21 m long side spars will result in the

most stable configuration for the buoy since the magnitude of its maximum trim angle (i.e. 0.5°) is less than those of the other side spar lengths (i.e. 3.3°, 1.2°, 0.7°, and 0.8° for the 11 m, 16 m, 26 m, and 31 m long side spars respectively).

The results for cases 3 and 4 are presented below (full results can be found in **Appendices C.1-7 to C.1-11**).

Side Spar Length	Case	Vessel Offset	Current Return Period	Current Direction	Flexible Jumpers		Buoy Trim Angle	Hang-off Angle	Maximum Values for SCRs			
					MBR	H_{min}			Max. Von Mises Stress (Top)	Max. Von Mises Stress (Sagbend)	Von Mises Utilization (Top)	Von Mises Utilization (Sagbend)
(m)		(m)	(yr)	(deg)	(m)	(m)	(deg)	(deg)	(MPa)	(MPa)		
11	3	-30	100	0	78	36	1.6	11	275	303	0.61	0.68
			0		54	53	1.7	8	276	262	0.62	0.58
	4	30	100	180	55	54	3.6	8	278	246	0.62	0.55
			0		76	40	1.9	9	276	256	0.62	0.57
16	3	-30	100	0	71	40	0.1	11	275	301	0.61	0.67
			0		50	55	0.5	8	276	261	0.62	0.58
	4	30	100	180	54	55	1.3	8	278	246	0.62	0.55
			0		73	42	0.7	9	276	256	0.62	0.57
21	3	-30	100	0	64	44	-0.5	11	275	298	0.61	0.67
			0		47	58	-0.1	8	276	261	0.62	0.58
	4	30	100	180	52	56	0.5	8	278	246	0.62	0.55
			0		69	44	0.1	9	276	256	0.62	0.57
26	3	-30	100	0	59	47	-0.7	11	275	296	0.61	0.66
			0		43	60	-0.4	8	276	260	0.62	0.58
	4	30	100	180	51	57	0.0	8	278	246	0.62	0.55
			0		66	46	-0.3	9	276	256	0.62	0.57
31	3	-30	100	0	54	51	-0.9	11	275	294	0.61	0.66
			0		40	62	-0.6	9	276	260	0.62	0.58
	4	30	100	180	49	58	-0.2	7	278	246	0.62	0.55
			0		63	48	-0.5	9	276	256	0.62	0.57

Table 5 - 3: Static Analysis Results for Conventional Buoy Length Variation at Near and Far Vessel Positions, and 0- and 100-year currents.

Just as for cases 1 and 2, the side spar lengths for cases 3 and 4 satisfy the minimum bend radius and H_{min} criteria for the flexible jumpers, and also fairly satisfy the maximum Von Mises stress requirements at the top and sagbend regions of the steel catenary risers. The buoy trim angles also show that the most stable buoy results when the side spar length is 21 m (just as obtained in cases 1 and 2).

Thus, a conventional buoy with a side spar length of 21 m will be the basis of subsequent parametric studies in this section.

5.1.2 Sensitivity to Riser Anchor Length

The riser anchor length refers to the horizontal distance between the hang-off point of the steel catenary risers at the subsurface buoy and the connection point of the same risers to the sea bed. The anchor length to a large extent influences the stability of a given size of buoy and the hang-off angle of the steel catenary risers. As the anchor length increases, the free hanging portion of the steel catenary risers also increases and this has the tendency to increase the top tension of the risers.

A study of five different anchor lengths is conducted for the conventional buoy with 21 m long side spars below.

Analysis Parameters

- Riser anchor lengths   1265, 1315, 1350, 1400, and 1450 m
- Side spar length   21 m
- Internal content of flowlines   Oil
- Drag coefficient of buoy (C_d)   1.4
- Added mass coefficient of buoy (C_a)
  - Main spar   0.741
  - Back spar   0.862
- Vessel offset   Nominal position (0 m)
- Current case   No current

The following results were obtained for the five anchor lengths (full results can be found in **Appendix C.1-12**):

Riser Anchor Length	Flexible Jumpers		Buoy Trim Angle	Maximum Values for SCRs					
	Minimum Bend Radius (MBR)	H_{min}		Hang-off Angle	Top Tension (Tension at Buoy)	Max. Von Mises Stress (Top)	Max. Von Mises Stress (Sagbend)	Von Mises Utilization (Top)	Von Mises Utilization (Sagbend)
(m)	(m)	(m)	(deg)	(deg)	(kN)	(MPa)	(MPa)		
1265	46	59	-0.4	7	1426	275	275	0.61	0.61
1315	52	54	-0.2	8	1492	276	264	0.62	0.59
1350	57	51	0.0	9	1490	276	259	0.62	0.58
1400	66	46	0.2	10	1541	276	252	0.62	0.56
1450	76	40	0.5	12	1606	277	248	0.62	0.55

Table 5 - 4: Summary Static Analysis Results for Riser Anchor Length Variation at Zero Vessel Offset and No Current – Conventional Buoy

The above results show that the top tension of the steel catenary risers increases as the anchor length increases. This leads to higher maximum Von Mises stress values at the top end of the risers when compared with the values at the sagbend area. The minimum bend radius and H_{min} values of the flexible jumpers, and the top and sagbend maximum Von Mises stress values satisfy the design criteria given in **section 4.4**.

It can also be seen that the minimum bend radius of the flexible jumpers decreases with reduction in anchor length, while the H_{min} values decrease with increase in anchor length. The implication of this is that there is high tendency for the minimum bend radius criterion to be breached as the anchor length decreases, and there is high tendency for the H_{min} criterion to be breached as the anchor length increases. A reasonable anchor length would thus be one with some degree of balance between the minimum bend radius and H_{min}. This anchor length must also be such that affords stability to the buoy. These conditions are satisfied by the 1350 m long anchor length. A buoy trim angle of 0.0° is achieved with this anchor length and this offers the best stability possible to the buoy. In addition, this riser anchor length meets the hang-off angle requirement (i.e. 9°) of the steel catenary risers as given in **section 4.4**. Thus, an anchor length of 1350 m will be utilized for subsequent analysis in this section.

The results in **Table 5-4** are plotted in **Figures 5-5, 5-6, 5-7** and **5-8** below.

Figure 5 - 5: Sensitivity of SCR Top Tension to Riser Anchor Length, with Zero Vessel Offset and No Current – Conventional Buoy
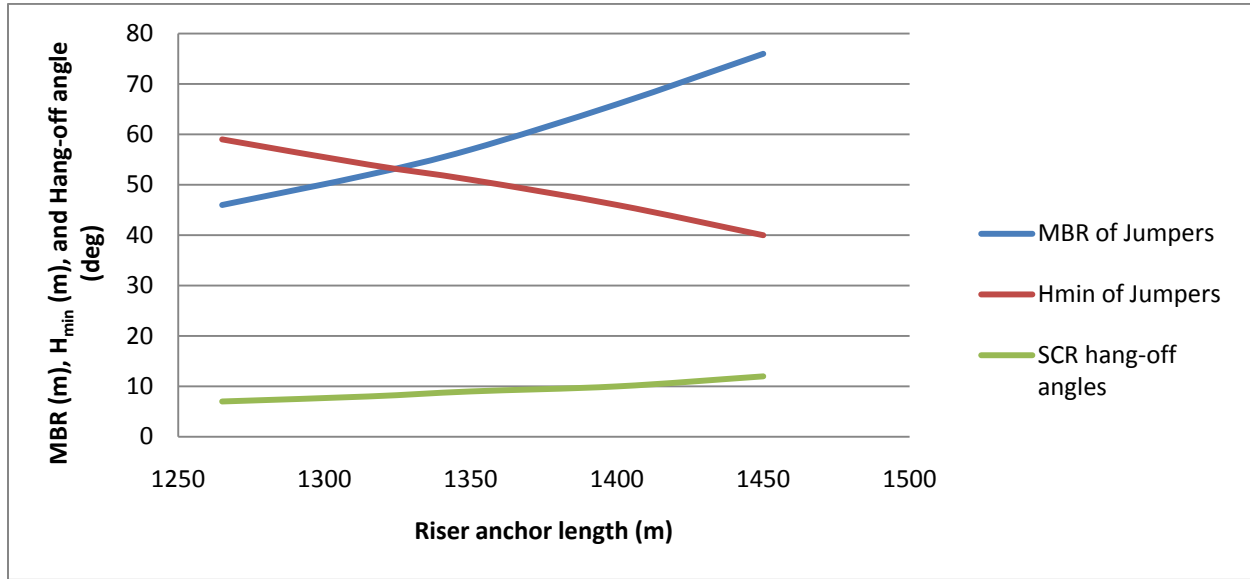
Figure 5 - 6: Sensitivity of H$_{min}$ and MBR of Jumpers, and Hang-off angle of SCRs to Riser Anchor Length, with Zero Vessel Offset and No Current – Conventional Buoy
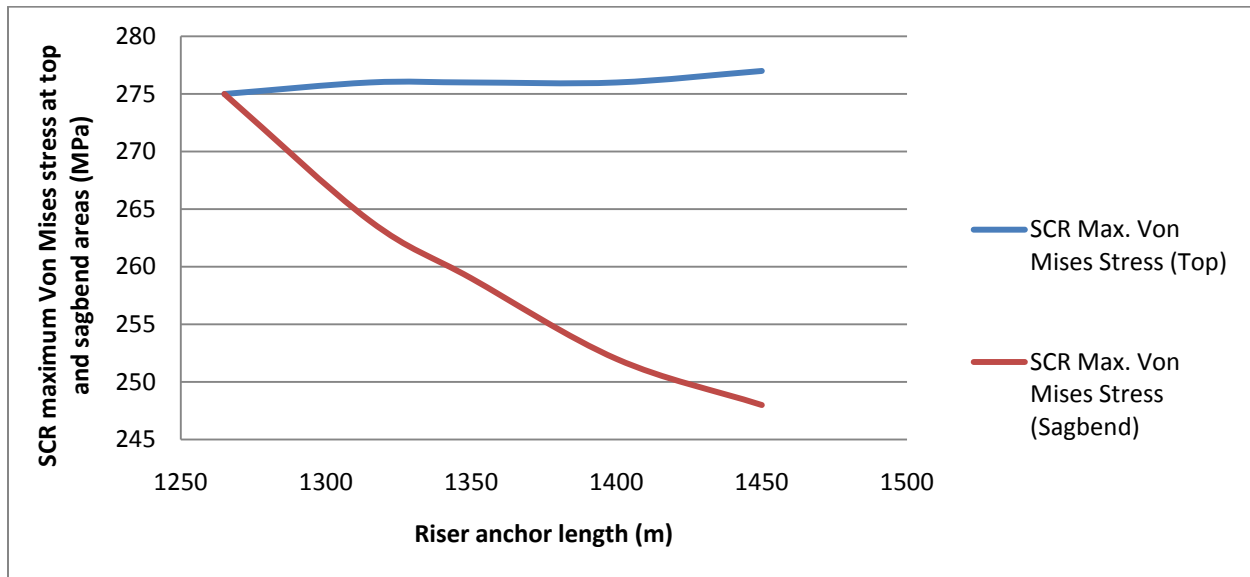
Figure 5 - 7: Sensitivity of Top and Sagbend region Von Mises Stresses of SCRs to Riser Anchor Length, with Zero Vessel Offset and No Current – Conventional Buoy
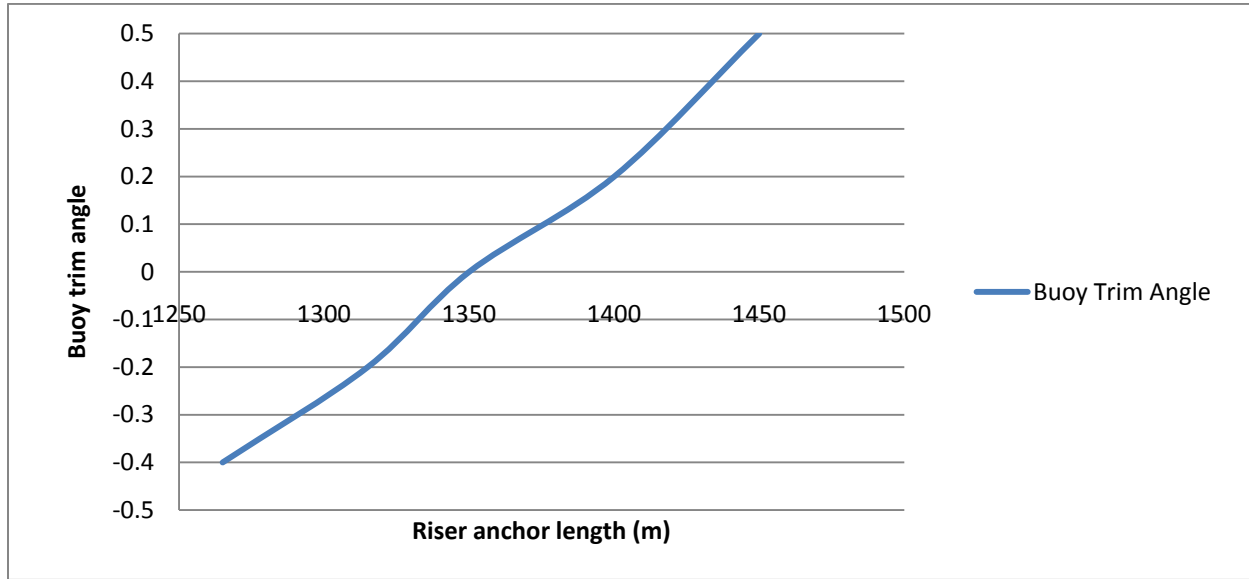
Figure 5 - 8: Sensitivity of Buoy Trim Angle to Riser Anchor Length, with Zero Vessel Offset and No Current – Conventional Buoy

5.1.3 Sensitivity to Internal Content of Flowlines

As mentioned in **section 4.1.2.6**, three internal fluid conditions namely content, empty, and flooded will be considered in this study. Here, analysis will be carried out separately for each internal fluid condition and necessary comparisons will be made based on results obtained. The analysis will be done at the near, nominal and far vessel offset positions.

Analysis Parameters

- Internal fluid condition of flowlines   Content, Empty, and Flooded
- Side spar length   21 m
- Riser anchor length   1350 m
- Drag coefficient of buoy (C_d)   1.4
- Added mass coefficient of buoy (C_a)
    - Main spar   0.741
    - Back spar   0.862
- Current and vessel offset cases
    - Case 1
        - Vessel offset   Near position (-50 m)
        - Current return period   10 years, No current (i.e. 0 years)
        - Current direction   0°

- Case 2
  - Vessel offset   Nominal position (0 m)
  - Current return period   10 years, No current (i.e. 0 years)
  - Current direction   0°, 180°
- Case 3
  - Vessel offset   Far position (50 m)
  - Current return period   10 years, No current (i.e. 0 years)
  - Current direction   180°
- Case 4
  - Vessel offset   Near position (-30 m)
  - Current return period   100 years, No current (i.e. 0 years)
  - Current direction   0°
- Case 5
  - Vessel offset   Nominal position (0 m)
  - Current return period   100 years, No current (i.e. 0 years)
  - Current direction   0°, 180°
- Case 6
  - Vessel offset   Far position (30 m)
  - Current return period   100 years, No current (i.e. 0 years)
  - Current direction   180°

Result summary of analysis done with the content-filled flowlines for cases 1, 2, and 3 are presented as follows (full results can be found in **Appendix C.1-15**):

				Flexible Jumpers		Buoy Trim Angle	Maximum Values for SCRs				
Case	Vessel Offset	Current Return Period	Current Direction	MBR	H_{min}		Hang-off Angle	Max. Von Mises Stress (Top)	Max. Von Mises Stress (Sagbend)	Von Mises Utilization (Top)	Von Mises Utilization (Sagbend)
	(m)	(yr)	(deg)	(m)	(m)	(deg)	(deg)	(MPa)	(MPa)		
1	-50	10	0	54	50	-0.5	10	275	294	0.61	0.66
		0	-	40	62	-0.1	8	276	262	0.62	0.58
2	0	10	0	74	39	-0.3	11	275	283	0.61	0.63
		0	-	57	51	0.0	9	276	259	0.62	0.58
		10	180	44	61	0.3	7	278	248	0.62	0.55
3	50	10	180	62	49	0.5	8	278	247	0.62	0.55
		0	-	78	39	0.1	10	276	255	0.62	0.57

Table 5 - 5: Summary Static Analysis Results for Riser System (with Content-filled flowlines) supported by Conventional Buoy, at Near, Zero, and Far Vessel Offsets, with 0- and 10-year Currents

The result summary of cases 4, 5, and 6 for content-filled flowlines are presented below (full results can be found in **Appendix C.1-16**).

Content-Filled Flowlines											
				Flexible Jumpers		**Buoy Trim Angle**	**Maximum Values for SCRs**				
Case	Vessel Offset	Current Return Period	Current Direction	MBR	H_{min}		Hang-off Angle	Max. Von Mises Stress (Top)	Max. Von Mises Stress (Sagbend)	Von Mises Utilization (Top)	Von Mises Utilization (Sagbend)
	(m)	(yr)	(deg)	(m)	(m)	(deg)	(deg)	(MPa)	(MPa)		
4	-30	100	0	64	44	-0.5	11	275	298	0.61	0.67
		0	-	47	58	-0.1	8	276	261	0.62	0.58
5	0	100	0	77	37	-0.4	11	275	290	0.61	0.65
		0	-	57	51	0.0	9	276	259	0.62	0.58
		100	180	42	62	0.4	7	278	247	0.62	0.55
6	30	100	180	52	56	0.5	8	278	246	0.62	0.55
		0	-	69	44	0.1	9	276	256	0.62	0.57

Table 5 - 6: Summary Static Analysis Results for Riser System (with Content-filled flowlines) supported by Conventional Buoy, at Near, Zero, and Far Vessel Offsets, with 0- and 100-year Currents

For empty flowlines situation, the result summary is presented below for cases 1, 2, and 3 (full results can be found in **Appendix C.1-21**).

Empty Flowlines											
				Flexible Jumpers		**Buoy Trim Angle**	**Maximum Values for SCRs**				
Case	Vessel Offset	Current Return Period	Current Direction	MBR	H_{min}		Hang-off Angle	Max. Von Mises Stress (Top)	Max. Von Mises Stress (Sagbend)	Von Mises Utilization (Top)	Von Mises Utilization (Sagbend)
	(m)	(yr)	(deg)	(m)	(m)	(deg)	(deg)	(MPa)	(MPa)		
1	-50	10	0	46	56	-2.1	12	50	221	0.11	0.49
		0	-	34	67	-1.7	9	53	147	0.12	0.33
2	0	10	0	65	44	-1.9	12	50	203	0.11	0.45
		0	-	50	56	-1.6	9	54	140	0.12	0.31
		10	180	39	65	-1.3	7	63	117	0.14	0.26
3	50	10	180	56	53	-1.2	8	64	115	0.14	0.26
		0	-	70	44	-1.4	10	54	133	0.12	0.30

Table 5 - 7: Summary Static Analysis Results for Riser System (with Empty flowlines) supported by Conventional Buoy, at Near, Zero, and Far Vessel Offsets, with 0- and 10-year Currents

Likewise, the result summary for empty flowlines condition for cases 4, 5, and 6 is as follows (full results can be found in **Appendix C.1-22**):

Empty Flowlines											
				Flexible Jumpers		Buoy Trim Angle	Maximum Values for SCRs				
Case	Vessel Offset	Current Return Period	Current Direction	MBR	H_min		Hang-off Angle	Max. Von Mises Stress (Top)	Max. Von Mises Stress (Sagbend)	Von Mises Utilization (Top)	Von Mises Utilization (Sagbend)
	(m)	(yr)	(deg)	(m)	(m)	(deg)	(deg)	(MPa)	(MPa)		
4	-30	100	0	56	49	-2.1	13	51	235	0.11	0.52
		0	-	40	63	-1.6	9	53	144	0.12	0.32
5	0	100	0	68	42	-2.0	13	51	221	0.11	0.49
		0	-	50	56	-1.6	9	54	140	0.12	0.31
		100	180	37	66	-1.2	7	65	115	0.15	0.26
6	30	100	180	46	60	-1.1	7	66	114	0.15	0.25
		0	-	61	49	-1.5	10	54	136	0.12	0.30

Table 5 - 8: Summary Static Analysis Results for Riser System (with Empty flowlines) supported by Conventional Buoy, at Near, Zero, and Far Vessel Offsets, with 0- and 100-year Currents

Result summary for flooded flowlines condition for cases 1, 2, and 3 is presented below (full results can be found in **Appendix C.1-27**).

Flooded Flowlines											
				Flexible Jumpers		Buoy Trim Angle	Maximum Values for SCRs				
Case	Vessel Offset	Current Return Period	Current Direction	MBR	H_min		Hang-off Angle	Max. Von Mises Stress (Top)	Max. Von Mises Stress (Sagbend)	Von Mises Utilization (Top)	Von Mises Utilization (Sagbend)
	(m)	(yr)	(deg)	(m)	(m)	(deg)	(deg)	(MPa)	(MPa)		
1	-50	10	0	62	45	1.5	9	79	228	0.18	0.51
		0	-	47	57	1.5	8	84	163	0.19	0.36
2	0	10	0	83	35	1.6	10	80	201	0.18	0.45
		0	-	65	46	1.6	8	85	151	0.19	0.34
		10	180	51	56	2.0	7	94	120	0.21	0.27
3	50	10	180	69	45	2.2	8	95	114	0.21	0.25
		0	-	87	35	1.8	9	87	138	0.19	0.31

Table 5 - 9: Summary Static Analysis Results for Riser System (with Flooded flowlines) supported by Conventional Buoy, at Near, Zero, and Far Vessel Offsets, with 0- and 10-year Currents

For cases 4, 5, and 6 pertaining to flooded flowlines condition, the results are summarized as follows (full results can be found in **Appendix C.1-28**):

| | | | | Flexible Jumpers | | | Maximum Values for SCRs | | | | |
Case	Vessel Offset	Current Return Period	Current Direction	MBR	H_{min}	Buoy Trim Angle	Hang-off Angle	Max. Von Mises Stress (Top)	Max. Von Mises Stress (Sagbend)	Von Mises Utilization (Top)	Von Mises Utilization (Sagbend)
	(m)	(yr)	(deg)	(m)	(m)	(deg)	(deg)	(MPa)	(MPa)		
4	-30	100	0	73	38	1.5	10	79	232	0.18	0.52
		0	-	54	53	1.6	8	84	158	0.19	0.35
5	0	100	0	87	32	1.6	10	80	214	0.18	0.48
		0	-	65	46	1.6	8	85	151	0.19	0.34
		100	180	49	58	2.1	7	95	116	0.21	0.26
6	30	100	180	59	52	2.3	8	96	113	0.21	0.25
		0	-	77	39	1.7	9	86	143	0.19	0.32

Table 5 - 10: Summary Static Analysis Results for Riser System (with Flooded flowlines) supported by Conventional Buoy, at Near, Zero, and Far Vessel Offsets, with 0- and 100-year Currents

The results in **Tables 5-5** to **5-10** above show that all the flowline internal conditions satisfy the minimum bend radius and H_{min} requirements of the flexible jumpers at all the considered vessel offset positions and the associated current return periods.

Comparisons of the buoy trim angles of all the flowline internal conditions when the vessel is at its nominal position with no current acting (i.e. cases 2 and 5 with no current acting for each flowline internal condition) shows that the oil-filled flowline condition (i.e. content flowlines) offers the best stability at this position with a trim angle of 0.0°, while the empty and flooded flowline conditions offer less stability with respective trim angles of -1.6° and 1.6°. This stability trend is also true for situations when the vessel is either at its near or far offset positions with all the considered current return periods (as seen in cases 1, 3, 4 and 6 for all the flowline internal conditions).

A look at the maximum Von Mises stress values at the top and sagbend areas shows that all the flowline internal conditions satisfy the steel catenary riser's maximum Von Mises stress requirements at all vessel offset positions with their associated current return periods. However, it can be seen that the Von Mises stress values at the top and sagbend regions for the content flowline internal condition is higher and closer to 300 MPa than those of the empty and flooded flowline internal conditions.

The above discussions show that the most important flowline internal condition with respect to the stability of the subsurface buoy and the strength performance of the steel catenary risers is the content flowline internal condition, and this will form the basis of subsequent dynamic analysis for the conventional buoy in this study.

5.1.4 Sensitivity to Drag Coefficient of the Buoy

The influence of variations in the drag coefficient of the buoy on the behaviours of the flexible jumpers, the steel catenary risers, and the buoy itself for each of the flowline internal fluid conditions considered in **section 5.1.3** is studied in this section. The study is carried out with the vessel at its near, nominal and far offset positions for three different buoy drag coefficient values as follows:

Analysis Parameters

- Drag coefficients of buoy (C_d)   1.2, 1.4, and 1.6
- Riser anchor length   1350 m
- Internal fluid condition of flowlines   Content, Empty, and Flooded
- Side spar length   21 m
- Added mass coefficient of buoy (C_a)
    - Main spar   0.741
    - Back spar   0.862
- Current and vessel offset cases
    - Case 1:
        - Vessel offset   Near position (-50 m)
        - Current return period   10 years
        - Current direction   0°
    - Case 2:
        - Vessel offset   Nominal position (0 m)
        - Current return period   10 years
        - Current direction   0°, 180°
    - Case 3:
        - Vessel offset   Far position (50 m)
        - Current return period   10 years
        - Current direction   180°
    - Case 4
        - Vessel offset   Near position (-30 m)
        - Current return period   100 years
        - Current direction   0°
    - Case 5
        - Vessel offset   Nominal position (0 m)
        - Current return period   100 years
        - Current direction   0°, 180°

- ▪ Case 6
  - ➢ Vessel offset   Far position (30 m)
  - ➢ Current return period   100 years
  - ➢ Current direction   180°

The following results were obtained for the content flowline internal fluid condition (full results can be found in **Appendices C.1-13** to **C.1-18**):

Content Flowlines with Buoy C_d = 1.2, and 10-year current										
Case	Vessel Offset	Current Return Period	Current Direction	Flexible Jumpers		Buoy		Maximum Values for SCRs			
				MBR	H_{min}	Buoy Trim Angle	Position Relative to Nominal with no current	Max. Von Mises Stress (Top)	Max. Von Mises Stress (Sagbend)	Von Mises Utilization (Top)	Von Mises Utilization (Sagbend)
	(m)	(yr)	(deg)	(m)	(m)	(deg)	(m)	(MPa)	(MPa)		
1	-50	10	0	53	51	-0.5	-51.65	274.58	293.30	0.61	0.65
2	0	10	0	73	40	-0.3	-30.58	274.83	282.27	0.61	0.63
		0	-	57	51	0.0	0	275.84	258.53	0.62	0.58
		10	180	45	61	0.3	33.51	277.82	248.19	0.62	0.55
3	50	10	180	63	49	0.4	49.20	278.10	246.81	0.62	0.55

Table 5 - 11: Summary Static Analysis Results for Riser System (with Content-filled flowlines) supported by Conventional Buoy with C_d = 1.2, at Near, Zero, and Far Vessel Offsets, with 10-year Current

Content Flowlines with Buoy C_d = 1.2, and 100-year current										
Case	Vessel Offset	Current Return Period	Current Direction	Flexible Jumpers		Buoy		Maximum Values for SCRs			
				MBR	H_{min}	Buoy Trim Angle	Position Relative to Nominal with no current	Max. Von Mises Stress (Top)	Max. Von Mises Stress (Sagbend)	Von Mises Utilization (Top)	Von Mises Utilization (Sagbend)
	(m)	(yr)	(deg)	(m)	(m)	(deg)	(m)	(MPa)	(MPa)		
4	-30	100	0	64	44	-0.5	-49.75	274.65	297.65	0.61	0.66
5	0	100	0	76	37	-0.4	-36.07	274.80	289.59	0.61	0.65
		0	-	57	51	0.0	0	275.84	258.53	0.62	0.58
		100	180	43	62	0.4	40.24	278.26	246.98	0.62	0.55
6	30	100	180	53	55	0.5	48.80	278.42	246.31	0.62	0.55

Table 5 - 12: Summary Static Analysis Results for Riser System (with Content-filled flowlines) supported by Conventional Buoy with C_d = 1.2, at Near, Zero, and Far Vessel Offsets, with 100-year Current

Content Flowlines with Buoy C_d = 1.4, and 10-year current											
Case	Vessel Offset	Current Return Period	Current Direction	Flexible Jumpers		Buoy		Maximum Values for SCRs			
				MBR	H_{min}	Buoy Trim Angle	Position Relative to Nominal with no current	Max. Von Mises Stress (Top)	Max. Von Mises Stress (Sagbend)	Von Mises Utilization (Top)	Von Mises Utilization (Sagbend)
	(m)	(yr)	(deg)	(m)	(m)	(deg)	(m)	(MPa)	(MPa)		
1	-50	10	0	54	50	-0.5	-52.55	274.57	293.82	0.61	0.66
2	0	10	0	74	39	-0.3	-31.36	274.80	282.62	0.61	0.63
		0	-	57	51	0.0	0	275.84	258.53	0.62	0.58
		10	180	44	61	0.3	34.50	277.84	248.10	0.62	0.55
3	50	10	180	62	49	0.5	50.08	278.12	246.74	0.62	0.55

Table 5 - 13: Summary Static Analysis Results for Riser System (with Content-filled flowlines) supported by Conventional Buoy with C_d = 1.4, at Near, Zero, and Far Vessel Offsets, with 10-year Current

Content Flowlines with Buoy C_d = 1.4, and 100-year current											
Case	Vessel Offset	Current Return Period	Current Direction	Flexible Jumpers		Buoy		Maximum Values for SCRs			
				MBR	H_{min}	Buoy Trim Angle	Position Relative to Nominal with no current	Max. Von Mises Stress (Top)	Max. Von Mises Stress (Sagbend)	Von Mises Utilization (Top)	Von Mises Utilization (Sagbend)
	(m)	(yr)	(deg)	(m)	(m)	(deg)	(m)	(MPa)	(MPa)		
4	-30	100	0	64	44	-0.5	-50.76	274.64	298.32	0.61	0.67
5	0	100	0	77	37	-0.4	-36.99	274.79	290.08	0.61	0.65
		0	-	57	51	0.0	0	275.84	258.53	0.62	0.58
		100	180	42	62	0.4	41.45	278.28	246.89	0.62	0.55
6	30	100	180	52	56	0.5	49.93	278.44	246.22	0.62	0.55

Table 5 - 14: Summary Static Analysis Results for Riser System (with Content-filled flowlines) supported by Conventional Buoy with C_d = 1.4, at Near, Zero, and Far Vessel Offsets, with 100-year Current

Content Flowlines with Buoy C_d = 1.6, and 10-year current											
Case	Vessel Offset	Current Return Period	Current Direction	Flexible Jumpers		Buoy		Maximum Values for SCRs			
				MBR	H_{min}	Buoy Trim Angle	Position Relative to Nominal with no current	Max. Von Mises Stress (Top)	Max. Von Mises Stress (Sagbend)	Von Mises Utilization (Top)	Von Mises Utilization (Sagbend)
	(m)	(yr)	(deg)	(m)	(m)	(deg)	(m)	(MPa)	(MPa)		
1	-50	10	0	54	50	-0.5	-53.45	274.56	294.33	0.61	0.66
2	0	10	0	74	39	-0.3	-32.14	274.82	283.03	0.61	0.63
		0	-	57	51	0.0	0	275.84	258.53	0.62	0.58
		10	180	44	61	0.3	35.49	277.86	248.00	0.62	0.55
3	50	10	180	62	50	0.5	50.96	278.14	246.68	0.62	0.55

Table 5 - 15: Summary Static Analysis Results for Riser System (with Content-filled flowlines) supported by Conventional Buoy with C_d = 1.6, at Near, Zero, and Far Vessel Offsets, with 10-year Current

Content Flowlines with Buoy C_d = 1.6, and 100-year current											
Case	Vessel Offset	Current Return Period	Current Direction	Flexible Jumpers		Buoy		Maximum Values for SCRs			
				MBR	H_{min}	Buoy Trim Angle	Position Relative to Nominal with no current	Max. Von Mises Stress (Top)	Max. Von Mises Stress (Sagbend)	Von Mises Utilization (Top)	Von Mises Utilization (Sagbend)
	(m)	(yr)	(deg)	(m)	(m)	(deg)	(m)	(MPa)	(MPa)		
4	-30	100	0	65	43	-0.5	-51.76	274.63	298.98	0.61	0.67
5	0	100	0	78	36	-0.4	-37.89	274.78	290.58	0.61	0.65
		0	-	57	51	0.0	0	275.84	258.53	0.62	0.58
		100	180	42	63	0.4	42.65	278.30	246.79	0.62	0.55
6	30	100	180	52	56	0.5	51.07	278.46	246.14	0.62	0.55

Table 5 - 16: Summary Static Analysis Results for Riser System (with Content-filled flowlines) supported by Conventional Buoy with C_d = 1.6, at Near, Zero, and Far Vessel Offsets, with 100-year Current

With respect to the 10-year current, **Tables 5-11**, **5-13**, and **5-15** show that the minimum bend radius and H_{min} values of the flexible jumpers, and the buoy trim angle for each of the study cases (i.e. cases 1 to 3) remain fairly constant over the considered buoy drag coefficient values, and the values satisfy the design criteria given in **section 4.4**.

The Von Mises stress values of the steel catenary risers also remain fairly constant for corresponding load cases over the studied buoy drag coefficient values, with less than 1% increase and decrease in maximum Von Mises stress values (sagbend) experienced respectively at the near (cases 1 and 4) and far (cases 3 and 6) vessel positions over the considered buoy drag coefficient values. The same trend is witnessed for the maximum Von Mises stress values at the hang-off region, with less than 1% decrease and increase experienced respectively at the near and far vessel positions (see **Table 5-17** below). It should be noted that all these values satisfy the design acceptance criteria as given in **section 4.4**.

Comparison of the values for the position of the buoy when the vessel is at its near and far offset positions with that when the vessel is at its nominal position (with no current) shows that the relative horizontal displacement (designated as the "position relative to the nominal with no current" on the tables above) of the buoy slightly increases as the drag coefficient of the buoy increases. This is as anticipated because the amount of drag a body experiences is proportional to its drag coefficient.

All these observations also hold for the 100-year current (see **Tables 5-12**, **5-14**, and **5-16**).

Based on the above observations, a drag coefficient value of 1.4 can be adopted for the conventional buoy in this design analysis.

Content Flowlines with C_d = 1.2, 1.4, and 1.6					
Case	Buoy Drag Coefficient	Vessel Offset	Position Relative to Nominal	Max. Von Mises Stress (Top)	Max. Von Mises Stress (Sagbend)
		(m)	(m)	(MPa)	(MPa)
1	1.2	-50	-51.65	274.58	293.30
	1.4		-52.55 (+1.74%)	274.57 (-0.004%)	293.82 (+0.18%)
	1.6		-53.45 (+1.71%)	274.56 (-0.004%)	294.33 (+0.17%)
3	1.2	50	49.20	278.10	246.81
	1.4		50.08 (+1.79%)	278.12 (+0.007%)	246.74 (-0.03%)
	1.6		50.96 (+1.76%)	278.14 (+0.007%)	246.68 (-0.02%)
4	1.2	-30	-49.75	274.65	297.65
	1.4		-50.76 (+2.03)	274.64 (-0.004%)	298.32 (+0.23%)
	1.6		-51.76 (+1.97)	274.63 (-0.004%)	298.98 (+0.22%)
6	1.2	30	48.80	278.42	246.31
	1.4		49.93 (+2.32%)	278.44 (+0.007%)	246.22 (-0.04%)
	1.6		51.07 (+2.28%)	278.46 (+0.007%)	246.14 (-0.03%)

Table 5 - 17: Comparison of Summary Static Analysis Results for Riser System (with Content-filled flowlines) supported by Conventional Buoy with C_d = 1.2, 1.4, and 1.6

The following plots further explain the results in **Table 5-17:**
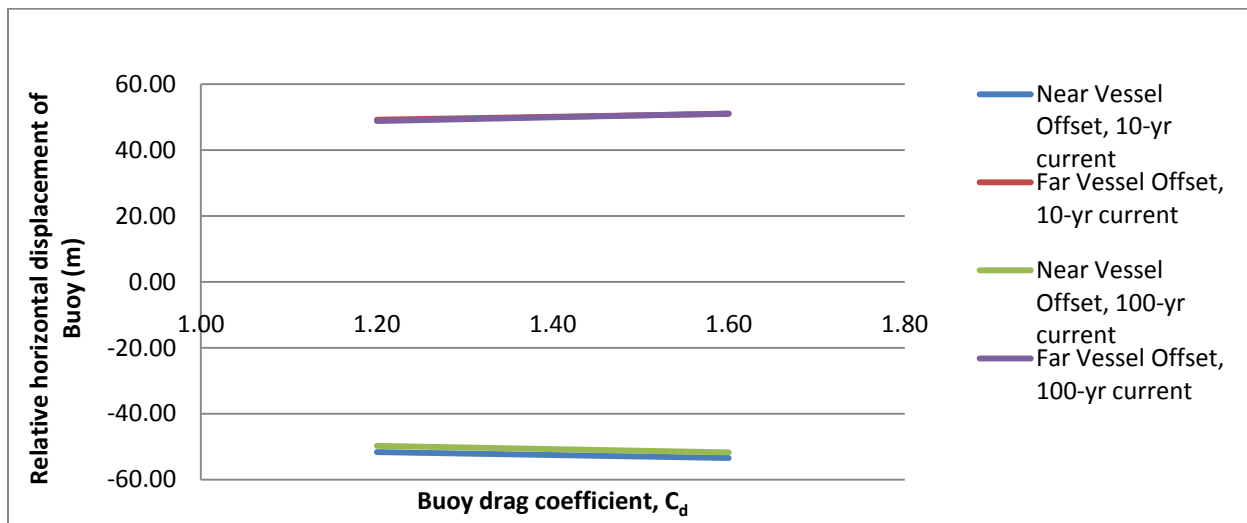
Figure 5 - 9: Relationship between Relative Horizontal Displacement of Conventional Buoy and its Drag Coefficient at Near and Far Vessel Offsets with 10- and 100-year Currents
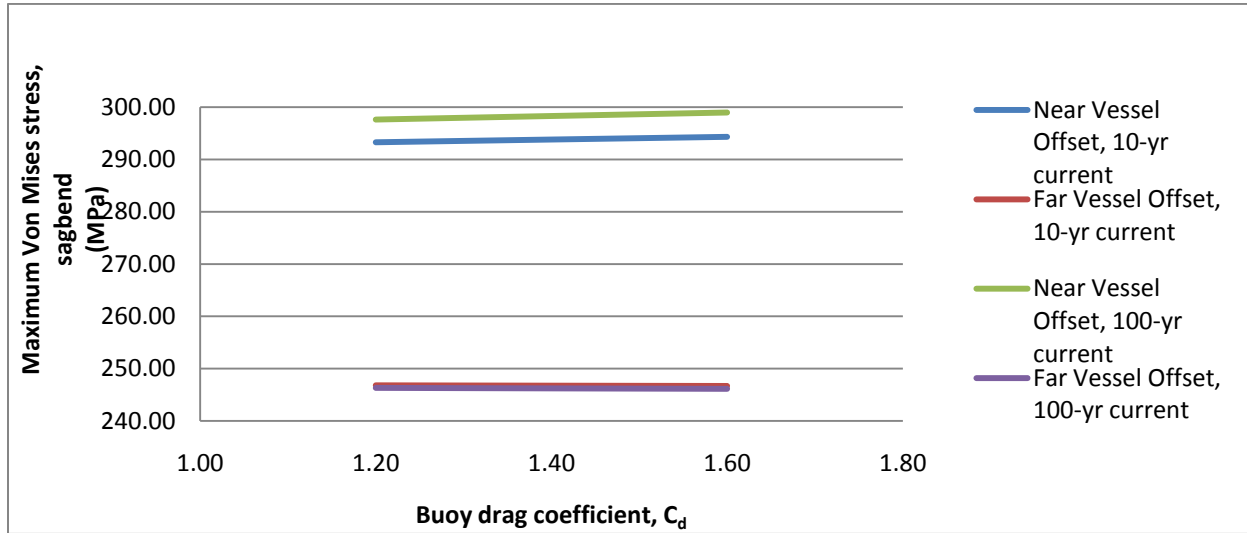
Figure 5 - 10: Relationship between Maximum Von Mises Stress at Sagbend of SCRs and Drag Coefficient of Conventional Buoy, at Near and Far Vessel Offsets with 10- and 100-year Currents
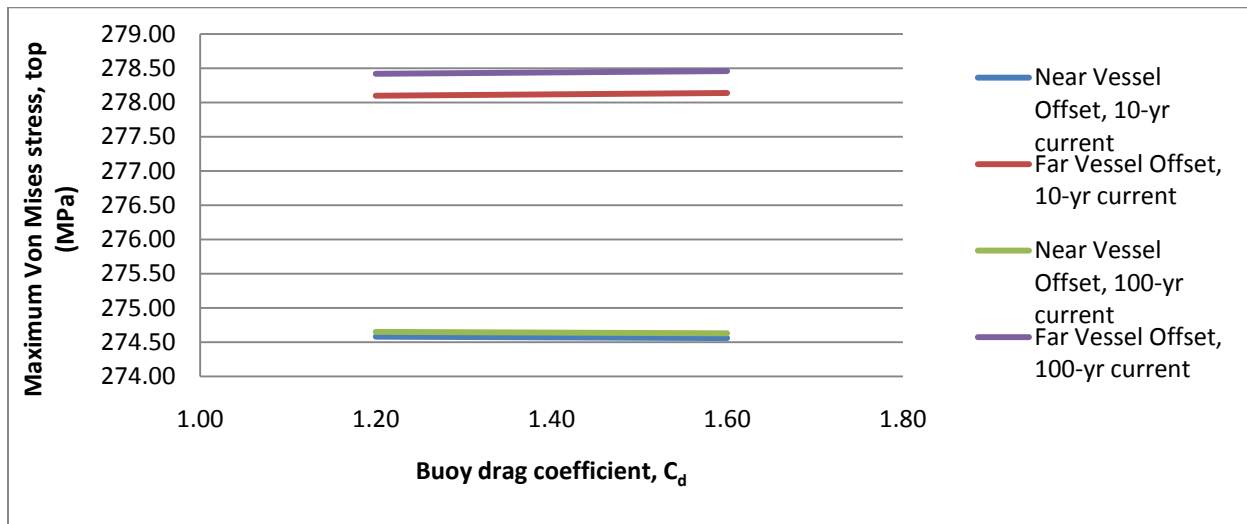
Figure 5 - 11: Relationship between Maximum Von Mises Stress at Top region of SCRs and Drag Coefficient of Conventional Buoy, at Near and Far Vessel Offsets with 10- and 100-year Currents

Similar trends are observed for flooded and empty flowline scenarios with respect to the minimum bend radius and H_{min} of the flexible jumpers, the trim angle and relative horizontal displacement of the buoy, and the maximum Von Mises stress values at the top and sagbend regions of the steel catenary risers. **Tables 5-18** and **5-19** below present a summary of results obtained for the empty and flooded flowline scenarios (full results can be found in **Appendices C.1-19** to **C.1-30**).

Empty Flowlines with C_d = 1.2, 1.4, and 1.6					
Case	Buoy Drag Coefficient	Vessel Offset	Position Relative to Nominal	Max. Von Mises Stress (Top)	Max. Von Mises Stress (Sagbend)
		(m)	(m)	(MPa)	(MPa)
1	1.2	-50	-51.38	49.89	220.41
	1.4		-52.36 (+1.91%)	49.86 (-0.06%)	221.48 (+0.49%)
	1.6		-53.34 (+1.87%)	49.84 (-0.04%)	222.38 (+0.41%)
3	1.2	50	48.74	63.99	115.14
	1.4		49.68 (+1.93%)	64.04 (+0.08%)	115.01 (-0.11%)
	1.6		50.63 (+1.91%)	64.09 (+0.09%)	114.88 (-0.11%)
4	1.2	-30	-51.12	50.61	233.92
	1.4		-52.22 (+2.15%)	50.58 (-0.06%)	235.08 (+0.50%)
	1.6		-53.32 (+2.11%)	50.56 (-0.04%)	236.38 (+0.55%)
6	1.2	30	49.67	65.65	113.89
	1.4		50.87 (+2.42%)	65.71 (+0.09%)	113.74 (-0.13%)
	1.6		52.08 (+2.38%)	65.77 (+0.09%)	113.60 (-0.12%)

Table 5 - 18: Comparison of Summary Static Analysis Results for Riser System (with Empty flowlines) supported by Conventional Buoy with C_d = 1.2, 1.4, and 1.6

Flooded Flowlines with C_d = 1.2, 1.4, and 1.6					
Case	Buoy Drag Coefficient	Vessel Offset	Position Relative to Nominal	Max. Von Mises Stress (Top)	Max. Von Mises Stress (Sagbend)
		(m)	(m)	(MPa)	(MPa)
1	1.2	-50	-51.87	79.07	226.74
	1.4		-52.68 (+1.56%)	79.03 (-0.05%)	227.65 (+0.40%)
	1.6		-53.50 (+1.56%)	78.99 (-0.05%)	228.58 (+0.41%)
3	1.2	50	49.84	94.99	114.61
	1.4		50.65 (+1.63%)	95.06 (+0.07%)	114.36 (-0.22%)
	1.6		51.47 (+1.62%)	95.12 (+0.06%)	114.10 (-0.23%)
4	1.2	-30	-48.21	79.39	231.16
	1.4		-49.10 (+1.85%)	79.34 (-0.06%)	232.21 (+0.45%)
	1.6		-50.00 (+1.83%)	79.30 (-0.05%)	233.43 (+0.53%)
6	1.2	30	48.03	95.99	113.45
	1.4		49.09 (+2.21%)	96.08 (+0.09%)	113.13 (-0.28%)
	1.6		50.16 (+2.18%)	96.17 (+0.09%)	112.81 (-0.28%)

Table 5 - 19: Comparison of Summary Static Analysis Results for Riser System (with Flooded flowlines) supported by Conventional Buoy with C_d = 1.2, 1.4, and 1.6

Comparison of **Tables 5-17**, **5-18**, and **5-19** affirms the discussion in **section 5.1.3** that the Von Mises stress values of the content-filled steel catenary risers approach 300 MPa faster than those in empty or flooded conditions. Thus, the content-filled situation will form the basis of subsequent dynamic analysis for the conventional buoy in this study.

5.2 Design Analysis of Steel Catenary Risers supported by Conventional Buoy (Dynamic Analysis)

Here, the content-filled flowlines scenario studied in **section 5.1.3** will be subjected to dynamic analysis, firstly, by keeping the added mass coefficients of the main and back spars of the conventional buoy fixed (i.e. using the same values they had in the static analysis). This will be called base case dynamic analysis. It will then be subjected to sensitivity analysis by varying the added mass coefficient values of the main and back spars of the buoy. Also, the influence of reduction in submerged weight of the buoy due to water ingress will be studied.

5.2.1 Base Case Dynamic Analysis for Conventional Buoy

Table 5-5 of **section 5.1.3** shows that the most critical of the static analysis results of the content-filled flowlines scenario are case 1 (with 10-year current) and case 3 (with 10-year current). This is because the Von Mises stress values at the sagbend region for case 1 (with current) and that at the top region for case 3 (with current) are the highest of all the different vessel offsets considered. The same also holds for case 4 (with 100-year current) and case 6 (with 100-year current) of **Table 5-6**. Thus, these cases will be subjected to dynamic analysis as follows:

Analysis Parameters (with 10-year current + 100-year wave)

Load Case 1:

- Vessel offset   Near position (-50 m)
- Environmental load combination   10-year current + 100-year wave
- Environmental load direction   0°

Load Case 3:

- Vessel offset   Far position (50 m)
- Environmental load combination   10-year current + 100-year wave
- Environmental load direction   180°

Below are tables with summaries of key static and dynamic analysis results for the steel catenary risers, flexible jumpers, and the buoy (full dynamic analysis results can be found in **Appendices C.2-1** and **C.2-2**).

Load Case	Static Analysis				Dynamic analysis					
	Max. Von Mises Stress		Max. Von Mises Utilization		Max. Von Mises Stress		Max. Von Mises Utilization		Max. Buckling Utilization	
	Top	Sagbend	Top	Sagbend	Top	Sagbend	Top	Sagbend	Top	Sagbend
	(MPa)				(MPa)					
1	274.57	293.82	0.61	0.66	275.49	302.85	0.61	0.68	0.11	0.61
3	278.12	246.74	0.62	0.55	278.60	247.32	0.62	0.55	0.12	0.28

Table 5 - 20: Base Case Static and Dynamic Analysis Results for SCRs with 10-yr Current + 100-yr Wave – Conventional Buoy

Load Case	Static Analysis	Dynamic Analysis	
	Minimum Bend Radius	Minimum Bend Radius	Minimum Tension
	(m)	(m)	(kN)
1	54	40	19
3	62	56	84

Table 5 - 21: Base Case Static and Dynamic Analysis Results for Flexible Jumpers with 10-yr Current + 100-yr Wave – Conventional Buoy

Load Case	Static Analysis			Dynamic Analysis						
	Trim Angle	Relative Vertical Displacement	Relative Horizontal Displacement	Trim Angle			Relative Vertical Displacement		Relative Horizontal Displacement	
				Min	Max	Variation	Min	Max	Min	Max
	(deg)	(m)	(m)	(deg)	(deg)	(deg)	(m)	(m)	(m)	(m)
1	-0.48	-2.79	-52.55	-0.85	-0.09	0.76	-3.38	-2.60	-58.73	-51.85
3	0.45	0.54	50.08	0.07	0.83	0.76	0.34	0.71	49.11	54.35

Table 5 - 22: Base Case Static and Dynamic Analysis Results for Buoy with 10-yr Current + 100-yr Wave – Conventional Buoy

The dynamics results of the steel catenary risers presented in **Table 5-20** show that the Von Mises stresses at the top and sagbend areas of the risers does not increase much in comparison with the static analysis results when the risers are subjected to combined environmental loads (i.e. wave and current loads). The Von Mises utilization factors are well below the 0.8 limit required by design codes (and also given in **section 4.4**). Also, the buckling utilization factors being less than one satisfy the design requirement. This implies usage of the conventional buoy helped to reduce the amount of stresses experienced by the risers, particularly at the sagbend area which is the most critical region with respect to buckling issues.

The dynamic results of the flexible jumpers show that although the minimum bend radius of the flexible jumpers reduced when the flowlines were subjected to dynamic environmental loads, the resultant values are still greater than the acceptance limit for minimum bend radius with

respect to static analysis (i.e. 25 m), and compression is not recorded along the jumpers. This suggests the results are acceptable.

Furthermore, the dynamic results in **Table 5-22** buoy show that the trim angle, relative vertical and horizontal displacements of the buoy do not increase much as a result of application of dynamic environmental loads when compared with the static results.

Similar analysis is done for the 100-year current as follows:

Analysis Parameters (with 100-year current + 10-year wave)

Load Case 4:

- Vessel offset   Near position (-30 m)
- Environmental load combination   100-year current + 10-year wave
- Environmental load direction   0°

Load Case 6:

- Vessel offset   Far position (30 m)
- Environmental load combination   100-year current + 10-year wave
- Environmental load direction   180°

Summaries of key static and dynamic analysis results obtained for load cases 4 and 6 are presented below (full dynamic analysis results can be found in **Appendices C.2-3** and **C.2-4**):

Load Case	Static Analysis				Dynamic analysis					
	Max. Von Mises Stress		Max. Von Mises Utilization		Max. Von Mises Stress		Max. Von Mises Utilization		Max. Buckling Utilization	
	Top	Sagbend	Top	Sagbend	Top	Sagbend	Top	Sagbend	Top	Sagbend
	(MPa)				(MPa)					
4	274.64	298.32	0.61	0.67	275.61	306.48	0.62	0.68	0.11	0.64
6	278.44	246.22	0.62	0.55	278.84	246.65	0.62	0.55	0.12	0.27

Table 5 - 23: Base Case Static and Dynamic Analysis Results for SCRs with 100-yr Current + 10-yr Wave – Conventional Buoy

Load Case	Static Analysis	Dynamic Analysis	
	Minimum Bend Radius	Minimum Bend Radius	Minimum Tension
	(m)	(m)	(kN)
4	64	46	38
6	52	48	77

Table 5 - 24: Base Case Static and Dynamic Analysis Results for Flexible Jumpers with 100-yr Current + 10-yr Wave – Conventional Buoy

Load Case	Static Analysis			Dynamic Analysis						
	Trim Angle	Relative Vertical Displacement	Relative Horizontal Displacement	Trim Angle			Relative Vertical Displacement		Relative Horizontal Displacement	
				Min	Max	Variation	Min	Max	Min	Max
	(deg)	(m)	(m)	(deg)	(deg)	(deg)	(m)	(m)	(m)	(m)
4	-0.47	-2.66	-50.76	-0.73	-0.14	0.59	-3.15	-2.52	-55.84	-50.22
6	0.47	0.51	49.93	0.17	0.74	0.57	0.37	0.64	49.19	52.77

Table 5 - 25: Base Case Static and Dynamic Analysis Results for Buoy with 100-yr Current + 10-yr Wave – Conventional Buoy

 Just like what was obtained for 10-year current + 100-year wave, load cases 4 and 6 for 100-yr current + 10-year wave show that the Von Mises stresses at the top and sagbend regions of the steel catenary risers only increase slightly (in comparison with the static analysis result) when dynamic environmental loads are applied to the risers. The Von Mises utilization factors are also below 0.8 which implies the Von Mises acceptance criterion is fulfilled. Also, the buckling check criterion is satisfied since the maximum buckling utilization values are less than 1.0.

Also, it can be seen that the minimum bend radius values of the flexible jumpers still satisfy the requirement for static analysis (which implies the requirement for dynamic analysis will also be satisfied since the limiting value for minimum bend radius in dynamic analysis will in reality be less than that in static analysis). In addition, there is no compression along the flexible jumpers.

Furthermore, **Table 5-25** shows that the trim angle, relative vertical and horizontal dynamic displacements of the buoy do not differ much from those obtained from static analysis.

In summary, the dynamic analysis results for the 10-year current + 100-year wave and 100-year current + 10-year wave show that the riser system under study satisfies the design acceptance criteria given in **section 4.4**.

5.2.2 Sensitivity to Added Mass Coefficient of Conventional Buoy
Here, the influence of 20 percent reduction and increase in the added mass coefficients of the main and back spars of the conventional buoy on the strength performance of the flowlines and the stability of the buoy is studied. The load cases considered in **section 5.2.1** are considered in addition to the new added mass coefficients of the buoy. Thus, the analysis is done as follows:

 New Buoy Added Mass Coefficient values

- 20% reduction in added mass coefficient of buoy
    - Main spar   0.593
    - Back spar   0.690
- 20% increase in added mass coefficient of buoy
    - Main spar   0.889

▪ Back spar   1.034

Tables 5-26 to **5-28** below present comparisons of the dynamic analysis results for the 20% buoy added mass coefficient reduction, base case added mass, and 20% buoy added mass coefficient increase.

Load Case	Buoy Added Mass Coefficient (C_a)	Max. Von Mises Stress		Max. Von Mises Utilization	
		Top	Sagbend	Top	Sagbend
		(MPa)			
1	20% lower	275.58	303.17	0.62	0.68
	Base Case	275.49	302.85	0.61	0.68
	20% higher	275.41	302.58	0.61	0.68
3	20% lower	278.64	247.25	0.62	0.55
	Base Case	278.60	247.32	0.62	0.55
	20% higher	278.57	247.38	0.62	0.55
4	20% lower	275.64	306.35	0.62	0.68
	Base Case	275.61	306.48	0.62	0.68
	20% higher	275.48	306.01	0.61	0.68
6	20% lower	278.87	246.61	0.62	0.55
	Base Case	278.84	246.65	0.62	0.55
	20% higher	278.80	246.69	0.62	0.55

Table 5 - 26: Sensitivity of Strength Performance of SCRs to Variations in Added Mass Coefficient of Conventional Buoy

Load Case	Buoy Added Mass Coefficient (C_a)	Minimum Bend Radius	Minimum Tension
		(m)	(kN)
1	20% lower	40	20
	Base Case	40	19
	20% higher	40	18
3	20% lower	56	84
	Base Case	56	84
	20% higher	56	83
4	20% lower	47	39
	Base Case	46	38
	20% higher	46	37
6	20% lower	48	77
	Base Case	48	77
	20% higher	48	77

Table 5 - 27: Sensitivity of Strength Performance of Flexible Jumpers to Variations in Added Mass Coefficient of Conventional Buoy

Load Case	Buoy Added Mass Coefficient (C_A)	Trim Angle Variation	Relative Vertical Displacement		Relative Horizontal Displacement	
			Min	Max	Min	Max
		(deg)	(m)	(m)	(m)	(m)
1	20% lower	0.73 (-3.94%)	-3.40 (0.59%)	-2.61 (0.38%)	-58.92 (0.32%)	-51.84 (-0.02%)
	Base Case	0.76	-3.38	-2.60	-58.73	-51.85
	20% higher	0.79 (3.94%)	-3.37 (-0.30%)	-2.60 (0.00%)	-58.55 (-0.31%)	-51.86 (0.02%)
3	20% lower	0.70 (-7.89%)	0.35 (2.94%)	0.69 (-2.82%)	49.13 (0.04%)	54.38 (0.06%)
	Base Case	0.76	0.34	0.71	49.11	54.35
	20% higher	0.82 (7.89%)	0.32 (-5.88%)	0.73 (2.82%)	49.09 (-0.04)	54.32 (-0.06%)
4	20% lower	0.57 (-3.39%)	-3.14 (-0.32%)	-2.52 (0.00%)	-55.68 (-0.29%)	-50.19 (-0.06%)
	Base Case	0.59	-3.15	-2.52	-55.84	-50.22
	20% higher	0.64 (8.47%)	-3.12 (-0.95%)	-2.51 (-0.40%)	-55.44 (-0.72%)	-50.18 (-0.08%)
6	20% lower	0.54 (-5.26%)	0.38 (2.70%)	0.63 (-1.56%)	49.19 (0.00%)	52.79 (0.04%)
	Base Case	0.57	0.37	0.64	49.19	52.77
	20% higher	0.62 (8.77%)	0.35 (-5.41%)	0.65 (1.56%)	49.19 (0.00%)	52.75 (-0.04%)

Table 5 - 28: Sensitivity of Stability and Motions of Conventional Buoy to Variations in its Added Mass Coefficient

Comparisons of the dynamic results of the steel catenary risers at the top and sagbend areas of the risers (**Table 5-26**) shows that the maximum Von Mises utilization factors remain fairly constant as the added mass coefficient of the conventional buoy increases for each load case. This implies changing the added mass of the buoy has negligible effect on the strength performance of the SCRs.

A look at the dynamic results of the flexible jumpers (**Table 5-27**) also reveals that the minimum bend radius and minimum tension for each load case stays almost unchanged as the added mass coefficient of the conventional buoy changes. This suggests that varying the added mass coefficient of the buoy has very minute influence on the strength performance of the jumpers.

Furthermore, the dynamic results of the buoy (**Table 5-28**) also show that the buoy trim angle, relative vertical and horizontal displacements do not change much when the buoy added mass coefficient is reduced or increased. In effect, the influence of added mass variation on the stability of the buoy is neglibible.

In summary, increasing or reducing the added mass of the buoy has very minor impact on the strength performance of the flowlines and the stability of the conventional buoy.

5.2.3 Reduction in Submerged Weight of Conventional Buoy due to Water Ingress

In this section, the influence of reduction in submerged weight of the conventional buoy on the strength performance of the flowlines and the stability of the buoy is studied. The buoy is idealized as being compartmentalized and a 4 m long section of the main spar of the buoy is

assumed to experience water breakthrough which leads to 10 percent reduction in the submerged weight of the main spar. This reduces the submerged weight of the buoy from -1800.60 tonnes to -1696.3 tonnes (calculations are presented in **Appendix B.5**). The 4 m long section is taken from one of the ends of the main spar (see **B.5-1** in **Appendix B.5**).

This study is carried out based on load cases 1, 3, 4, and 6 of **section 5.2.1** with respect to accidental limit state (ALS) considerations. Presented below are the dynamic analysis results for load cases 1 and 3 (full dynamic analysis results can be found in **Appendices C.2-5** and **C.2-6**).

Load Case	Dynamic analysis					
	Max. Von Mises Stress		Max. Von Mises Utilization		Max. Buckling Utilization	
	Top	Sagbend	Top	Sagbend	Top	Sagbend
	(MPa)					
1	275.44	305.96	0.61	0.68	0.11	0.53
3	278.56	247.34	0.62	0.55	0.11	0.26

Table 5 - 29: Strength Performance of SCRs due to reduction in Submerged Weight of Conventional Buoy, with 10-yr Current + 100-yr Wave

| Load Case | Dynamic Analysis | |
| | Minimum Bend Radius | Minimum Tension |
	(m)	(kN)
1	41	16
3	56	84

Table 5 - 30: Strength Performance of Flexible Jumpers due to reduction in Submerged Weight of Conventional Buoy, with 10-yr Current + 100-yr Wave

Load Case	Dynamic Analysis						
	Trim Angle			Relative Vertical Displacement		Relative Horizontal Displacement	
	Min	Max	Variation	Min	Max	Min	Max
	(deg)	(deg)	(deg)	(m)	(m)	(m)	(m)
1	0.00	0.76	0.76	-3.69	-2.90	-61.16	-54.22
3	0.84	1.61	0.77	0.38	0.75	51.48	56.66

Table 5 - 31: Stability and Motions of Conventional Buoy due to reduction in its Submerged Weight, with 10-yr Current + 100-yr Wave

The dynamic results of the steel catenary risers show that the maximum Von Mises utilization factors at the top and sagbend areas of the riser are below 1.0 (which is the Von Mises acceptance limit for accidental limit state) for the two load cases considered. Also, the maximum buckling utilization factors are less than 1.0. This implies the SCRs exhibit satisfactory strength performance at the considered vessel offsets under the influence of reduced buoy submerged weight.

In addition, the dynamic results of the flexible jumpers show that no compression is observed along the length of the flexible jumpers, and the observed minimum bend radius values are less than the 5 m acceptance limit.

Also, the trim angle, relative vertical and horizontal displacements of the buoy are quite similar to those obtained in **Table 5-22** of **section 5.2.1** for the ULS scenario.

Similarly, results for load cases 4 and 6 are presented below (full dynamic analysis results can be found in **Appendices C.2-7** and **C.2-8**).

Load Case	Dynamic analysis					
	Max. Von Mises Stress		Max. Von Mises Utilization		Max. Buckling Utilization	
	Top	Sagbend	Top	Sagbend	Top	Sagbend
	(MPa)					
4	275.60	309.66	0.62	0.69	0.11	0.55
6	278.79	246.67	0.62	0.55	0.11	0.25

Table 5 - 32: Strength Performance of SCRs due to reduction in Submerged Weight of Conventional Buoy, with 100-yr Current + 10-yr Wave

Load Case	Dynamic Analysis	
	Minimum Bend Radius	Minimum Tension
	(m)	(kN)
4	46	35
6	47	77

Table 5 - 33: Strength Performance of Flexible Jumpers due to reduction in Submerged Weight of Conventional Buoy, with 100-yr Current + 10-yr Wave

Load Case	Dynamic Analysis						
	Trim Angle			Relative Vertical Displacement		Relative Horizontal Displacement	
	Min	Max	Variation	Min	Max	Min	Max
	(deg)	(deg)	(deg)	(m)	(m)	(m)	(m)
4	0.12	0.72	0.60	-3.43	-2.78	-57.87	-52.15
6	0.96	1.55	0.59	0.40	0.67	51.60	55.13

Table 5 - 34: Stability and Motions of Conventional Buoy due to reduction in its Submerged Weight, with 100-yr Current + 10-yr Wave

Just like what was obtained for load cases 1 and 3, the dynamic results in **Tables 5-32** to **5-34** above show that the steel catenary risers fulfill the maximum Von Mises and buckling acceptance criteria, the flexible jumpers will also experience no compression and they satisfy the minimum bend radius acceptance criterion, and the buoy motions are quite similar to those of **Table 5-25** in **section 5.2.1**.

In summary, the riser system behaves satisfactorily with respect to the buoy submerged weight studied.

5.3 Design Analysis of Steel Catenary Risers supported by H-shaped Buoy (Static Analysis)

Studies similar to those carried out in **section 5.1** using the conventional buoy are done here with the H-shaped buoy. These are as follows:

5.3.1 Sensitivity to Offset of the Main Spar relative to the mid-length of its Side Spars

This determines the trim angle of the buoy and its eventual stability. Seven different offset positions are studied as follows:

Analysis Parameters

- Offset of main spar   -5, -4, -3, -2, -1, 0, and 1 m
- Riser anchor length   1320 m
- Internal content of flowlines   Oil
- Drag coefficient of buoy (C_d)   1.4
- Added mass coefficient of buoy (C_a)
    - Main spar   0.801
    - Side spar   0.150
- Vessel offset   Nominal position (0 m)
- Current case   No current

Note that negative main spar offset values imply distances to the left of the mid-length position of the side spars, while the positive main spar offset value was measured to the right of the mid-length position of the side spars.

Presented below is a summary of results obtained for the seven main spar offset positions (full results can be found in **Appendix C.1-31**).

Main Spar Offset	Flexible Jumpers			Hang-off Angle	Maximum Values for SCRs			
	Minimum Bend Radius (MBR)	H_{min}	Buoy Trim Angle		Max. Von Mises Stress (Top)	Max. Von Mises Stress (Sagbend)	Von Mises Utilization (Top)	Von Mises Utilization (Sagbend)
(m)	(m)	(m)	(deg)	(deg)	(MPa)	(MPa)		
-5.0	57	52	-0.3	9	276	259	0.62	0.58
-4.0	57	52	0.0	9	276	259	0.62	0.58
-3.0	57	51	0.3	9	276	259	0.62	0.58
-2.0	57	51	0.6	9	276	259	0.62	0.58
-1.0	57	51	0.9	9	276	259	0.62	0.58
0.0	58	51	1.3	9	276	259	0.62	0.58
1.0	58	51	1.6	9	276	259	0.62	0.58

Table 5 - 35: Summary Static Analysis Results for Main Spar Offset Variation, at Zero Vessel Offset and No Current

In addition to the fact that **Table 5-35** above shows that changing the offset position of the main spar relative to the mid-length of its side spars does not significantly change the minimum bend radius and H_{min} of the flexible jumpers, and the hang-off angle and Von Mises stress values at the top and sagbend regions of the steel catenary risers, it also shows that these values satisfy the design acceptance criteria given in **section 4.4.** However, the buoy trim angles change significantly as the offset position of the main spar changes, with the most stable buoy configuration being when the main spar offset is -4.0 m since it gives a buoy trim angle of 0.0°. Thus, -4.0 m main spar offset will be used in subsequent analysis with respect to the H-shaped buoy.

A plot of the buoy trim angles is presented below.
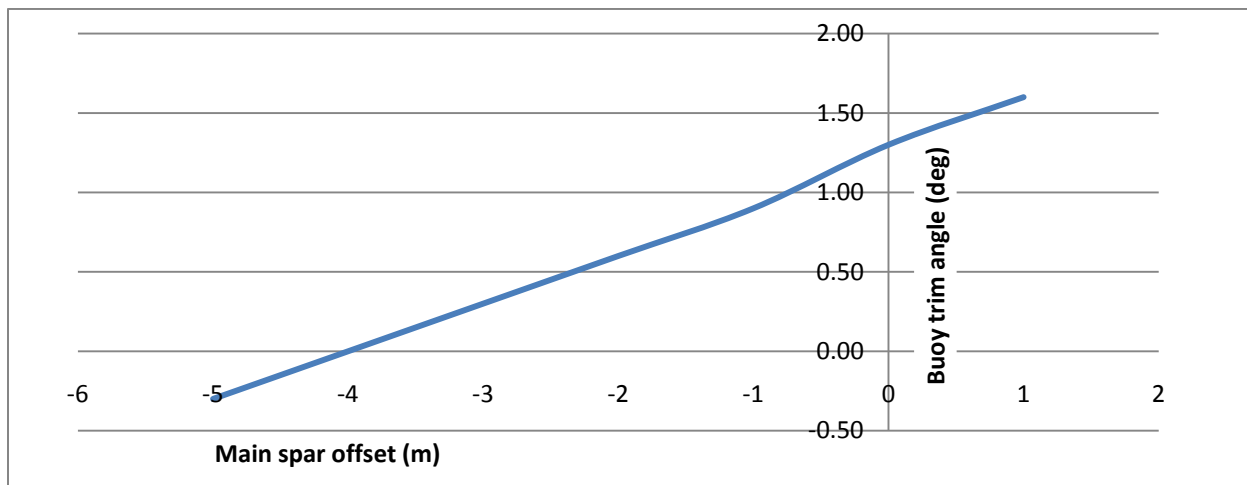
Figure 5 - 12: Relationship between Trim angle of H-shaped Buoy and its Main Spar Offset, at Zero Vessel Offset and No Current

5.3.2 Sensitivity to Riser Anchor Length

Just as the case was for the conventional buoy, five riser anchor lengths are studied with respect to the H-shaped buoy as follows:

Analysis Parameters

- Riser anchor length   1270, 1320, 1350, 1400, and 1450 m
- Offset of main spar   -4 m
- Internal content of flowlines   Oil
- Drag coefficient of buoy (C_d)   1.4
- Added mass coefficient of buoy (C_a)
  - Main spar   0.801
  - Side spar   0.150
- Vessel offset   Nominal position (0 m)
- Current case   No current

The following results were obtained for the five riser anchor lengths (full results are presented in **Appendix C.1-32**):

Riser Anchor Length	Flexible Jumpers		Buoy Trim Angle	Maximum Values for SCRs					
	Minimum Bend Radius (MBR)	H_{min}		Hang-off Angle	Top Tension (Tension at Buoy)	Max. Von Mises Stress (Top)	Max. Von Mises Stress (Sagbend)	Von Mises Utilization (Top)	Von Mises Utilization (Sagbend)
(m)	(m)	(m)	(deg)	(deg)	(kN)	(MPa)	(MPa)		
1270	49	57	0.0	7	1468	275	268	0.61	0.60
1320	57	52	0.0	9	1506	276	259	0.62	0.58
1350	62	48	0.0	10	1531	276	255	0.62	0.57
1400	72	42	0.0	11	1577	276	250	0.62	0.56
1450	84	35	0.0	13	1628	277	247	0.62	0.55

Table 5 - 36: Summary Static Analysis Results for Riser Anchor Length Variation at Zero Vessel Offset and No Current – H-shaped Buoy

The results above follow the same trend as the corresponding results obtained for the conventional buoy in **section 5.1.2**. The top tension of the steel catenary risers increases as the riser anchor length increases, leading to higher values of Von Mises stress at the top region when compared with those at the sagbend region. These Von Mises stress values (top and sagbend regions) together with the minimum bend radius and H_{min} values of the flexible jumpers are within the limits of the design acceptance criteria.

Although the buoy is stable (with 0.0° trim angle) for all the riser anchor lengths checked, only the 1320 m riser anchor length satisfies the hang-off angle acceptance criterion for the steel

catenary risers as given in **section 4.4** (i.e. the hang-off angle when there is no current acting while the vessel is at its nominal offset position must be 9°). In addition to this, the minimum bend radius decreases as the anchor length decreases, while H_{min} decreases as the anchor length increases. This means too low or too high anchor length will not only contravene the hang-off angle criterion for the steel catenary risers but also probably breach the acceptable minimum bend radius and H_{min} values when subjected to dynamic analysis. Hence, a riser anchor length of 1320 m will form the basis of subsequent analysis in this study.

5.3.3 Sensitivity to Internal Content of Flowlines

The stability of the buoy and the strength performance of the flowlines are studied with respect to the internal condition (content, empty, and flooded) of the flowlines as follows:

Analysis Parameters

- Internal fluid condition of flowlines   Content, Empty, and Flooded
- Offset of main spar   -4 m
- Riser anchor length   1320 m
- Drag coefficient of buoy (C_d)   1.4
- Added mass coefficient of buoy (C_a)
  - Main spar   0.801
  - Side spar   0.150
- Current and vessel offset cases
  - Case 1
    - Vessel offset   Near position (-50 m)
    - Current return period   10 years, No current (i.e. 0 years)
    - Current direction   0°
  - Case 2
    - Vessel offset   Nominal position (0 m)
    - Current return period   10 years, No current (i.e. 0 years)
    - Current direction   0°, 180°
  - Case 3
    - Vessel offset   Far position (50 m)
    - Current return period   10 years, No current (i.e. 0 years)
    - Current direction   180°
  - Case 4
    - Vessel offset   Near position (-30 m)
    - Current return period   100 years, No current (i.e. 0 years)
    - Current direction   0°

- Case 5
  - ➢ Vessel offset   Nominal position (0 m)
  - ➢ Current return period   100 years, No current (i.e. 0 years)
  - ➢ Current direction   0°, 180°
- Case 6
  - ➢ Vessel offset   Far position (30 m)
  - ➢ Current return period   100 years, No current (i.e. 0 years)
  - ➢ Current direction   180°

The result summaries for the oil-filled flowlines scenario for cases 1 to 6 are presented in **Tables 5-37** and **5-38** below (full results can be found in **Appendices C.1-35** and **C.1-36**).

				Content-Filled Flowlines								
				Flexible Jumpers				**Maximum Values for SCRs**				
Case	**Vessel Offset**	**Current Return Period**	**Current Direction**	**MBR**	**H_{min}**	**Buoy Trim Angle**	**Hang-off Angle**	**Max. Von Mises Stress (Top)**	**Max. Von Mises Stress (Sagbend)**	**Von Mises Utilization (Top)**	**Von Mises Utilization (Sagbend)**
	(m)	(yr)	(deg)	(m)	(m)	(deg)	(deg)	(MPa)	(MPa)		
1	-50	10	0	56	49	0.1	10	274	298	0.61	0.67
		0	-	41	62	0.0	8	275	263	0.61	0.59
2	0	10	0	75	39	0.1	11	275	285	0.61	0.64
		0	-	57	52	0.0	9	276	259	0.62	0.58
		10	180	43	62	-0.1	8	278	248	0.62	0.55
3	50	10	180	60	51	-0.1	8	278	247	0.62	0.55
		0	-	77	40	0.0	10	276	255	0.62	0.57

Table 5 - 37: Summary Static Analysis Results for Riser System (with Content-filled flowlines) supported by H-shaped Buoy, at Near, Zero, and Far Vessel Offsets, with 0- and 10-year Currents

				Content-Filled Flowlines								
				Flexible Jumpers				**Maximum Values for SCRs**				
Case	**Vessel Offset**	**Current Return Period**	**Current Direction**	**MBR**	**H_{min}**	**Buoy Trim Angle**	**Hang-off Angle**	**Max. Von Mises Stress (Top)**	**Max. Von Mises Stress (Sagbend)**	**Von Mises Utilization (Top)**	**Von Mises Utilization (Sagbend)**
	(m)	(yr)	(deg)	(m)	(m)	(deg)	(deg)	(MPa)	(MPa)		
4	-30	100	0	67	43	0.1	11	274	303	0.61	0.68
		0	-	47	58	0.0	8	275	262	0.63	0.58
5	0	100	0	79	36	0.1	11	274	293	0.61	0.65
		0	-	57	52	0.0	9	276	259	0.62	0.58
		100	180	41	64	-0.1	7	278	247	0.62	0.55
6	30	100	180	50	58	-0.1	8	278	246	0.62	0.55
		0	-	68	45	0.0	9	276	257	0.62	0.57

Table 5 - 38: Summary Static Analysis Results for Riser System (with Content-filled flowlines) supported by H-shaped Buoy, at Near, Zero, and Far Vessel Offsets, with 0- and 100-year Currents

Similarly, the result summaries for the empty flowlines scenario are presented in **Tables 5-39** and **5-40** below (check **Appendices C.1-41** and **C.1-42** for full results).

Empty Flowlines											
				Flexible Jumpers		Buoy Trim Angle	Maximum Values for SCRs				
Case	Vessel Offset	Current Return Period	Current Direction	MBR	H_{min}		Hang-off Angle	Max. Von Mises Stress (Top)	Max. Von Mises Stress (Sagbend)	Von Mises Utilization (Top)	Von Mises Utilization (Sagbend)
	(m)	(yr)	(deg)	(m)	(m)	(deg)	(deg)	(MPa)	(MPa)		
1	-50	10	0	47	56	0.3	12	49	228	0.11	0.51
		0	-	34	68	0.2	9	53	149	0.12	0.33
2	0	10	0	66	44	0.3	12	50	207	0.11	0.46
		0	-	49	57	0.2	9	53	141	0.12	0.31
		10	180	37	67	0.1	7	63	117	0.14	0.26
3	50	10	180	53	56	0.1	8	64	115	0.14	0.26
		0	-	68	45	0.2	10	54	134	0.12	0.30

Table 5 - 39: Summary Static Analysis Results for Riser System (with Empty flowlines) supported by H-shaped Buoy, at Near, Zero, and Far Vessel Offsets, with 0- and 10-year Currents

Empty Flowlines											
				Flexible Jumpers		Buoy Trim Angle	Maximum Values for SCRs				
Case	Vessel Offset	Current Return Period	Current Direction	MBR	H_{min}		Hang-off Angle	Max. Von Mises Stress (Top)	Max. Von Mises Stress (Sagbend)	Von Mises Utilization (Top)	Von Mises Utilization (Sagbend)
	(m)	(yr)	(deg)	(m)	(m)	(deg)	(deg)	(MPa)	(MPa)		
4	-30	100	0	57	49	0.3	13	50	243	0.11	0.54
		0	-	40	64	0.2	9	53	146	0.12	0.33
5	0	100	0	70	42	0.3	13	50	227	0.11	0.51
		0	-	49	57	0.2	9	53	141	0.12	0.31
		100	180	35	69	0.1	7	65	114	0.15	0.25
6	30	100	180	44	62	0.1	8	65	113	0.15	0.25
		0	-	60	50	0.2	10	54	137	0.12	0.31

Table 5 - 40: Summary Static Analysis Results for Riser System (with Empty flowlines) supported by H-shaped Buoy, at Near, Zero, and Far Vessel Offsets, with 0- and 100-year Currents

The result summaries for the flooded flowlines scenarios are presented in **Tables 5-41** and **5-42** below (full results are presented in **Appendices C.1-47** and **C.1-48**).

				Flexible Jumpers			Maximum Values for SCRs				
Flooded Flowlines											
Case	Vessel Offset	Current Return Period	Current Direction	MBR	H_{min}	Buoy Trim Angle	Hang-off Angle	Max. Von Mises Stress (Top)	Max. Von Mises Stress (Sagbend)	Von Mises Utilization (Top)	Von Mises Utilization (Sagbend)
	(m)	(yr)	(deg)	(m)	(m)	(deg)	(deg)	(MPa)	(MPa)		
1	-50	10	0	65	43	-0.1	9	78	236	0.17	0.53
		0	-	48	56	-0.2	7	83	166	0.19	0.37
2	0	10	0	85	33	-0.1	10	80	206	0.18	0.46
		0	-	65	46	-0.2	8	85	153	0.19	0.34
		10	180	50	57	-0.3	7	93	121	0.21	0.27
3	50	10	180	68	46	-0.3	8	95	114	0.21	0.25
		0	-	86	35	-0.2	9	87	139	0.19	0.31

Table 5 - 41: Summary Static Analysis Results for Riser System (with Flooded flowlines) supported by H-shaped Buoy, at Near, Zero, and Far Vessel Offsets, with 0- and 10-year Currents

				Flexible Jumpers			Maximum Values for SCRs				
Flooded Flowlines											
Case	Vessel Offset	Current Return Period	Current Direction	MBR	H_{min}	Buoy Trim Angle	Hang-off Angle	Max. Von Mises Stress (Top)	Max. Von Mises Stress (Sagbend)	Von Mises Utilization (Top)	Von Mises Utilization (Sagbend)
	(m)	(yr)	(deg)	(m)	(m)	(deg)	(deg)	(MPa)	(MPa)		
4	-30	100	0	76	37	-0.1	10	79	240	0.18	0.54
		0	-	55	52	-0.2	8	84	161	0.19	0.36
5	0	100	0	89	31	0.0	10	79	220	0.18	0.49
		0	-	65	46	-0.2	8	85	153	0.19	0.34
		100	180	47	59	-0.3	7	95	116	0.21	0.26
6	30	100	180	57	53	-0.3	8	96	113	0.21	0.25
		0	-	77	40	-0.2	9	86	145	0.19	0.32

Table 5 - 42: Summary Static Analysis Results for Riser System (with Flooded flowlines) supported by H-shaped Buoy, at Near, Zero, and Far Vessel Offsets, with 0- and 100-year Currents

Like the results obtained in **Tables 5-5** to **5-10** for the conventional buoy, **Tables 5-37** to **5-42** show that the design criteria for the minimum bend radius and H_{min} of the flexible jumpers, and the Von Mises stress values of the steel catenary risers are satisfied at all the considered vessel offsets and associated current return periods by all the flowline internal conditions.

Comparisons of the buoy trim angles of all the flowline internal conditions when the vessel is at its nominal position with no current acting (i.e. cases 2 and 5 with no current acting for each flowline internal condition) reveals that the oil-filled flowline condition (i.e. content flowlines) gives the best stability with a trim angle of 0.0° at this position, while the empty and flooded flowline conditions offer less stability with respective trim angles of 0.2° and -0.2°. It is also observed that this stability trend remains true for situations when the vessel is either at its near or far offset positions with all the considered current return periods (as seen in cases 1, 3, 4,

and 6 for all the flowline internal conditions). This implies the flowline internal condition that offers the best stability to the buoy is the content flowline internal condition.

The Von Mises stress values at the top and sagbend areas of the steel catenary risers show that the empty and flooded flowline internal conditions satisfy the Von Mises stress acceptance criterion (as stated in **section 4.4**) at all the vessel offset positions. The Von Mises stress values in **Tables 5-37** to **5-38** show that the oil-filled flowlines scenario has higher values at all vessel offsets when compared with the empty and flooded flowline conditions. While at all vessel offset positions and their associated current return periods, the Von Mises stress values at the top area for the oil-filled flowlines condition clearly satisfy the acceptance criterion, the value at the sagbend area for case 4 (with 100-year current) is a bit over 300 MPa. However, this can still be considered as being within the acceptance limit as stated in **section 4.4**). This shows that that the most critical flowline internal condition with respect to the strength performance of the steel catenary risers is the content flowline internal condition.

5.3.4 Sensitivity to Drag Coefficient of the Buoy

Here, the influence of variations in the drag coefficient of the H-shaped buoy on the performance of the flexible jumpers, steel catenary risers, and the buoy itself with respect to each of the flowline internal conditions considered in **section 5.3.3** is studied. This is as follows:

Analysis Parameters

- Drag coefficients of buoy (C_d)   1.2, 1.4, and 1.6
- Riser anchor length   1320 m
- Internal fluid condition of flowlines   Content, Empty, and Flooded
- Offset of main spar   -4 m
- Added mass coefficient of buoy (C_a)
    - Main spar   0.801
    - Side spar   0.150
- Current and vessel offset cases
    - Case 1:
        - Vessel offset   Near position (-50 m)
        - Current return period   10 years
        - Current direction   0°
    - Case 2:
        - Vessel offset   Nominal position (0 m)
        - Current return period   10 years
        - Current direction   0°, 180°

- Case 3:
    - Vessel offset   Far position (50 m)
    - Current return period   10 years
    - Current direction   180°
- Case 4
    - Vessel offset   Near position (-30 m)
    - Current return period   100 years
    - Current direction   0°
- Case 5
    - Vessel offset   Nominal position (0 m)
    - Current return period   100 years
    - Current direction   0°, 180°
- Case 6
    - Vessel offset   Far position (30 m)
    - Current return period   100 years
    - Current direction   180°

The following results were obtained for the content flowline internal condition:

Content Flowlines with Buoy C_d = 1.2, and 10-year current											
Case	Vessel Offset	Current Return Period	Current Direction	Flexible Jumpers		Buoy		Maximum Values for SCRs			
				MBR	H_{min}	Buoy Trim Angle	Position Relative to Nominal with no current	Max. Von Mises Stress (Top)	Max. Von Mises Stress (Sagbend)	Von Mises Utilization (Top)	Von Mises Utilization (Sagbend)
	(m)	(yr)	(deg)	(m)	(m)	(deg)	(m)	(MPa)	(MPa)		
1	-50	10	0	55	50	0.1	-55.15	274.27	297.09	0.61	0.66
2	0	10	0	74	39	0.1	-32.75	274.53	284.66	0.61	0.64
		0	-	57	52	0.0	0.00	275.58	259.13	0.62	0.58
		10	180	43	62	-0.1	36.42	277.58	248.22	0.62	0.55
3	50	10	180	60	51	-0.1	52.49	277,87	246,81	0.62	0.55

Table 5 - 43: Summary Static Analysis Results for Riser System (with Content-filled flowlines) supported by H-shaped Buoy with C_d = 1.2, at Near, Zero, and Far Vessel Offsets, with 10-year Current

				Flexible Jumpers		Buoy		Maximum Values for SCRs			
Case	**Vessel Offset**	**Current Return Period**	**Current Direction**	**MBR**	**H$_{min}$**	**Buoy Trim Angle**	**Position Relative to Nominal with no current**	**Max. Von Mises Stress (Top)**	**Max. Von Mises Stress (Sagbend)**	**Von Mises Utilization (Top)**	**Von Mises Utilization (Sagbend)**
	(m)	(yr)	(deg)	(m)	(m)	(deg)	(m)	(MPa)	(MPa)		
4	-30	100	0	66	43	0.1	-53.08	274.20	301.61	0.61	0.67
5	0	100	0	78	37	0.1	-38.56	274.36	292.40	0.61	0.65
		0	-	57	52	0.0	0.00	275.58	259.13	0.62	0.58
		100	180	41	64	-0.1	43.77	277,89	246,84	0.62	0.55
6	30	100	180	51	57	-0.1	52.53	278,05	246,15	0.62	0.55

Table 5 - 44: Summary Static Analysis Results for Riser System (with Content-filled flowlines) supported by H-shaped Buoy with C$_d$ = 1.2, at Near, Zero, and Far Vessel Offsets, with 100-year Current

				Flexible Jumpers		Buoy		Maximum Values for SCRs			
Case	**Vessel Offset**	**Current Return Period**	**Current Direction**	**MBR**	**H$_{min}$**	**Buoy Trim Angle**	**Position Relative to Nominal with no current**	**Max. Von Mises Stress (Top)**	**Max. Von Mises Stress (Sagbend)**	**Von Mises Utilization (Top)**	**Von Mises Utilization (Sagbend)**
	(m)	(yr)	(deg)	(m)	(m)	(deg)	(m)	(MPa)	(MPa)		
1	-50	10	0	56	49	0.1	-56.28	274.25	297.82	0.61	0.66
2	0	10	0	75	39	0.1	-33.73	274.52	285.15	0.61	0.64
		0	-	57	52	0.0	0.00	275.58	259.13	0.62	0.58
		10	180	43	62	-0.1	37.69	277.60	248.11	0.62	0.55
3	50	10	180	60	51	-0.1	53.63	277.89	246.71	0.62	0.55

Table 5 - 45: Summary Static Analysis Results for Riser System (with Content-filled flowlines) supported by H-shaped Buoy with C$_d$ = 1.4, at Near, Zero, and Far Vessel Offsets, with 10-year Current

				Flexible Jumpers		Buoy		Maximum Values for SCRs			
Case	**Vessel Offset**	**Current Return Period**	**Current Direction**	**MBR**	**H$_{min}$**	**Buoy Trim Angle**	**Position Relative to Nominal with no current**	**Max. Von Mises Stress (Top)**	**Max. Von Mises Stress (Sagbend)**	**Von Mises Utilization (Top)**	**Von Mises Utilization (Sagbend)**
	(m)	(yr)	(deg)	(m)	(m)	(deg)	(m)	(MPa)	(MPa)		
4	-30	100	0	67	43	0.1	-54.33	274.32	302.58	0.61	0.68
5	0	100	0	79	36	0.1	-39.70	274.48	293.19	0.61	0.65
		0	-	57	52	0.0	0.00	275.58	258.13	0.62	0.58
		100	180	41	64	-0.1	45.33	278.05	246.84	0.62	0.55
6	30	100	180	50	58	-0.1	54.00	278.21	246.17	0.62	0.55

Table 5 - 46: Summary Static Analysis Results for Riser System (with Content-filled flowlines) supported by H-shaped Buoy with C$_d$ = 1.4, at Near, Zero, and Far Vessel Offsets, with 100-year Current

			Flexible Jumpers		Buoy		Maximum Values for SCRs			
Case	**Vessel Offset**	**Current Return Period**	**Current Direction**			**Buoy Trim Angle**	**Position Relative to Nominal with no current**	**Max. Von Mises Stress (Top)**	**Max. Von Mises Stress (Sagbend)**	**Von Mises Utilization (Top)**	**Von Mises Utilization (Sagbend)**
			MBR	H_{min}						
	(m)	(yr)	(deg)	(m)	(m)	(deg)	(m)	(MPa)	(MPa)		
1	-50	10	0	56	49	0.1	-57.41	274.24	298.54	0.61	0.67
2	0	10	0	76	38	0.1	-34.70	274.50	285.63	0.61	0.64
		0	-	57	52	0.0	0.00	275.58	258.13	0.62	0.58
		10	180	42	63	-0.1	38.97	277.62	247.98	0.62	0.55
3	50	10	180	59	52	-0.1	54.77	277.92	246.62	0.62	0.55

Content Flowlines with Buoy C_d = 1.6, and 10-year current

Table 5 - 47: Summary Static Analysis Results for Riser System (with Content-filled flowlines) supported by H-shaped Buoy with C_d = 1.6, at Near, Zero, and Far Vessel Offsets, with 10-year Current

			Flexible Jumpers		Buoy		Maximum Values for SCRs			
Case	**Vessel Offset**	**Current Return Period**	**Current Direction**			**Buoy Trim Angle**	**Position Relative to Nominal with no current**	**Max. Von Mises Stress (Top)**	**Max. Von Mises Stress (Sagbend)**	**Von Mises Utilization (Top)**	**Von Mises Utilization (Sagbend)**
			MBR	H_{min}						
	(m)	(yr)	(deg)	(m)	(m)	(deg)	(m)	(MPa)	(MPa)		
4	-30	100	0	68	42	0.1	-55.57	274.17	303.23	0.61	0.68
5	0	100	0	80	36	0.1	-40.83	274.33	293.77	0.61	0.66
		0	-	57	52	0.0	0.00	275.58	258.13	0.62	0.58
		100	180	40	65	-0.1	46.90	277.95	246.59	0.62	0.55
6	30	100	180	49	58	-0.1	55.47	278.11	245.93	0.62	0.55

Content Flowlines with Buoy C_d = 1.6, and 100-year current

Table 5 - 48: Summary Static Analysis Results for Riser System (with Content-filled flowlines) supported by H-shaped Buoy with C_d = 1.6, at Near, Zero, and Far Vessel Offsets, with 100-year Current

Tables 5-43, **5-45**, and **5-47** for the 10-year current show that the minimum bend radius and H_{min} of the flexible jumpers, and the buoy trim angles remain fairly constant at corresponding vessel offset positions if comparison is made between the three buoy drag coefficients. The tables also show that the minimum bend radius and H_{min} values satisfy the design criteria for the flexible jumpers. The same also holds for the 100-year current as seen in **Tables 5-44**, **5-46**, and **5-48**

In addition, **Tables 5-43** to **5-48** reveal that the relative horizontal displacement of the buoy increases (albeit small) as its drag coefficient increases. This can be seen by comparing corresponding current and vessel offset cases (for instance, case 1 of **Tables 5-43**, **5-45**, and **5-47**; case 2 of **Tables 5-43**, **5-45**, and **5-47**, and so on). This is as expected because the amount of drag a body experiences is proportional to its drag coefficient.

Furthermore, **Tables 5-43** to **5-48** also show that the maximum Von Mises stress values at the top and sagbend areas of the steel catenary risers do not change much when comparison is made between corresponding current and vessel offset cases as the drag coefficient changes. The change trend observed at the near and far vessel offset positions is presented in **Table 5-49** below.

Case	Buoy Drag Coefficient	Vessel Offset	Position Relative to Nominal	Max. Von Mises Stress (Top)	Max. Von Mises Stress (Sagbend)
			Content Flowlines with C_d = 1.2, 1.4, and 1.6		
		(m)	(m)	(MPa)	(MPa)
1	1.2	-50	-55.15	274.27	297.09
	1.4		-56.28 (+2.05%)	274.25 (-0.007%)	297.82 (+0.23%)
	1.6		-57.41(+2.01%)	274.24 (-0.004%)	298.54 (+0.24%)
3	1.2	50	52.49	277.87	246.81
	1.4		53.63 (+2.17%)	277.89 (+0.007%)	246.71 (-0.04%)
	1.6		54.77 (+2.13%)	277.92 (+0.011%)	246.62 (-0.04%)
4	1.2	-30	-53.08	274.20	301.61
	1.4		-54.33 (+2.35%)	274.32 (+0.044%)	302.58 (+0.32%)
	1.6		-55.57 (+2.28%)	274.17 (-0.055%)	303.23 (+0.21%)
6	1.2	30	52.53	278.05	246.15
	1.4		54.00 (+2.80%)	278.21 (+0.058%)	246.17 (0.008%)
	1.6		55.47 (+2.72%)	278.11 (-0.036%)	245.93 (-0.097%)

Table 5 - 49: Comparison of Summary Static Analysis Results for Riser System (with Content-filled flowlines) supported by H-shaped Buoy with C_d = 1.2, 1.4, and 1.6

A drag coefficient of 1.4 can thus be adopted for the H-shaped buoy in subsequent dynamic analysis.

The following plots further explain the results in **Table 5-49** above:
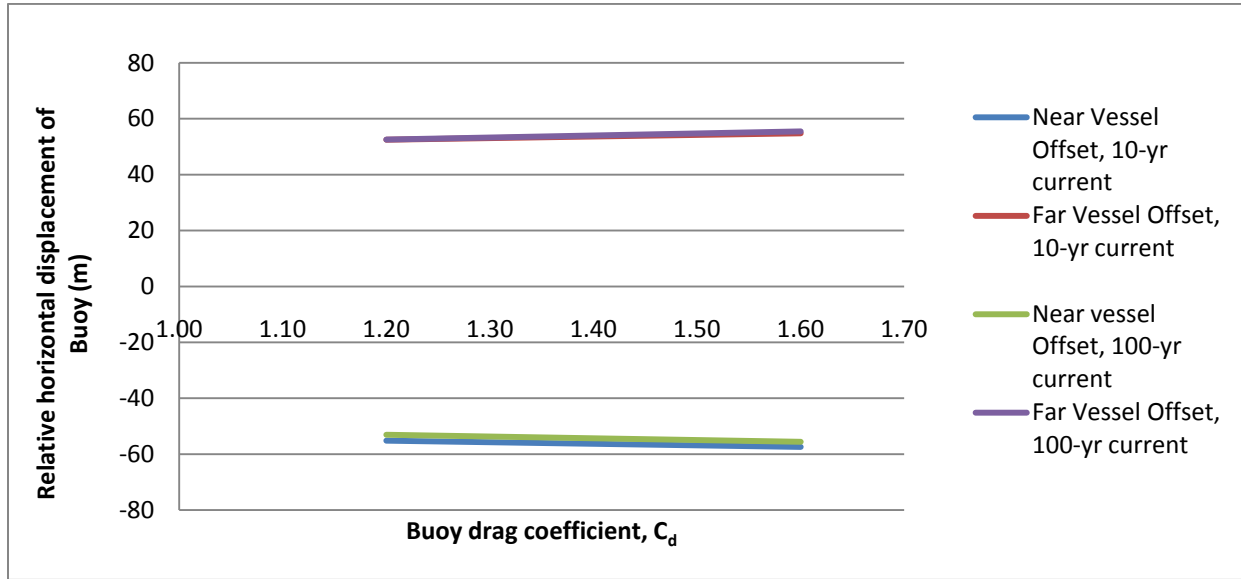
Figure 5 - 13: Relationship between Relative Horizontal Displacement of H-shaped Buoy and its Drag Coefficient, at Near and Far Vessel Offsets with 10- and 100-year Currents
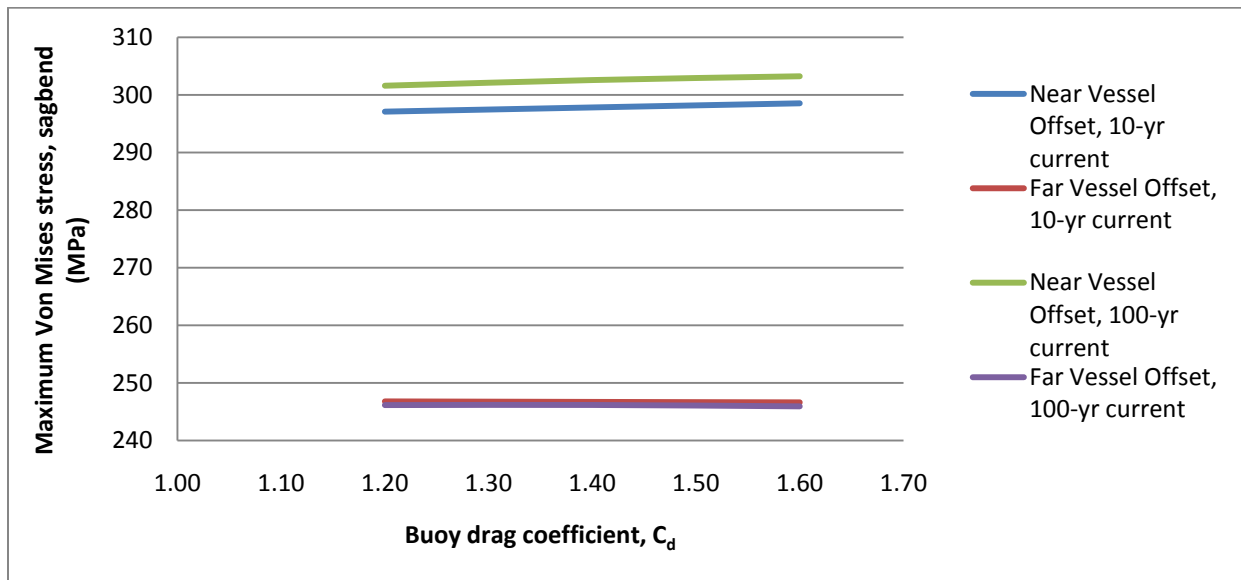
Figure 5 - 14: Relationship between Maximum Von Mises Stress at Sagbend of SCRs and Drag Coefficient of H-shaped Buoy, at Near and Far Vessel Offsets with 10- and 100-year Currents
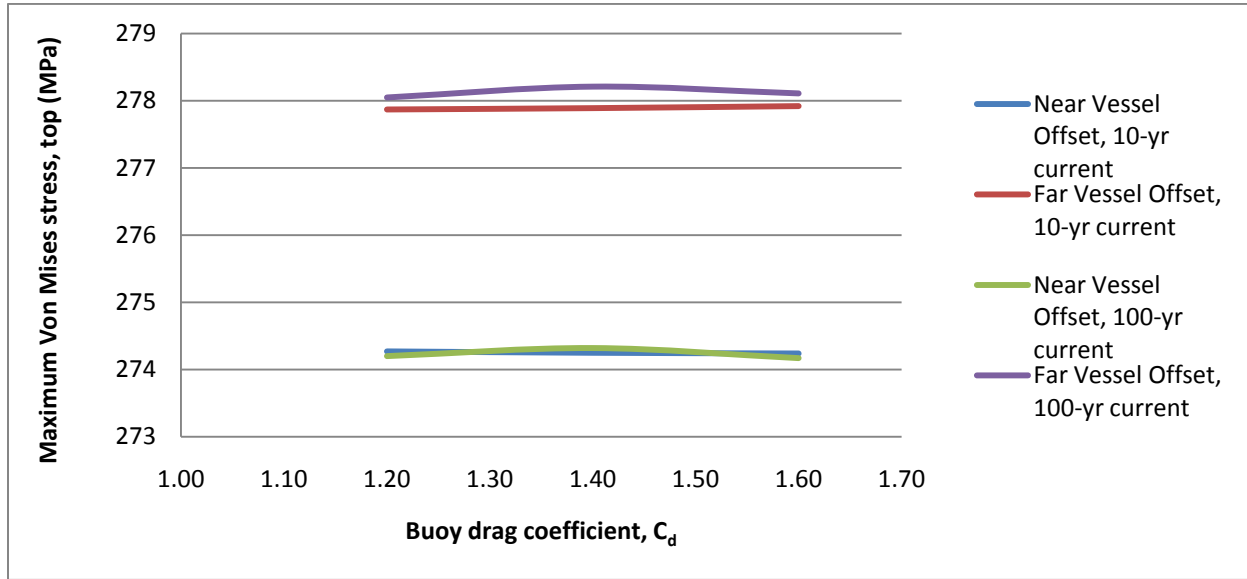
Figure 5 - 15: Relationship between Maximum Von Mises Stress at Top region of SCRs and Drag Coefficient of H-shaped Buoy, at Near and Far Vessel Offsets with 10- and 100-year Currents

Similar trends are observed for the minimum bend radius, H_{min}, trim angle, relative horizontal displacement, and Von Mises stress values for the empty and flooded flowlines scenarios. Summary results for these scenarios are presented below (check **Appendices C.1-39** to **C.1-50** for full results).

	Empty Flowlines with C_d = 1.2, 1.4, and 1.6				
Case	Buoy Drag Coefficient	Vessel Offset	Position Relative to Nominal	Max. Von Mises Stress (Top)	Max. Von Mises Stress (Sagbend)
		(m)	(m)	(MPa)	(MPa)
1	1.2	-50	-55.20	49.42	226.93
	1.4		-56.44 (+2.25%)	49.39 (-0.061%)	228.40 (+0.65%)
	1.6		-57.68 (+2.20%)	49.36 (-0.061%)	229.86 (+0.64%)
3	1.2	50	52.28	63.70	114.95
	1.4		53.51 (+2.35%)	63.77 (+0.110%)	114.79 (-0.14%)
	1.6		54.74 (+2.30%)	63.84 (+0.110%)	114.62 (-0.15%)
4	1.2	-30	-54.95	50.03	241.04
	1.4		-56.35 (+2.55%)	50.00 (-0.060%)	242.91 (+0.78%)
	1.6		-57.73 (+2.45%)	49.97 (-0.060%)	244.59 (+0.69%)
6	1.2	30	53.77	65.33	113.66
	1.4		55.34 (+2.92%)	65.41 (+0.122%)	113.47 (-0.17%)
	1.6		56.91 (+2.84%)	65.50 (+0.138%)	113.29 (-0.16%)

Table 5 - 50: Comparison of Summary Static Analysis Results for Riser System (with Empty flowlines) supported by H-shaped Buoy with C_d = 1.2, 1.4, and 1.6

Flooded Flowlines with C_d = 1.2, 1.4, and 1.6					
Case	Buoy Drag Coefficient	Vessel Offset	Position Relative to Nominal	Max. Von Mises Stress (Top)	Max. Von Mises Stress (Sagbend)
		(m)	(m)	(MPa)	(MPa)
1	1.2	-50	-55.02	78,28	234.48
	1.4		-56.03 (+1.84%)	78.24 (-0.051%)	235.73 (+0.53%)
	1.6		-57.03 (+1.78%)	78.19 (-0.064%)	236.97 (+0.53%)
3	1.2	50	52.72	94.55	114.59
	1.4		53.75 (+1.95%)	94.64 (+0.095%)	114.26 (-0.29%)
	1.6		54.80 (+1.95%)	94.73 (+0.095%)	113.93 (-0.29%)
4	1.2	-30	-50.99	78.61	238.62
	1.4		-52.09 (+2.16%)	78.56 (-0.064%)	240.05 (+0.60%)
	1.6		-53.19 (+2.11%)	78.54 (-0.025%)	241.46 (+0.59%)
6	1.2	30	51.16	95.55	113.36
	1.4		52.53 (+2.68%)	95.66 (+0.115%)	112.94 (-0.37%)
	1.6		53.89 (+2.59%)	95.79 (+0.136%)	112.54 (-0.35%)

Table 5 - 51: Comparison of Summary Static Analysis Results for Riser System (with Flooded flowlines) supported by H-shaped Buoy with C_d = 1.2, 1.4, and 1.6

While the relative displacement values of the buoy when the flowlines are in empty or flooded conditions do not differ much from those obtained when the flowlines are in content-filled condition (this is seen by comparing column 4 of **Tables 5-49**, **5-50**, and **5-51**), the Von Mises stress values for the latter (content-filled) can be seen to be higher than those of the former (empty and flooded) for all considered buoy drag coefficients and all vessel offsets. Thus, the content-filled flowlines conditions will be the subject of subsequent dynamic analysis.

5.4 Design Analysis of Steel Catenary Risers supported by H-shaped Buoy (Dynamic Analysis)

In this section, analyses similar to those carried out with respect to the conventional buoy in **section 5.2** are carried out. First off, a base case dynamic analysis will be carried out for the content-filled flowlines scenario studied in **section 5.3.3**, with the added mass coefficients of the main and side spars of the buoy kept fixed. A sensitivity study will then be done to study the effect of variations in the added mass coefficient of the buoy on the riser system.

5.4.1 Base Case Dynamic Analysis for H-shaped Buoy

Cases 1 and 3 (both with 10-year current), and cases 4 and 6 (both with 100-year current) from **section 5.3.3** are subjected to dynamic analyses at the near and far vessel offset positions as follows:

Analysis Parameters (with 10-year current + 100-year wave)

Load Case 1:

- Vessel offset   Near position (-50 m)
- Environmental load combination   10-year current + 100-year wave
- Environmental load direction   0°

Load Case 3:

- Vessel offset   Far position (50 m)
- Environmental load combination   10-year current + 100-year wave
- Environmental load direction   180°

The following results were obtained (full dynamic analysis results can be found in **Appendices C.2-9** and **C.2-10**):

Load Case	Static Analysis				Dynamic analysis					
	Max. Von Mises Stress		Max. Von Mises Utilization		Max. Von Mises Stress		Max. Von Mises Utilization		Max. Buckling Utilization	
	Top	Sagbend	Top	Sagbend	Top	Sagbend	Top	Sagbend	Top	Sagbend
	(MPa)				(MPa)					
1	274.25	297.82	0.61	0.66	275.43	311.38	0.61	0.70	0.11	0.66
3	277.89	246.71	0.62	0.55	278.71	248.36	0.62	0.55	0.12	0.28

Table 5 - 52: Base Case Static and Dynamic Analysis Results for SCRs with 10-yr Current + 100-yr Wave – H-shaped Buoy

Load Case	Static Analysis	Dynamic Analysis	
	Minimum Bend Radius	Minimum Bend Radius	Minimum Tension
	(m)	(m)	(kN)
1	56	43	19
3	60	54	82

Table 5 - 53: Base Case Static and Dynamic Analysis Results for Flexible Jumpers with 10-yr Current + 100-yr Wave – H-shaped Buoy

Load Case	Static Analysis			Dynamic Analysis							
	Trim Angle	Relative Vertical Displacement	Relative Horizontal Displacement	Trim Angle			Relative Vertical Displacement		Relative Horizontal Displacement	
				Min	Max	Variation	Min	Max	Min	Max
	(deg)	(m)	(m)	(deg)	(deg)	(deg)	(m)	(m)	(m)	(m)
1	0.09	-3.28	-56.28	-0.17	0.38	0.55	-4.15	-2.81	-62.93	-55.60
3	-0.08	0.68	53.63	-0.31	0.16	0.47	0.32	1.10	52.69	57.88

Table 5 - 54: Base Case Static and Dynamic Analysis Results for Buoy with 10-yr Current + 100-yr Wave – H-shaped Buoy

The dynamic results of the steel catenary risers show that the Von Mises utilization and buckling utilization acceptance criteria are satisfied for both load cases at the top and sagbend areas, and that the dynamic environmental loads do not lead to much increase in the Von Mises stresses when compared with the static analysis results.

The dynamic results of the flexible jumpers also show that the minimum bend radius of the jumpers does not change much under the influence of dynamic loads and that no compression is obtained along the jumpers. In addition, the minimum bend radius values for both load cases are well above the limiting minimum bend radius value.

Also, the trim angle, relative horizontal and vertical displacements of the buoy do not change much when compared with the static analysis results.

Similar analysis is done for the 100-year current as follows:

Analysis Parameters (with 100-year current + 10-year wave)

Load Case 4:

- Vessel offset   Near position (-30 m)
- Environmental load combination   100-year current + 10-year wave
- Environmental load direction   0°

Load Case 6:

- Vessel offset   Far position (30 m)
- Environmental load combination   100-year current + 10-year wave
- Environmental load direction   180°

Summaries of key static and dynamic analysis results obtained for load cases 4 and 6 are presented below (full dynamic analysis results can be found in **Appendices C.2-11** and **C.2-12**).

Load Case	Static Analysis				Dynamic analysis					
	Max. Von Mises Stress		Max. Von Mises Utilization		Max. Von Mises Stress		Max. Von Mises Utilization		Max. Buckling Utilization	
	Top	Sagbend	Top	Sagbend	Top	Sagbend	Top	Sagbend	Top	Sagbend
	(MPa)				(MPa)					
4	274.32	302.58	0.61	0.68	275.60	315.64	0.62	0.70	0.11	0.69
6	278.21	246.17	0.62	0.55	278.89	247.11	0.62	0.55	0.12	0.27

Table 5 - 55: Base Case Static and Dynamic Analysis Results for SCRs with 100-yr Current + 10-yr Wave – H-shaped Buoy

Load Case	Static Analysis	Dynamic Analysis	
	Minimum Bend Radius	Minimum Bend Radius	Minimum Tension
	(m)	(m)	(kN)
4	67	48	26
6	50	46	73

Table 5 - 56: Base Case Static and Dynamic Analysis Results for Flexible Jumpers with 100-yr Current + 10-yr Wave – H-shaped Buoy

Load Case	Static Analysis			Dynamic Analysis						
	Trim Angle	Relative Vertical Displacement	Relative Horizontal Displacement	Trim Angle			Relative Vertical Displacement		Relative Horizontal Displacement	
				Min	Max	Variation	Min	Max	Min	Max
	(deg)	(m)	(m)	(deg)	(deg)	(deg)	(m)	(m)	(m)	(m)
4	0.13	-3.11	-54.33	-0.12	0.38	0.50	-3.85	-2.74	-59.89	-53.85
6	-0.10	0.63	54.00	-0.29	0.11	0.40	0.34	0.95	53.30	56.82

Table 5 - 57: Base Case Static and Dynamic Analysis Results for Buoy with 100-yr Current + 10-yr Wave – H-shaped Buoy

Like what was obtained for load cases 1 and 3, the dynamic results for cases 4 and 6 also satisfy the maximum Von Mises stress and buckling utilization criteria for the steel catenary risers, the minimum bend radius and "no compression" criteria for the flexible jumpers. The buoy results also show that buoy motion doesn't differ much from that obtained through static analysis.

5.4.2 Sensitivity to Added Mass Coefficient of H-shaped Buoy

The response of the flowlines and the H-shaped buoy to 20 percent reduction and increase in the added mass coefficient of the buoy is studied in this section. Load cases 1, 3, 4, and 6 considered in **section 5.4.1** are also considered here in addition to the new added mass coefficients of the buoy. The added mass variation is achieved by varying the added mass coefficients of the main and side spars of the H-shaped Buoy. The analysis is presented below.

New Buoy Added Mass Coefficient values

- 20% reduction in added mass coefficient of buoy
  - Main spar   0.641
  - Side spar   0.12
- 20% increase in added mass coefficient of buoy
  - Main spar   0.961
  - Side spar   0.18

Comparisons of the dynamic analysis results for the 20% buoy added mass coefficient reduction, base case buoy added mass coefficient, and 20% buoy added mass coefficient increase are presented in **Tables 5-58** to **5-60** below.

Load Case	Buoy Added Mass Coefficient (C_a)	Max. Von Mises Stress		Max. Von Mises Utilization	
		Top	Sagbend	Top	Sagbend
		(MPa)			
1	20% lower	275.48	311.44	0.61	0.70
	Base Case	275.43	311.38	0.61	0.70
	20% higher	275.38	311.27	0.61	0.69
3	20% lower	278.73	248.36	0.62	0.55
	Base Case	278.71	248.36	0.62	0.55
	20% higher	278.71	248.36	0.62	0.55
4	20% lower	275.64	315.80	0.62	0.70
	Base Case	275.60	315.64	0.62	0.70
	20% higher	275.56	315.52	0.62	0.70
6	20% lower	278.90	247.10	0.62	0.55
	Base Case	278.89	247.11	0.62	0.55
	20% higher	278.88	247.12	0.62	0.55

Table 5 - 58: Sensitivity of Strength Performance of SCRs to Variations in Added Mass Coefficient of H-shaped Buoy

Load Case	Buoy Added Mass Coefficient (C_a)	Minimum Bend Radius	Minimum Tension
		(m)	(kN)
1	20% lower	43	19
	Base Case	43	19
	20% higher	42	18
3	20% lower	54	82
	Base Case	54	82
	20% higher	54	82
4	20% lower	49	27
	Base Case	48	26
	20% higher	48	26
6	20% lower	46	73
	Base Case	46	73
	20% higher	46	73

Table 5 - 59: Sensitivity of Strength Performance of Flexible Jumpers to Variations in Added Mass Coefficient of Conventional Buoy

Load Case	Buoy Added Mass Coefficient (C_A)	Trim Angle Variation	Relative Vertical Displacement		Relative Horizontal Displacement	
			Min	Max	Min	Max
		(deg)	(m)	(m)	(m)	(m)
1	20% lower	0.54 (-1.82%)	-4.15 (0.00%)	-2.81 (0.00%)	-63.03 (0.16%)	-55.60 (0.00%)
	Base Case	0.55	-4.15	-2.81	-62.93	-55.60
	20% higher	0.56 (1.82%)	-4.15 (0.00%)	-2.80 (-0.36%)	-62.82 (-0.17%)	-55.61 (0.02%)
3	20% lower	0.46 (-2.13%)	0.32 (0.00%)	1.09 (-0.91%)	52.72 (0.06%)	57.89 (0.02%)
	Base Case	0.47	0.32	1.10	52.69	57.88
	20% higher	0.48 (2.13%)	0.31 (-3.13%)	1.11 (0.91%)	52.68 (-0.02)	57.87 (-0.02%)
4	20% lower	0.49 (-2.00%)	-3.85 (0.00%)	-2.75 (0.36%)	-59.96 (0.12%)	-53.85 (0.00%)
	Base Case	0.50	-3.85	-2.74	-59.89	-53.85
	20% higher	0.50 (0.00%)	-3.85 (0.00%)	-2.74 (0.00%)	-59.81 (-0.13%)	-53.85 (0.00%)
6	20% lower	0.39 (-2.50%)	0.35 (2.94%)	0.94 (-1.05%)	53.31 (0.02%)	56.82 (0.00%)
	Base Case	0.40	0.34	0.95	53.30	56.82
	20% higher	0.41 (2.50%)	0.33 (-2.94%)	0.95 (0.00%)	53.30 (0.00%)	56.82 (0.00%)

Table 5 - 60: Sensitivity of Stability and Motions of H-shaped Buoy to Variations in its Added Mass Coefficient

Like what was obtained in **section 5.2.2** for the conventional buoy, the dynamic results of the steel catenary risers and the flexible jumpers (**Tables 5-58** and **5-59**) show that the maximum Von Mises utilization factors at top and sagbend areas of the SCRs, and the minimum bend radius and minimum tension of the flexible jumpers remain fairly constant as the added mass coefficient of the buoy changes for all the considered load cases.

Also, the dynamic results of the buoy presented in **Table 5-60** above reveal that the trim angle variation, relative vertical and horizontal displacements of the buoy witness very minor changes as the added mass coefficient of the buoy changes, which implies varying the added mass coefficient does not have much influence on the stability of the buoy.

In summary, the presented results show that changing the added mass of the buoy has very little effect on the strength performance of the steel catenary risers and flexible jumpers, likewise on the stability of the buoy.

5.5 Line Clashing Check

To study the performance of the riser system (with content-filled flowlines) supported by H-shaped buoy when exposed to cross-flow currents, the riser system was subjected to wave and current loads in the 90° direction with varying vessel cross offset positions. At a **vessel cross offset position** of 70 m, clashing was observed between one of the steel catenary risers and one of the mooring lines. This is seen in the approximately zero clearance distance between the SCR and the mooring line as shown in the plot below at 85 m arc length along the SCR.
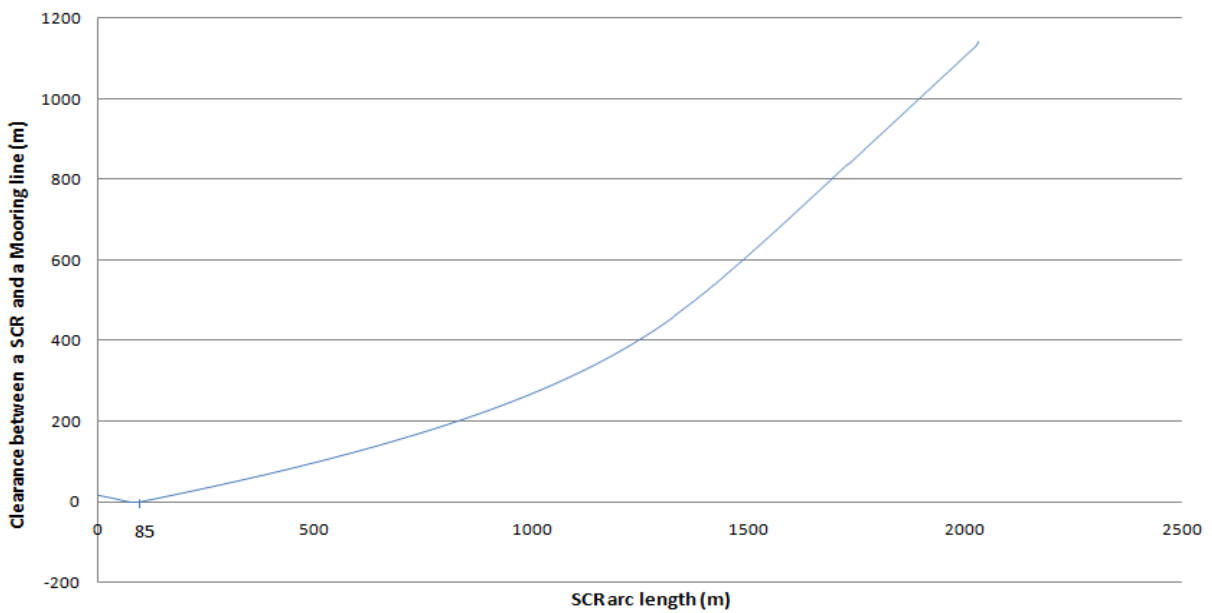
Figure 5 - 16: Plot to show Clearance between a SCR and a Mooring Line used with the H-shaped Buoy
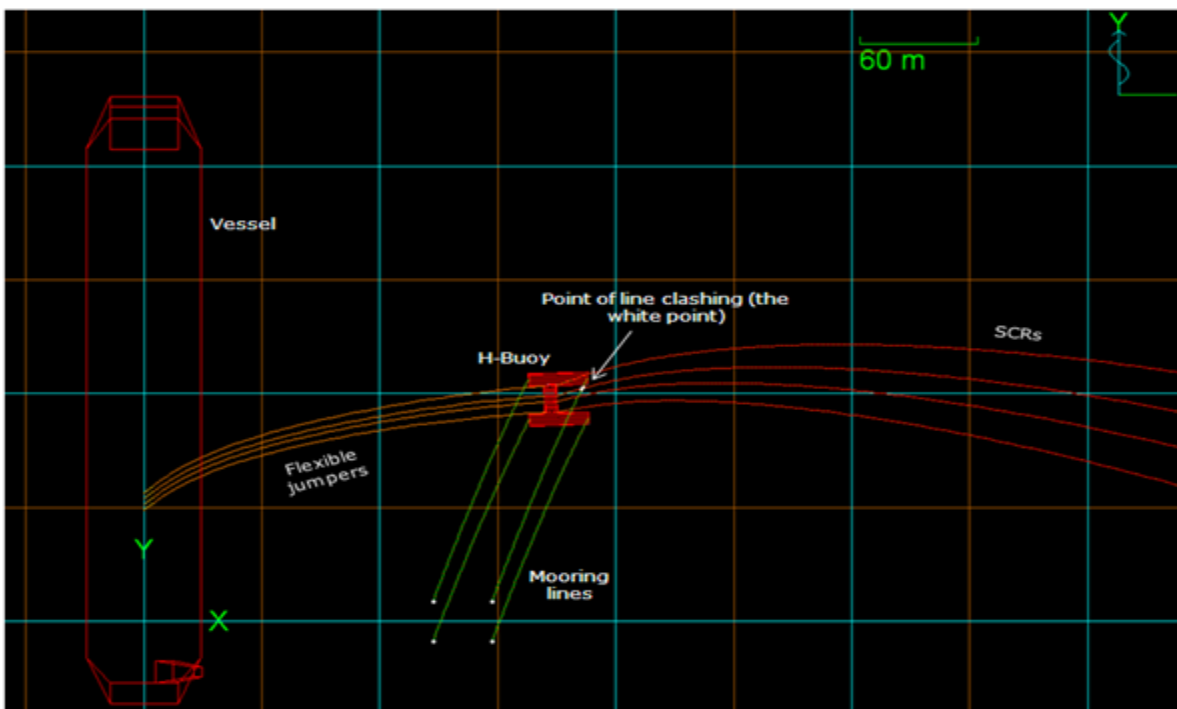
Figure 5 - 17: Plan View of Steel Catenary Risers supported by H-shaped Buoy to illustrate Line Clashing

To eliminate this undesirable situation, the **Modified H-buoy** was studied at the same offset position and at larger vessel offset positions (up to 150 m) and **no clashing** was reported in the

riser system. In addition, the modified H-buoy gave satisfactory results with respect to the strength performance of the steel catenary risers and the flexible risers, and the stability of the buoy itself at the considered cross offset positions. Results for the riser system with modified H-buoy at 70 m vessel cross offset position are presented below.

Vessel Cross Offset	Environmental Load Combination	SCRs			
		Max. Von Mises Stress	Max. Von Mises Stress	Max. Von Mises Utilization	Min. Von Mises Utilization
(m)		(MPa)	(MPa)		
70	10-yr current + 100-yr wave	278.75	256.52	0.64	0.57

Table 5 - 61: Strength Performance of SCRs, with Modified H-Buoy and 10-yr Current + 100-yr Wave in Cross flow direction

Vessel Cross Offset	Environmental Load Combination	Flexible Jumpers	
		MBR	Minimum Tension
(m)		(m)	(kN)
70	10-yr current + 100-yr wave	46	106

Table 5 - 62: Strength Performance of Flexible Jumpers, with Modified H-Buoy and 10-yr Current + 100-yr Wave in Cross flow direction

Vessel Cross Offset	Environmental Load Combination	Buoy Trim Angle		
		Min.	Max.	Variation
(m)		(deg)	(deg)	(deg)
70	10-yr current + 100-yr wave	1.36	1.56	0.2

Table 5 - 63: Stability of Modified H-Buoy, with 10-yr Current + 100-yr Wave in Cross flow direction

The above results show that at a vessel cross offset position of 70 m, the maximum Von Mises utilization factors of the SCRs at the top and sagbend regions, and the minimum bend radius and minimum tension recorded along the flexible jumpers satisfy the design acceptance criteria given in **section 4.4**. Also, the small values of the buoy trim angle and its variation show that the modified H-buoy has appreciable stability when exposed to cross-flow environmental loads.

Chapter 6: PERIODS OF BUOY MOTIONS

6.0   Introduction

As a result of exposure of the subsurface buoy to in-line environmental loads (i.e. environmental loads in 0° or 180° direction, it undergoes prominent translation motions in directions parallel and perpendicular (in the direction of the water depth) to the environmental loads. The parallel motion is known as sway while the perpendicular motion is known as heave.

In this section, analysis models for computing periods in the aforementioned directions are presented and periods of motion of the buoys considered in **sections 5.2.1**, **5.2.3**, and **5.4.1** are computed based on the models.

6.1   Analysis Model for Sway Motion

Presented below is a diagram that typifies the sway motion of the buoy.
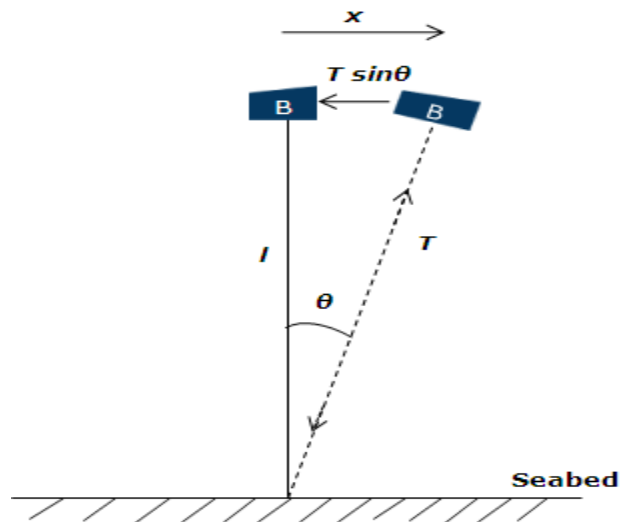
Figure 6 - 1: Illustration of Buoy Sway Motion

The above diagram shows a buoy (B) of mass m tethered to the seabed by a mooring line of length l with tension T. The sway motion of the buoy is in the direction of x. As the buoy moves through an angle θ and distance x, a force of magnitude $T\,sin\theta$ tends to restore it to its initial position. However, for very small values of θ, $sin\theta \approx \theta$, which implies $T\,sin\theta \approx T\theta$.

From elementary mathematics, $x = \theta l$, where θ is measured in radians. This implies $\theta = x/l$.

Thus, restoring force = $T\frac{x}{l}$. In addition to the restoring force, a force due to the added mass of water that moves with the buoy as the buoy undergoes sway motion also opposes the motion of the buoy. Thus, the resultant force acting on the buoy can be written as:

$$\sum F = -T\frac{x}{l} - m_a\ddot{x},$$

where:

m_a = added mass of water

$\ddot{x}$ = acceleration of the body

$\sum F$ = summation of forces acting on the buoy in the direction of x

Applying Newton's 2nd law of motion in the x direction,

$$\sum F = m\ddot{x},$$

Hence,

$$-T\frac{x}{l} - m_a\ddot{x} = m\ddot{x}$$

$$\Rightarrow (m + m_a)\ddot{x} + T\frac{x}{l} = 0$$

$$\Rightarrow \ddot{x} + \frac{T/l}{(m+m_a)}x = 0 \quad\text{...} \quad (1)$$

According to Rao S.S. (2005), the equation of motion of a one degree of freedom (1-DOF) system with mass m and stiffness k undergoing free vibration in the x direction can be expressed as:

$$m\ddot{x} + kx = 0$$

$$\Rightarrow \ddot{x} + \omega^2 x = 0 \quad\text{...} \quad (2)$$

where:

ω = angular frequency of the body = $\sqrt{\dfrac{k}{m}}$

Comparing equations (1) and (2) gives

$$\omega^2 = \frac{T/l}{(m + m_a)}$$

$$\Rightarrow \omega = \sqrt{\frac{T/l}{(m+m_a)}} \quad\text{...} \quad (3)$$

Equation (3) thus gives the angular frequency of the sway motion of the buoy.

The natural period, T_{ps}, of the sway motion is obtained as follows:

$$T_p = \frac{2\pi}{\omega}$$

$$\Rightarrow T_{ps} = \frac{2\pi}{\sqrt{\frac{T/l}{(m + m_a)}}}$$

$$\Rightarrow T_{ps} = 2\pi\sqrt{\left(\frac{m+m_a}{T/l}\right)} \quad\text{..} \quad (4)$$

6.2   Analysis Model for Heave Motion

The heave motion of the buoy can be modelled by a 1-DOF mass-spring system as shown below.
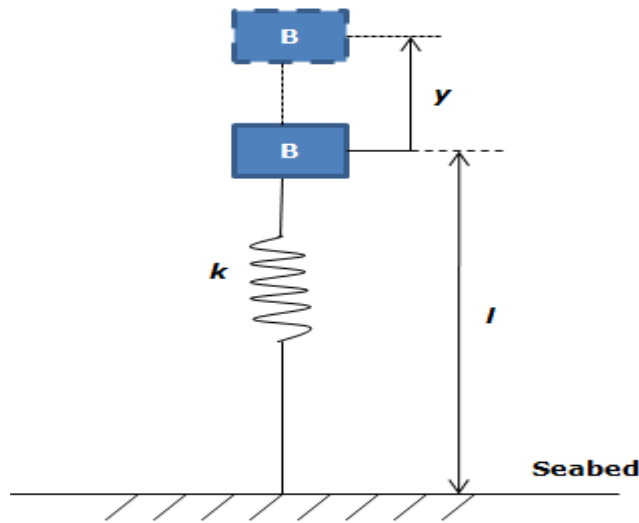
Figure 6 - 2: Illustration of Buoy Heave Motion

The above diagram shows buoy B with mass m, moored to the seabed by means of a mooring line with length l and stiffness k. The heave motion of the buoy is in the direction of y. As the buoy moves up a distance y, force $k.y$ opposes the motion and tends to restore it to its original position. In addition to this force, force $m_a\ddot{y}$ due to the added mass of water that moves with the buoy as a result of the heave motion also opposes the motion of the buoy. Hence, the total force acting on the buoy can be expressed as:

$$\sum F = -ky - m_a\ddot{y},$$

where:

$\ddot{y}$ = acceleration of the buoy

$\sum F$ = summation of forces in the y direction

Applying Newton's 2nd law of motion in the y direction,

$$\sum F = m\ddot{y},$$

Thus,

$$-ky - m_a\ddot{y} = m\ddot{y}$$

$$\Rightarrow (m + m_a)\ddot{y} + ky = 0$$

$$\Rightarrow \ddot{y} + \frac{k}{(m+m_a)}y = 0 \dots\dots\dots\dots\dots\dots\dots\dots\dots\dots\dots\dots\dots\dots\dots (5)$$

Comparing equation (5) with the y direction form of equation (2) (i.e. $\ddot{y} + \omega^2 y = 0$) gives

$$\omega^2 = \frac{k}{(m + m_a)}$$

$$\Rightarrow \omega = \sqrt{\frac{k}{(m+m_a)}} \dots\dots\dots\dots\dots\dots\dots\dots\dots\dots\dots\dots\dots\dots\dots (6)$$

Equation (6) thus gives the angular frequency of the buoy in heave motion.

The natural period, T_{ph}, of the heave motion is then obtained as follows:

$$T_p = \frac{2\pi}{\omega}$$

$$\Rightarrow T_{ph} = \frac{2\pi}{\sqrt{\frac{k}{(m + m_a)}}}$$

$$\Rightarrow T_{ph} = 2\pi\sqrt{\left(\frac{m+m_a}{k}\right)} \dots\dots\dots\dots\dots\dots\dots\dots\dots\dots\dots\dots (7)$$

Note that for a single mooring line,

$$k = \frac{EA}{L}$$

where E and A are the Young's modulus and cross sectional area of the mooring line respectively, and EA is the axial stiffness of the mooring line. However, since four parallel mooring lines are utilized in the riser system being studied, the effective stiffness of the mooring lines becomes

$$k_{eff} = \frac{4EA}{L}$$

Hence, the natural period of the heave motion of the buoy becomes

$$T_{ph} = 2\pi \sqrt{\left(\frac{m+m_a}{\frac{4EA}{L}}\right)} \dots\dots\dots\dots\dots\dots\dots\dots\dots\dots\dots\dots\dots (8)$$

6.3 Calculation of Sway and Heave Periods of Buoys

In this section, the respective sway and heave periods of the conventional and H-shaped buoys considered in **sections 5.2.1**, **5.2.3**, and **5.4.1** are calculated based on Equations (4) and (8).

6.3.1 Period Calculations for Section 5.2.1 (Base Case Conventional Buoy)

- Mass of main spar, m_m: 688800 kg
- Mass of side spar, m_s: 206600 kg
- Mass of back spar, m_b: 98400 kg
- Added mass of main spar, $m_{m,a}$: $C_a \times m_m$ = 510400.8 kg
- Added mass of back spar, $m_{b,a}$: $C_a \times m_b$ = 84820.8 kg
- Total added mass of bouy, m_a: $m_{m,a} + m_{b,a}$ = 595221.6 kg
- Mass of buoy, m: $m_m + 2m_s + m_b$ = 1200400 kg
- Overall mass of buoy, including added mass: $m + m_a$ = 1589021.6 kg

C_a values for the main spar and back spar of the conventional buoy can be found in **Table 4-9**.

The sway and heave periods of the base case conventional buoy of **section 5.2.1** are calculated and recorded below.

Load Case	Min. Mooring Line Tension	Max. Mooring Line Tension	Min. Sway Period of Buoy ($T_{ps, min}$)	Max. Sway Period of Buoy ($T_{ps, max}$)	Heave Period of Buoy (T_{ph})
	(kN)	(kN)	(sec)	(sec)	(sec)
1	699	1640	194	297	4.11
3	560	1466	205	331	4.11
4	715	1603	196	293	4.11
6	589	1437	207	323	4.11

Table 6 - 1: Computation of Sway and Heave Periods of the Base Case Conventional Buoy of Section 5.2.1

The sway and heave periods recorded in **Table 6-1** above are much different from the peak wave periods for the 10- and 100-year sea states (i.e. 18.8 sec and 17.5 sec) provided in **section 4.1.1.2**. This means the buoy considered in **section 5.2.1** is safe with respect to resonance with the peak waves in the sea states.

6.3.2 Period Calculations for Section 5.2.3 (Flooded Conventional Buoy)

- Mass of main spar, m_m: 792120 kg
- Mass of side spar, m_s: 206600 kg
- Mass of back spar, m_b: 98400 kg
- Added mass of main spar, $m_{m,a}$: $C_a \times m_m$ = 586960.92 kg
- Added mass of back spar, $m_{b,a}$: $C_a \times m_b$ = 84820.8 kg
- Total added mass of bouy, m_a: $m_{m,a} + m_{b,a}$ = 671781.72 kg
- Mass of buoy, m: $m_m + 2m_s + m_b$ = 1303720 kg
- Overall mass of buoy, including added mass: $m + m_a$ = 1975501.72 kg

The calculated sway and heave periods of the conventional buoy for the scenario of 10% reduction in the submerged weight of the main spar of the conventional buoy are presented below.

Load Case	Min. Mooring Line Tension	Max. Mooring Line Tension	Min. Sway Period of Buoy ($T_{ps,\,min}$)	Max. Sway Period of Buoy ($T_{ps,\,max}$)	Heave Period of Buoy (T_{ph})
	(kN)	(kN)	(sec)	(sec)	(sec)
1	509	1542	256	445	5.27
3	222	1556	255	675	5.27
4	535	1540	256	434	5.27
6	253	1529	257	632	5.27

Table 6 - 2: Computation of Sway and Heave Periods of the Flooded Conventional Buoy of Section 5.2.3

The results show that the sway and heave periods of the buoy are much different from the peak periods of the considered 10- and 100-year sea states, which means the buoy is safe with respect to resonance with the waves with the peak period.

6.3.3 Period Calculations for Section 5.4.1 (H-shaped Buoy)

- Mass of main spar, m_m: 221400 kg
- Mass of side spar, m_s: 442800 kg
- Added mass of main spar, $m_{m,a}$: $C_a \times m_m$ = 177341.4 kg
- Added mass of side spar, $m_{s,a}$: $C_a \times m_s$ = 66420 kg
- Total added mass of bouy, m_a: $m_{m,a} + 2m_{s,a}$ = 310181.4 kg
- Mass of buoy, m: $m_m + 2m_s$ = 1107000 kg

- Overall mass of buoy, including added mass: $m + m_a = 1417181.4$ kg

C_a values for the main and side spars of the H-shaped buoy can be found in **Table 4-9**.

The following sway and heave periods were obtained for the H-shaped buoy:

Load Case	Min. Mooring Line Tension	Max. Mooring Line Tension	Min. Sway Period of Buoy ($T_{ps,\ min}$)	Max. Sway Period of Buoy ($T_{ps,\ max}$)	Heave Period of Buoy (T_{ph})
	(kN)	(kN)	(sec)	(sec)	(sec)
1	638	1415	226	337	4.47
3	529	1247	241	370	4.47
4	665	1394	228	330	4.47
6	541	1200	246	366	4.47

Table 6 - 3: Computation of Sway and Heave Periods of the H-shaped Buoy of Section 5.4.1

Like the results in **sections 6.3.1** and **6.3.2**, the sway and heave periods of the H-shaped buoy reported in **Table 6-3** show that the buoy will exhibit satisfactory motion under exposure to waves with peak periods in the 10- and 100-year sea states, without resonance concerns.

Chapter 7: FATIGUE ANALYSIS OF STEEL CATENARY RISERS SUPPORTED BY SUBSURFACE BUOY

7.0 Introduction

Risers, being slender structures, are sensitive to fatigue. Riser fatigue mainly arises due to the random nature of environmental loads coupled with complex vessel movements (Ruswandi M.I., 2009). DNV-OS-F201 (2010) says riser fatigue analysis should consider all relevant cyclic load effects including:

- First order wave effects (direct wave loads and associated floater motions)
- Second order floater motions
- Thermal and pressure induced stress cycles
- Vortex induced vibrations
- Collisions

Wave induced fatigue contributes significantly to the total fatigue performance of steel catenary risers, through wave induced vessel motions. The SCR wave fatigue loading is related to the combined effect of various parameters such as environmental conditions, riser content density, riser diameter, water depth, host vessel type and its motion behaviour. Wave loading fatigue damage in SCRs is generally greatest in the wave zone and at the touchdown point on the seabed (Xia J., 2008). Hence, only wave-induced riser fatigue is considered in this chapter.

As mentioned in **section 2.3.2.2.3**, fatigue assessment based on S-N curves will be utilized in this study in accordance with DNV-OS-F201 (2010) and DNV-RP-C203 (2010). This fatigue analysis is carried out with the adoption of the conventional buoy as the subsurface buoy.

7.1 Fatigue Assessment using S-N Curves

The following are considered when S-N curves are used to carry out fatigue check:

- Assessment of short-term distribution of nominal stress range
- Selection of appropriate S-N curve
- Incorporation of thickness correction factor
- Determination of stress concentration factor (SCF)
- Determination of accumulated fatigue damage (D_{fat}) over all short term conditions.

These are discussed below.

7.1.1 Nominal Stress Range, S-N curve selection, and Thickness Correction Factor

The basic fatigue capacity is given in terms of S-N curves expressing the number of stress cycles to failure (N) for a given constant stress range (S). This is expressed as:

$$N = \bar{a}S^{-m}$$

In logarithmic form, it can be written as:

$$\log N = \log \bar{a} - m \log S,$$

where $\bar{a}$ and m are empirical constants established by experiments.

The stress range (S) to be applied in fatigue damage calculations is found by application of a stress concentration factor (SCF) as well as a thickness correction to the nominal stress range as follows:

$$S = S_o \cdot SCF \cdot \left(\frac{t}{t_{ref}}\right)^k$$

where:

S_o Nominal stress range

$\left(\frac{t}{t_{ref}}\right)^k$ Thickness correction factor

t Thickness through which a crack will most likely grow. $t = t_{ref}$ is used for thickness t_{ref}.

t_{ref} Reference thickness equals 25 mm for welded connections other than tubular joints.

           For tubular joints, the reference thickness is 32 mm. For bolts, t_{ref} = 25 mm.

k Thickness exponent (a function of the actual structural design) on fatigue strength

           = 0.10 for tubular butt welds made from one side

           = 0.25 for threaded bolts subjected to stress variations in the axial direction

A number of S-N curves are given by DNV-RP-C203 (2010) for welded, tubular and other types of joints, and whichever curve is selected for a particular task depends on:

- The geometrical arrangement of the detail
- The direction of the fluctuating stress relative to the detail

- The method of fabrication and inspection of the detail.

For this present study, the F1 curve (with k = 0.25) of the S-N curves for seawater environment with cathodic protection is used. Below is a diagram of the different S-N curves for seawater environment with cathodic protection.
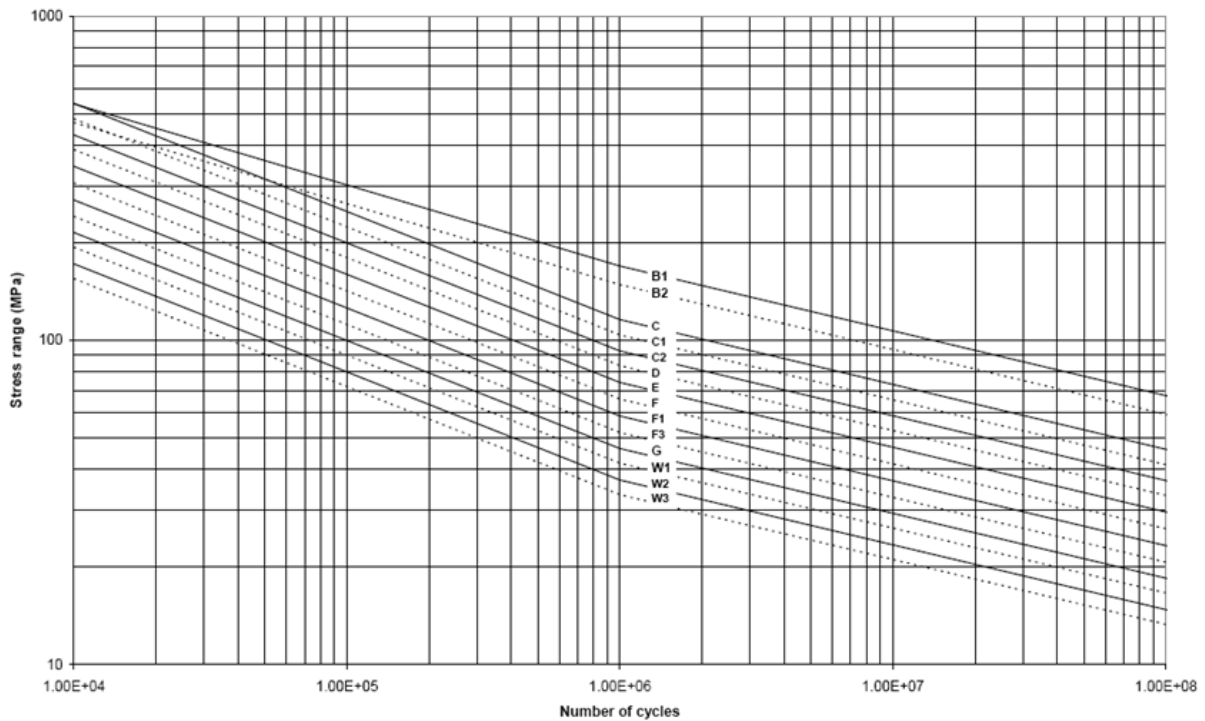
Figure 7 - 1: S-N Curves for Seawater Environment with Cathodic Protection (DNV-RP-C203, 2010)

7.1.2 Stress Concentration Factor (SCF)

This is defined as the ratio of the hot spot (structural) stress to local nominal stress. (Hot spot refers to a point in a structure where a fatigue crack may initiate due to the combined effect of structural stress fluctuation and the weld geometry or a similar notch). Stress concentration could arise from cracks, changes in cross-sectional area of a pipe, and geometrical misalignments as pipes are fitted together. These lead to local increase in the intensity of a stress field (Ruswandi M.I., 2009).

To account for this effect in this study, a SCF value of 1.2 is utilized.

7.1.3 Accumulated Fatigue Damage (D$_{fat}$)

The fatigue criterion to be satisfied is written as:

$$D_{fat} \cdot DFF \leq 1.0$$

where:

D_{fat} Accumulated fatigue damage (Palmgren-Miner rule)

DFF   Design fatigue factor = 10.0 due to the high safety class of the riser system under study since its failure would yield extreme consequences like significant environmental pollution and huge economic loss, coupled with the fact that it is difficult to conduct structural inspections in deep waters.

According to Palmgren-Miner rule,

$$D_{fat} = \sum_i \frac{n(S_i)}{N(S_i)}$$

where $n(S_i)$ is the number of stress cycles with range S_i and $N(S_i)$ is the number of stress cycles to failure.

7.2 Fatigue Analysis Procedure

The general approach for calculation of wave- and low- frequency fatigue damage contributions is given below:

- The wave environment scatter diagram is subdivided into a number of representative blocks.
- Within each block, a single sea-state is selected to represent all the sea states within the block. This representative sea state has the highest probability of occurrence within the block.
- The fatigue damage is estimated for each selected short-term sea state for all the blocks.
- The fatigue damage over all the blocks is summed up, taken into consideration directional probabilities, to obtain the weighted fatigue damage from all sea states.
- The fatigue life is the reciprocal of this weighted fatigue damage.

It should be noted that a conservative 1-year wave is adopted in this present study. This is because based on a previous confidential study, it was found out that wave induced fatigue response of the riser system is negligible.

7.3   Fatigue Analysis Result

The optimal conventional buoy drag and added mass coefficients, conventional buoy length, and oil-filled flowlines with riser anchor length of 1350 m obtained in **sections 5.1 and 5.2** are utilized in obtaining the results presented below.

Location along SCR	Fatigue Life (years)
Top region	1373
Sagbend region	> 10000

Table 7 - 1: Fatigue Analysis Result

Based on the results above, it can be concluded that usage of subsurface buoys with SCRs gives robust fatigue performance to the risers.

Chapter 8: CONCLUSION AND RECOMMENDATIONS

8.0   Introduction

The present study has looked into the improved strength performance, stability, and fatigue performance which results from the usage of the riser system known as steel catenary risers supported by subsurface buoy. A review of some riser systems used in deepwater applications was firstly carried out, followed by a review of important design codes that govern riser design. The strength performance, stability, and fatigue performance of the riser system were evaluated by studying three different subsurface buoy shapes (rectangular buoy, H-shaped buoy, and the modified H-buoy). The first two buoy shapes were utilized in studying the strength performance and stability of the riser system but only the rectangular buoy was used in studying the fatigue performance of the riser system. The third buoy shape was utilized as a modification of the H-shaped buoy to eliminate line clashing concerns which occur when the riser system is subjected to cross flow environmental loads.

The thesis example riser system was subjected to static and dynamic analysis, and the results are summarized as follows:

8.1   Summary

- Buoy size: For the conventional buoy, this was checked by varying the length of its side spar while for the H-shaped buoy, the check was done by varying the offset of its main spar from the mid-length position of its side spars (i.e. the location of its main spar relative to the mid-length position of its side spars). The following were observed:
  - Static analysis results for the conventional buoy under the influence of no current (**Table 5-1**) show that with very short and long buoy lengths, the magnitude of the trim angle of the buoy increases. However, the static analysis results under the influence of 10-year and 100-year currents (**Tables 5-2** and **5-3**) reveal that not only do short buoy lengths lead to high trim angles, they also lead to high Von Mises stress value (around 300 MPa) at the sagbend region of the SCRs when the vessel is at its near offset position.
  - Static analysis results for the H-shaped buoy under the influence of no current (**Table 5-35**) show that the closer the main spar of the H-buoy is to the mid-length position of its side spars (i.e. the smaller the main spar offset), the higher the magnitude of the buoy trim angle. Also, when the magnitude of the main spar offset gets too large (around -5 m), the magnitude of the trim angle starts to increase.
- Riser anchor length: It was observed from the static analysis results in **Table 5-4** that under the influence of no current, increase in the riser anchor length leads to increase in the SCR hang-off angle, while too long and too short riser anchor lengths were found to lead to increase in the magnitude of the trim angle of the conventional buoy. On the other hand,

Table 5-46 shows that the trim angle of the H-shaped buoy is not affected by the riser anchor length. However, it was also noted that the longer the riser anchor length for the H-shaped buoy, the higher the SCR hang-off angle.

- Flowline content: Static analysis results in **sections 5.1.3** and **5.3.3** show that at all vessel offset positions and under the action of in-line currents, both the rectangular buoy and the H-shaped buoy are more stable when the flexible jumpers and steel catenary risers are oil-filled than when they are empty or flooded with water. This is because the least buoy trim angles are obtained when the flowlines are oil-filled. It was also observed that the highest Von Mises stress values were obtained when the oil-filled flowlines are used with the two buoys.

- Drag coefficient of buoy: Static analysis results for the conventional buoy and the H-shaped buoy in **sections 5.1.4** and **5.3.4** respectively show that for a particular vessel offset value and applied current, increasing the drag coefficient of each buoy from 1.2 to 1.6 leads to negligible changes in its trim angle and much less than 1% change in the strength parameters of the flowlines (see **Tables 5-17** and **5-49**).

- Added mass coefficient of buoy: Like what was obtained when the drag coefficient of both the conventional buoy and H-shaped buoy were varied, dynamic analysis results in **sections 5.2.2** and **5.4.2** show that reducing or increasing the added mass coefficient of the buoy (conventional buoy or H-shaped buoy) by 20 percent leads to no significant changes in the trim angle and displacement values of both buoys, and very negligible changes in the strength parameters of the flowlines.

- Flooding of Conventional Buoy: Comparison of dynamic analysis results of the base case conventional buoy (**section 5.2.1**) and those of the flooded conventional buoy (**section 5.2.3**) show that reduction in submerged weight of the conventional buoy as a result of water ingress into a compartment of its main spar results in higher and slightly reduced Von Mises stress values at the sagbend and top regions of the SCRs respectively, and reduced maximum buckling utilization factor at the sagbend while the value at the top end of the SCRs remained fairly constant compared with the base case conventional buoy. In addition, the sagbend Von Mises stress when the vessel is at its near position is observed to have the highest value out of all the load cases checked for the flooded buoy situation.

- Line clashing check: The riser system when used with the H-shaped buoy was found to be susceptible to collision of some of its lines (flexible jumpers, SCRs, and mooring lines) when exposed to cross flow environmental loads in the 90° direction and at a cross vessel offset of 70 m. This can be seen in **Figure 5-16**. However, usage of the modified H-buoy (which has a wider distance between its side spars than what obtains with the H-shaped buoy) helped to eliminate the line clashing issue. Dynamic analysis results of the modified H-buoy in **Tables 5-61**, **5-62**, and **5-63** for cross vessel offset of 70 m also show that the Von Mises

utilization factors of the SCRs is less than 0.8 (as required by design codes), there is no compression in the jumpers, and the buoy trim angle magnitude is not high coupled with having low variation value of 0.2.

- Sway and heave periods of buoys: Generally, the heave periods of the base case conventional buoy (**section 6.3.1**), flooded conventional buoy (**section 6.3.2**), and the H-shaped buoy (**section 6.3.3**) were found to be small (i.e. 4.11, 5.27, and 4.47 sec respectively). However, the sway periods were observed to be on the high side (see **Tables 6-1**, **6-2**, and **6-3**). It was also noted that the sway and heave period values differ from the peak wave periods associated with the 10- and 100-year sea states utilized in the study.

- Fatigue analysis: It was observed that the riser system has a very robust fatigue performance with respect to wave induced fatigue loading, with fatigue lives of 1373 years and over 10000 years at the top and sagbend regions of the SCRs respectively.

8.2 Conclusion

On the basis of the above summary and the results presented in Chapters 5, 6, and 7, the following conclusions can be drawn:

- The length of the conventional buoy influences its stability and the strength performance of the SCRs of the riser system. In particular, too short buoy length would adversely affect the stability of the buoy and the strength performance of the SCRs. Also, the main spar offset of the H-shaped buoy determines to a large extent the stability of the buoy.

- Too long and too short riser anchor lengths will have much negative influence on the stability of the conventional buoy and the hang-off angle of the SCRs when the riser system is subjected to dynamic environmental loads. The same applies to the H-shaped buoy also.

- The oil-filled flowline situation gives the best buoy (both conventional and H-shaped buoys) stability, and it is also the most critical flowline internal fluid condition to the strength performance of the SCRs as it gives the highest SCR Von Mises values.

- Variations in drag and added mass coefficients of both the conventional and H-shaped buoys have negligible effects on the stability of the buoys and the strength performance of the flowlines.

- Flooding of the conventional buoy could negatively affect the sagbend Von Mises stress values of the SCRs.

- Usage of the modified H-buoy helps eliminate line clashing concerns, coupled with the fact that it also has acceptable stability and gives satisfactory strength performance to flowlines.

- The riser system has robust fatigue performance.

In addition to the above, the following comparisons can be made between the conventional buoy and the H-shaped buoy:

- Strength performance of the SCRs: Comparison of the base case dynamic analysis results of the riser system when the subsurface buoy is the conventional buoy (**section 5.2.1**) and that when it is the H-shaped buoy (**section 5.4.1**) shows that the former offers better strength performance to the SCRs because the Von Mises and buckling utilization factor values of the SCRs recorded with the former are less than those recorded with the latter.
- Stability of buoys: Comparison of the base case dynamic analysis results also reveals that the trim angle values and variations of the H-shaped buoy are less than those of the conventional buoy. This implies the H-shaped buoy offers better stability to the riser system in comparison with the conventional buoy.

8.3   Recommendations

- Further studies could be done to evaluate effects of failure of mooring lines on the strength performance and stability of the riser system.
- Tests can be carried out in a wave tank to verify the behaviour of the buoys and the observed interference between the mooring lines and the SCRs when the H-shaped buoy is used.
- Fatigue loading due to vortex induced vibrations can also be studied.

References

1. Alexander, W.L., Mason, W., and Mark Chang, S.H./Aker Engineering, Inc. (1999): Dynamic Performance Comparison of Deepwater Riser Systems for a Turret-Moored FPS. Paper prepared for presentation at the Offshore Technology Conference, Houston, USA.

2. Andresen, T. (2007): Umbilical and Flexible Pipeline Installation Analysis Guideline. Subsea 7

3. API RP 2RD (2006): Design of Risers for Floating Production Systems (FPSs) and Tension-Leg Platforms (TLPs). American Petroleum Institute, USA.

4. Bai, Y. and Bai, Q. (2005): Subsea Pipelines and Risers (First Edition). Amsterdam: Elsevier.

5. Bell, J.M., Chin, Y.D., and Hanrahan, S. (2005): State-of-the-Art of Ultra Deepwater Production Technologies. Paper prepared for presentation at the Offshore Technology Conference, Houston, USA.

6. Dale, N. and Karunakaran, D. (2007): The Grouped SLOR: Design and Implementation. 26th International Conference on Offshore Mechanics and Arctic Engineering, San Diego, USA.

7. DNV-OS-F201 (2010): Dynamic Risers. Det Norske Veritas, Norway.

8. DNV-RP-C203 (2010): Fatigue Design of Offshore Steel Structures. Det Norske Veritas, Norway.

9. DNV-RP-H103 (2011): Modelling and Analysis of Marine Operations. Det Norske Veritas, Norway.

10. Franciss, R. (2005): Subsurface Buoy Configuration for Rigid Risers in Ultradeep Water. Paper prepared for presentation at the SPE Latin American and Caribbean Petroleum Engineering Conference, Rio de Janeiro, Brazil.

11. Hoffman, D., Ismail, N.M., Nielsen, R., and Chandwani, R. (1991): Design of Flexible Marine Risers in Deep and Shallow Water. Paper presented at the 23rd Annual OTC in Houston, Texas, USA.

12. Karunakaran, D., Lee, D., and Mair, J., Subsea 7 (2009): Qualification of the Grouped SLOR Riser System. Paper prepared for presentation at the Offshore Technology Conference, Houston, USA.

13. Legras, J. and Saint-Marcoux, J. (2011): Management of Hybrid Riser Towers Integrity. Paper prepared for presentation at the Offshore Technology Conference, Houston, USA.

14. Lim, F. (2006): Installation of Risers in Deep Waters. 4th PetroMin Deepwater and Subsea Technology Conference and Exhibition, Kuala Lumpur, Malaysia.

15. Mungall, J.C.H., Garrett, D.L., and Alexander, C.H. (1997): Marine Steel Catenary Riser System. United States Patent (Patent Number: 5639187).

16. NORSOK Standard N-003 (2007): Actions and Action Effects. Norway.

17. O'Brien, P. and O'Sullivan, E. (1966): Deepwater Compliant Riser Systems – The Technical Challenges and Solutions. Society for Underwater Technology.

18. Phifer, E.H., Kopp, F., Swanson, R.C., Allen, D.W., and Langner, C.G. (1994): Design and Installation of Auger Steel Catenary Risers. Paper presented at the 26th Annual OTC in Houston, USA.

19. Rao, S.S. (2005): Mechanical Vibrations (Fourth Edition in SI Units). Prentice Hall, Pearson Education South Asia Pte Ltd, Singapore 629733.

20. Ruswandi, M.I. (2009): Improvisation of Deepwater Weight Distributed Steel Catenary Riser. Masters thesis, Faculty of Science and Technology, University of Stavanger, Norway.

21. Saint-Marcoux, J. and Legras, J. (2011): Lessons Learned on the Design and Construction of Hybrid Riser Towers. Paper prepared for presentation at the Offshore Technology Conference, Houston, USA.

22. SBM Atlantia: Steel Catenary Riser (SCR) Studies. As retrieved from http://www.sbmatlantia.comhttp://www.sbmatlantia.com/innovation/research-development/steel-catenary-riser-studies/ on March 3, 2011.

23. Serta, O.B., Longo, C.E.V., and Roveri, F.E. (2001): Riser Systems for Deep and Ultra-Deepwaters. Paper prepared for presentation at the Offshore Technology Conference, Houston, USA.

24. Shu, S., Seehausen, R., Bledsoe, S., and Powell, T.: Reviewing the state of Deepwater Production Risers. As retrieved from http://www.offshore-mag.com/index/article-display/3658771513/articles/offshore/volume-70/issue-11/subsea/reviewing-the-state-of-deepwater-production-risers.html on March 7, 2011.

25. Song, R. and Stanton, P. (2007): Deepwater Tieback SCR: Unique Design Challenges and Solutions. Paper prepared for presentation at the Offshore Technology Conference, Houston, USA.

26. Terje, C. and D'Souza, R. (2001): Deepwater E and P: Dynamic Risers key component for Deepwater Drilling, Floating Production. As retrieved from http://www.offshore-mag.com/index/article-display/100597/articles/offshore/volume-61/issue-5/news/deepwater-ep-dynamic-risers-key-component-for-deepwater-drilling-floating-production.html on March 14, 2011.

27. Xie, J. (2008): Weight-optimised Steel Catenary Risers and their Applications in harsh Deepwater Environment. Ph.D thesis, Department of Naval Architecture and Marine Engineering, Universities of Glasgow and Strathclyde.

Appendix A: WAVE SPECTRUM FORMULATION

Idealised wave spectra used to represent the characteristics of real waves found in offshore locations include the Pierson-Moskowitz model, Bretschneider or ITTC two parameter spectrum, JONSWAP model, and the Ochi-Hubble spectrum model. Out of these, the JONSWAP model is often used to model North Sea waves as it gives a good representation of the typical waves found at the location. The governing equation for the model is presented in the next section.

A.1: JONSWAP

The JONSWAP (Joint North Sea Wave Project) spectrum is often used to describe coastal waters where the fetch is limited. The governing equation for the spectrum is given as:

$$S(\omega) = \alpha g^2 \omega^{-5} exp\left(-1.25\left(\frac{\omega}{\omega_p}\right)^{-4}\right).\gamma^{\left(-(\omega-\omega_p)^2/2\sigma^2\omega_p^2\right)}$$

where:

ω Angular wave frequency $= \frac{2\pi}{T_\omega}$

T_ω Wave period

T_p Peak wave period

T_z Zero up-crossing wave period $\rightarrow \frac{T_p}{T_z} = 1.407(1 - 0.287 \ln\gamma)^{1/4}$

ω_p Angular spectral peak frequency $= \frac{2\pi}{T_p}$

g   Acceleration due to gravity

α $5.058(1 - 0.287 \ln\gamma)\frac{H_s^2}{T_p^4}$

σ Spectral width parameter

     $= 0.07$ for $\omega \leq \omega_p$

     $= 0.09$ for $\omega \geq \omega_p$

γ Peakedness parameter

= 1.0 for $\qquad$ $T_p \geq 5\sqrt{H_s}$

= $exp\left(5.75 - 1.15 \dfrac{T_p}{\sqrt{H_s}}\right)$ for $\qquad$ $3.6\sqrt{H_s} \leq T_p < 5\sqrt{H_s}$

= 5.0 for $\qquad$ $T_p < 3.6\sqrt{H_s}$

Appendix B: BUOY CALCULATIONS

B.1: H-Buoy Stability Calculations

$Te := 1000kg$

$$\rho := 1025\frac{kg}{m^3}$$

Assumption:

It is assumed in these calculations that the main spar and the side spars have submerged weights equal to 60% of each spar's displacement. Displacement herein refers to buoyancy which is the product of the submerged volume of an object and the density of the medium in which it is submerged.

Main Spar:

$L_1 := 15m$

$b_1 := 6m$

$h_1 := 6m$

$displ_1 := b_1 \cdot h_1 \cdot L_1 \cdot \rho$ $\qquad displ_1 = 5.535 \times 10^5 \, kg$

$w_{sub1} := displ_1 \cdot 0.6$ $\qquad w_{sub1} = 3.321 \times 10^5 \, kg$

$w_{air1} := displ_1 - w_{sub1}$ $\qquad w_{air1} = 2.214 \times 10^5 \, kg$

Side Spar (2off):

$L_2 := 30m$

$b_2 := 6m$

$h_2 := 6m$

$displ_2 := b_2 \cdot h_2 \cdot L_2 \cdot \rho$ $\qquad displ_2 = 1.107 \times 10^6 \, kg$

$w_{sub2} := displ_2 \cdot 0.6$ $\qquad w_{sub2} = 6.642 \times 10^5 \, kg$

$w_{air2} := displ_2 - w_{sub2}$ $\qquad w_{air2} = 4.428 \times 10^5 \, kg$

Total:

$displ_{tot} := displ_1 + 2 \cdot displ_2$ $\qquad displ_{tot} = 2.768 \times 10^6 \, kg$

$w_{sub\_tot} := w_{sub1} + 2 \cdot w_{sub2}$ $\qquad w_{sub\_tot} = 1.661 \times 10^6 \, kg$

$w_{air\_tot} := w_{air1} + 2 \cdot w_{air2}$ $\qquad w_{air\_tot} = 1.107 \times 10^6 \, kg$

B.2: Conventional Buoy Stability Calculations

$Te := 1000 kg$ $\rho := 1025 \dfrac{kg}{m^3}$

Assumption:
It is assumed in these calculations that the main spar, back spar and the side spars have submerged weights equal to 60% of each spar's displacement. Displacement herein refers to buoyancy which is the product of the submerged volume of an object and the density of the medium in which it is submerged.

Main Spar:

$L_1 := 15m$

$b_1 := 14m$

$h_1 := 8m$

$displ_m := L_1 \cdot b_1 \cdot h_1 \cdot \rho$ $displ_m = 1.722 \times 10^6 \, kg$

$w_{sub\_m} := displ_m \cdot 0.6$ $w_{sub\_m} = 1.033 \times 10^6 \, kg$

$w_{air\_m} := displ_m - w_{sub\_m}$ $w_{air\_m} = 6.888 \times 10^5 \, kg$

Back Spar:

$b_2 := 4m$

$h_2 := 4m$

$displ_b := L_1 \cdot b_2 \cdot h_2 \cdot \rho$ $displ_b = 2.46 \times 10^5 \, kg$

$w_{sub\_b} := displ_b \cdot 0.6$ $w_{sub\_b} = 1.476 \times 10^5 \, kg$

$w_{air\_b} := displ_b - w_{sub\_b}$ $w_{air\_b} = 9.84 \times 10^4 \, kg$

Side Spar (2 off):
- *Triangular part:*

$L_3 := 21m$

$b_3 := 4m$

$h_3 := 4m$

$displ_{st} := 0.5 \cdot L_3 \cdot b_3 \cdot h_3 \cdot \rho$ $displ_{st} = 1.722 \times 10^5 \, kg$

$w_{sub\_st} := displ_{st} \cdot 0.6$ $w_{sub\_st} = 1.033 \times 10^5 \, kg$

$w_{air\_st} := displ_{st} - w_{sub\_st}$ $w_{air\_st} = 6.888 \times 10^4 \, kg$

- *Rectangular part:*

$displ_{sr} := L_3 \cdot b_2 \cdot h_2 \cdot \rho$ $displ_{sr} = 3.444 \times 10^5 \, kg$

$$w_{sub\_sr} := displ_{sr} \cdot 0.6 \qquad\qquad w_{sub\_sr} = 2.066 \times 10^5 \, kg$$

$$w_{air\_sr} := displ_{sr} - w_{sub\_sr} \qquad\qquad w_{air\_sr} = 1.378 \times 10^5 \, kg$$

Therefore, for a side spar,

$$displ_s := displ_{st} + displ_{sr} \qquad\qquad displ_s = 5.166 \times 10^5 \, kg$$

$$w_{sub\_s} := w_{sub\_st} + w_{sub\_sr} \qquad\qquad w_{sub\_s} = 3.1 \times 10^5 \, kg$$

$$w_{air\_s} := displ_s - w_{sub\_s} \qquad\qquad w_{air\_s} = 2.066 \times 10^5 \, kg$$

Total:

$$displ_{tot} := displ_m + displ_b + 2 \cdot displ_s \qquad\qquad displ_{tot} = 3.001 \times 10^6 \, kg$$

$$w_{sub\_tot} := w_{sub\_m} + w_{sub\_b} + 2 \cdot w_{sub\_s} \qquad\qquad w_{sub\_tot} = 1.801 \times 10^6 \, kg$$

$$w_{air\_tot} := w_{air\_m} + w_{air\_b} + 2 \cdot w_{air\_s} \qquad\qquad w_{air\_tot} = 1.2 \times 10^6 \, kg$$

Since $w_{air\_tot} < displ_{tot}$ the buoy will float in water

B.3: Modified H-Buoy Calculations

Assumption:

It is assumed in these calculations that the main spar, back spar and the side spars have submerged weights equal to 60% of each spar's displacement. Displacement herein refers to buoyancy which is the product of the submerged volume of an object and the density of the medium in which it is submerged.

Main Spar:

The displacement, submerged weight, and weight in air are the same as those obtained for the main spar of the H-buoy. Thus,

$displ_m = 5.535 \times 10^5$ kg

$w_{sub, m} = 3.321 \times 10^5$ kg

$w_{air, m} = 2.214 \times 10^5$ kg

Side Spar (2 off):

As seen in **B.6-3**, each side spar is divided into two parts: Parts S_A and S_B.

- Part S_A: The displacement, submerged weight, and weight in air are the same as those obtained for the side spar of the H-buoy. Thus,

$displ_A = 1.107 \times 10^6$ kg

$w_{sub, A} = 6.642 \times 10^5$ kg

$w_{air, A} = 4.428 \times 10^5$ kg

- Part S_B:

$L_2 = 30$ m

$L_3 = 6$ m

$b_3 = 10$ m

$h_2 = 6$ m

Thus,

$displ_B = \frac{1}{2} \cdot (L_2 + L_3) \cdot b_3 \cdot h_2 \cdot \rho = 1107000$ Kg

$w_{sub, B}$ = displ$_B$. 0.6 = 664200 kg

$w_{air, B}$ = displ$_B$ - $w_{sub, B}$ = 442800 kg

Thus, total displacement, submerged weight and weight in air of side spar are:

displ$_S$ = displ$_A$ + displ$_B$ = 2214000 kg

$w_{sub, S}$ = $w_{sub, A}$ + $w_{sub, B}$ = 1328400 kg

$w_{air, S}$ = $w_{air, A}$ + $w_{air, B}$ = 885600 kg

Overall Displacement, Submerged Weight and Weight in Air of Modified H-buoy:

displ = displ$_m$ + 2.displ$_S$ = 4.982 × 10^6 kg

w_{sub} = $w_{sub, m}$ + 2.$w_{sub, S}$ = 2.989 × 10^6 kg

w_{air} = $w_{air, m}$ + 2.$w_{air, S}$ = 1.993 × 10^6 kg

B.4: Conventional Buoy Length Variation Calculations

As the side spar length of the conventional buoy varies, the following displacements, submerged weight, and weight in air values were obtained for the side spar of the conventional buoy based on **Appendix B.2**.

Side Spar Length (L_3)	$displ_{st}$	w_{sub_st}	W_{air_st}
(m)	(kg)	(kg)	(kg)
11	2.706×10^5	1.624×10^5	1.082×10^5
16	3.936×10^5	2.362×10^5	1.574×10^5
26	6.396×10^5	3.838×10^5	2.558×10^5
31	7.626×10^5	4.576×10^5	3.050×10^5

B.4 - 1: Conventional Buoy Length Variation Calculations

B.5: Flooded Conventional Buoy (Water Ingress)
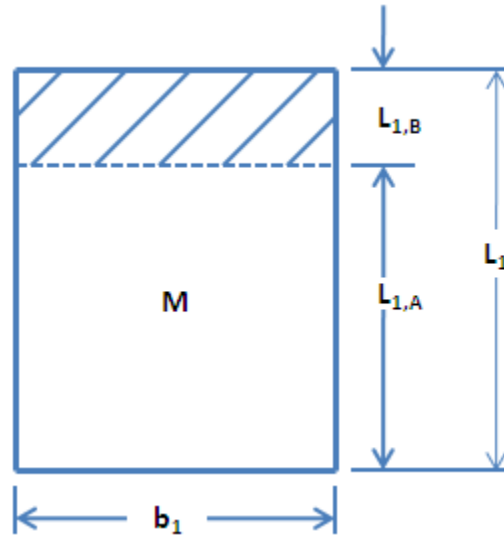
B.5 - 1: Plan View of Flooded Main Spar of Conventional Buoy

The above diagram shows the plan view of the main spar of the conventional buoy. The hatched portion represents the corner part flooded with water. The length of the flooded part is taken as $L_{1,B} = 4$ m. Thus, the length of the unflooded portion is $L_{1,A} = L_1 - L_{1,B} = 11$ m.

From **Appendix B.2**, submerged weight (w_{sub_m}) of the main spar is 1.033×10^6 kg. Due to flooding of the hatched section, the submerged weight of the main spar reduces by 10 percent. Hence, the new submerged weight of the main spar, $w_{sub\_new} = 0.9 \times 1.033 \times 10^6$ kg

$= 9.287 \times 10^5$ kg.

The following calculations can be made for the unflooded portion:

$displ_u = L_{1,A} \cdot b_1 \cdot h_1 \cdot \rho = 1.263 \times 10^6$ kg

$w_{sub, u} = displ_u \cdot 0.6 = 7.577 \times 10^5$ kg

$w_{air, u} = displ_u - w_{sub, u} = 5.053 \times 10^5$ kg

Therefore, the submerged weight ($w_{sub, f}$) of the flooded portions becomes:

$w_{sub, f} = w_{sub\_new} - w_{sub, u} = 1.71 \times 10^5$ kg

The displacement of the flooded portion is obtained as follows:

$\text{displ}_f = L_{1,B} \cdot b_1 \cdot h_1 \cdot \rho = 4.592 \times 10^5$ kg

Thus, weight in air ($w_{air,\,f}$) of the flooded portion is:

$w_{air,\,f} = \text{displ}_f - w_{sub,\,f} = 2.882 \times 10^5$ kg

(Note that L_1, b_1, and h_1 have the same values as those in **Appendix B.2**).

The **new overall submerged weight of the flooded buoy** can be found by:

$w_{sub\_total} = w_{sub\_new} + w_{sub\_b} + 2.w_{sub\_s} = (9.287 + 1.476 + (2 \times 3.1)) \times 10^5$ kg $= 1.6963 \times 10^6$ kg

$= 1693.3$ tonnes.

Note: w_{sub_b} and w_{sub_s} are the respective submerged weights of a side spar and the back spar of the conventional buoy as found in **Appendix B.2**.

B.6: Buoy Calculation Diagrams
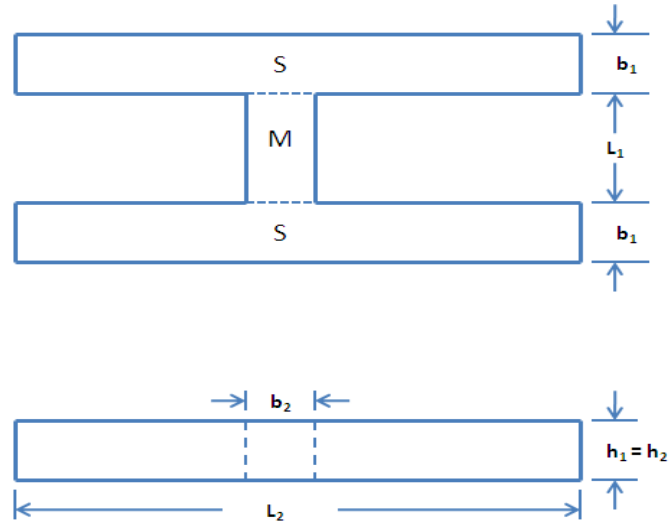
B.6 - 1: H-shaped Buoy
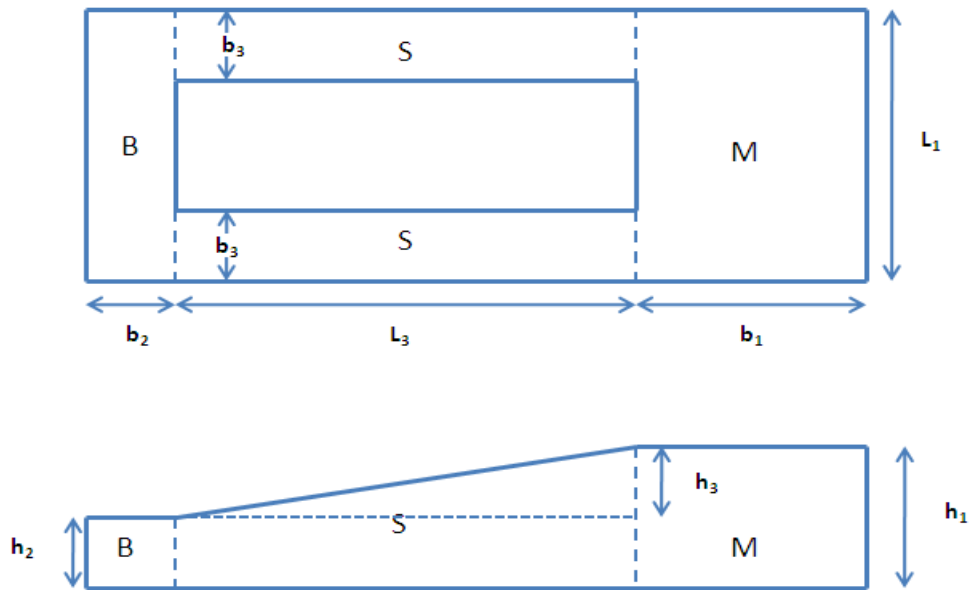
B.6 - 2: Conventional Buoy
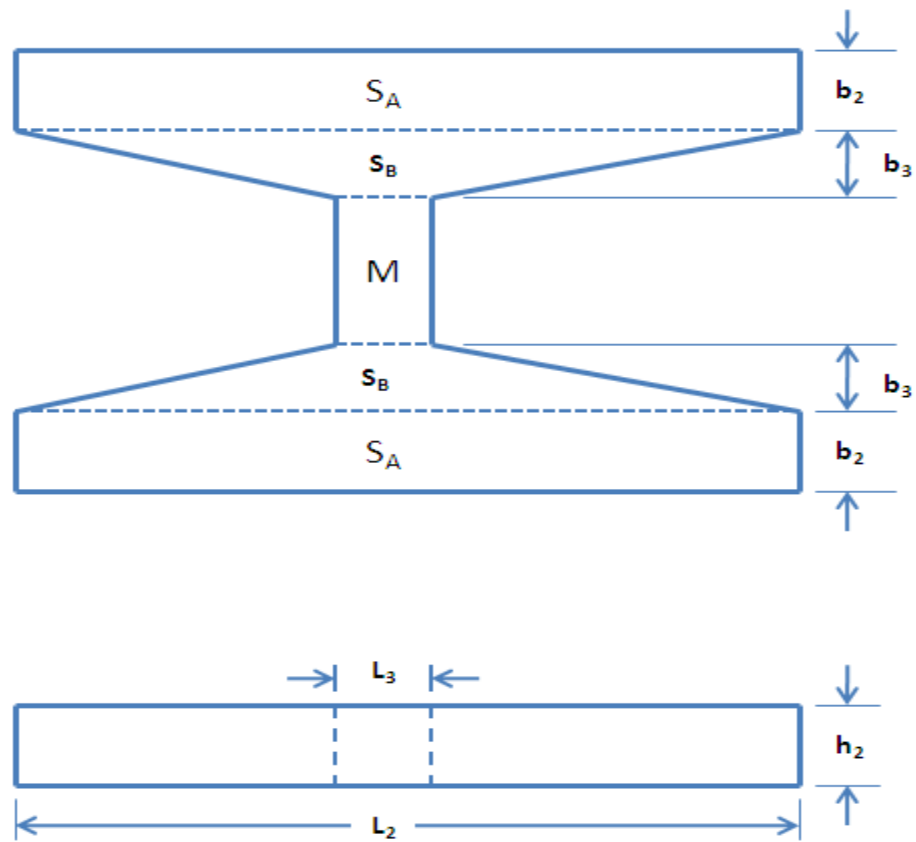
B.6 - 3: Modified H-buoy

Appendix C: RESULT TABLES

C.1 Full Static Analysis Results

Pipeline:	10"ID Riser, Wall thickness 26mm, 3" Coating
Water Depth:	1500m
Current:	-
Content:	0.5Te/m³

		Flexible (no1)							Buoy		Max values for SCR					Mooring line		
Side Spar Length	Current Case	Tension at FPSO	Tension at buoy	Declination at FPSO	Declination at Buoy	Horizontal projection	MBR	Hmin	Buoy trim angle	Depth in Water	Tension at buoy	Horizontal projection	Declination at buoy	Max von Mises Top	Max von Mises Sag	Max Top Tension	Max Anchor Tension	Min Anchor Tension
[m]	[-]	[kN]	[kN]	[deg]	[deg]	[m]	[m]	[m]	[deg]	[m]	[kN]	[m]	[deg]	[MPa]	[MPa]	[kN]	[kN]	[kN]
11		821	330	13	36	215	64	46	1.8	201	1514	602	9	276	259	1164	675	298
16		816	326	12	34	210	61	49	0.6	200	1519	603	9	276	259	1236	744	586
21	No current	812	314	11	33	204	57	51	0.0	200	1490	609	9	276	259	1337	849	841
26		809	310	11	31	198	54	53	-0.3	200	1522	609	9	276	258	1582	1091	957
31		806	307	10	29	192	51	55	-0.5	199	1494	610	9	276	258	1816	1324	1083

C.1 - 1: Full Static Analysis Results for Conventional Buoy Length Variation, at Zero Vessel Offset and No Current

Pipeline:	10"ID Riser, Wall thickness 26mm, 3" Coating
Buoy type:	Side spar length = 11m
Water Depth:	1500m
Current:	10-year
Content:	0.5Te/m³

			Flexible (no1)							Buoy			Max values for SCR					Mooring line		
Flexible length	Current Case	Vessel position	Tension at FPSO	Tension at buoy	Declination at FPSO	Declination at Buoy	Horizontal projection	MBR	Hmin	Position rel nominal	Buoy trim angle	Water Depth	Tension at buoy	Horizontal projection	Declination at buoy	Max von Mises Top	Max von Mises Sag	Max Top Tension	Max Anchor Tension	Min Anchor Tension
[m]	[-]	[m]	[kN]	[kN]	[deg]	[deg]	[m]	[m]	[m]	[m]	[deg]	[m]	[kN]	[m]	[deg]	[MPa]	[MPa]	[kN]	[kN]	[kN]
380	Near	-50	825	322	17	37	225	66	43	-59	1.5	204	1404	458	10	274	300	1149	658	445
380		0	848	354	20	47	248	86	33	-33	1.8	202	1431	509	11	275	285	1171	683	406
380	No current	-50	805	313	9	28	186	48	57	-21	1.6	202	1489	561	8	275	264	1145	654	335
380		0	821	330	13	36	215	64	46	0	1.8	201	1514	602	9	276	259	1164	675	298
380		50	846	352	16	45	241	85	36	24	2.0	200	1547	651	10	276	255	1197	705	253
380	Far	0	805	319	5	29	177	48	59	39	2.5	200	1616	705	7	278	248	1175	686	174
380		50	823	338	9	37	208	65	48	57	3.3	200	1642	744	8	278	246	1198	706	139

C.1 - 2: Full Static Analysis Results for Conventional Buoy with 11 m Side Spar Length and 10-year Current

Pipeline:	10"ID Riser, Wall thickness 26mm, 3" Coating
Buoy type:	Side spar length = 16m
Water Depth:	1500m
Current:	10-year
Content:	0.5Te/m³

			Flexible (no1)							Buoy			Max values for SCR					Mooring line		
Flexible length	Current Case	Vessel position	Tension at FPSO	Tension at buoy	Declination at FPSO	Declination at Buoy	Horizontal projection	MBR	Hmin	Position rel nominal	Buoy trim angle	Water Depth	Tension at buoy	Horizontal projection	Declination at buoy	Max von Mises Top	Max von Mises Sag	Max Top Tension	Max Anchor Tension	Min Anchor Tension
[m]	[-]	[m]	[kN]	[kN]	[deg]	[deg]	[m]	[m]	[m]	[m]	[deg]	[m]	[kN]	[m]	[deg]	[MPa]	[MPa]	[kN]	[kN]	[kN]
380	Near	-50	817	308	16	34	215	59	47	-56	0.1	204	1409	467	10	274	297	1226	736	721
380	Near	0	839	338	19	44	242	79	36	-32	0.3	202	1434	516	11	275	284	1245	757	687
380	No current	-50	802	297	9	26	178	44	59	-18	0.4	201	1487	569	8	276	263	1219	727	617
380	No current	0	816	326	12	34	210	61	49	0	0.6	200	1519	603	9	276	259	1236	744	586
380	No current	50	841	356	16	44	238	81	38	22	0.8	200	1543	650	10	276	255	1262	769	549
380	Far	0	804	305	5	28	173	46	60	36	1.0	200	1601	704	7	278	248	1240	750	471
380	Far	50	822	334	8	36	206	64	48	53	1.2	200	1609	741	8	278	247	1261	769	438

C.1 - 3: Full Static Analysis Results for Conventional Buoy with 16 m Side Spar Length and 10-year Current

Pipeline:	10"ID Riser, Wall thickness 26mm, 3" Coating
Buoy type:	Side spar length = 21 m
Water Depth:	1500m
Current:	10-year
Content:	0.5Te/m³

			Flexible (no1)							Buoy			Max values for SCR					Mooring line		
Flexible length	Current Case	Vessel position	Tension at FPSO	Tension at buoy	Declination at FPSO	Declination at Buoy	Horizontal projection	MBR	Hmin	Position rel nominal	Buoy trim angle	Water Depth	Tension at buoy	Horizontal projection	Declination at buoy	Max von Mises Top	Max von Mises Sag	Max Top Tension	Max Anchor Tension	Min Anchor Tension
[m]	[-]	[m]	[kN]	[kN]	[deg]	[deg]	[m]	[m]	[m]	[m]	[deg]	[m]	[kN]	[m]	[deg]	[MPa]	[MPa]	[kN]	[kN]	[kN]
380	Near	-50	810	311	15	31	206	54	50	-53	-0.5	203	1408	476	10	275	294	1463	975	835
380	Near	0	831	337	18	41	235	74	39	-31	-0.3	201	1406	517	11	275	283	1437	946	853
380	No current	-50	798	308	8	24	170	40	62	-16	-0.1	201	1501	572	8	276	262	1363	875	826
380	No current	0	812	314	11	33	204	57	51	0	0.0	200	1490	609	9	276	259	1337	849	841
380	No current	50	836	351	15	42	234	78	39	20	0.1	200	1546	649	10	276	255	1355	862	816
380	Far	0	802	317	4	27	169	44	61	34	0.3	199	1615	703	7	278	248	1336	844	739
380	Far	50	820	332	8	36	204	62	49	50	0.5	199	1637	738	8	278	247	1350	860	710

C.1 - 4: Full Static Analysis Results for Conventional Buoy with 21 m Side Spar Length and 10-year Current

Pipeline: 10"ID Riser, Wall thickness 26mm, 3" Coating
Buoy type: Side spar length = 26m
Water Depth: 1500m
Current: 10-year
Content: 0.5Te/m³

			Flexible (no1)							Buoy			Max values for SCR					Mooring line		
Flexible length	Current Case	Vessel position	Tension at FPSO	Tension at buoy	Declination at FPSO	Declination at Buoy	Horizontal projection	MBR	Hmin	Position rel nominal	Buoy trim angle	Water Depth	Tension at buoy	Horizontal projection	Declination at buoy	Max von Mises Top	Max von Mises Sag	Max Top Tension	Max Anchor Tension	Min Anchor Tension
[m]	[-]	[m]	[kN]	[kN]	[deg]	[deg]	[m]	[m]	[m]	[m]	[deg]	[m]	[kN]	[m]	[deg]	[MPa]	[MPa]	[kN]	[kN]	[kN]
380	Near	-50	805	296	14	28	197	49	54	-49	-0.7	202	1416	485	10	275	291	1700	1212	952
380		0	823	332	17	38	228	68	42	-30	-0.6	201	1408	524	11	275	282	1675	1187	968
380	No current	-50	796	308	7	22	163	37	65	-15	-0.4	200	1474	580	8	276	261	1605	1113	945
380		0	809	310	11	31	198	54	53	0	-0.3	200	1522	609	9	276	258	1582	1091	957
380		50	832	338	14	41	230	75	41	18	-0.2	199	1518	648	10	276	255	1551	1062	976
380	Far	0	800	315	4	26	165	43	62	33	-0.1	199	1614	702	7	278	248	1477	985	958
380		50	817	332	8	35	201	61	50	47	0.0	199	1605	731	8	278	247	1465	973	960

C.1 - 5: Full Static Analysis Results for Conventional Buoy with 26 m Side Spar Length and 10-year Current

Pipeline: 10"ID Riser, Wall thickness 26mm, 3" Coating
Buoy type: Side spar length = 31m
Water Depth: 1500m
Current: 10-year
Content: 0.5Te/m³

			Flexible (no1)							Buoy			Max values for SCR					Mooring line		
Flexible length	Current Case	Vessel position	Tension at FPSO	Tension at buoy	Declination at FPSO	Declination at Buoy	Horizontal projection	MBR	Hmin	Position rel nominal	Buoy trim angle	Water Depth	Tension at buoy	Horizontal projection	Declination at buoy	Max von Mises Top	Max von Mises Sag	Max Top Tension	Max Anchor Tension	Min Anchor Tension
[m]	[-]	[m]	[kN]	[kN]	[deg]	[deg]	[m]	[m]	[m]	[m]	[deg]	[m]	[kN]	[m]	[deg]	[MPa]	[MPa]	[kN]	[kN]	[kN]
380	Near	-50	800	292	13	25	189	44	57	-47	-0.8	202	1423	494	11	275	289	1932	1441	1079
380		0	817	316	16	35	222	63	45	-30	-0.7	200	1411	526	11	275	281	1907	1419	1093
380	No current	-50	794	291	7	20	156	34	67	-13	-0.6	200	1508	587	8	276	261	1836	1344	1072
380		0	806	307	10	29	192	51	55	0	-0.5	199	1494	610	9	276	258	1816	1324	1083
380		50	827	338	14	39	225	71	43	17	-0.4	199	1541	647	10	276	255	1790	1298	1100
380	Far	0	799	316	3	25	161	41	64	31	-0.3	199	1614	701	7	278	248	1713	1221	1083
380		50	815	329	7	34	198	59	52	44	-0.2	199	1633	729	8	278	247	1691	1199	1096

C.1 - 6: Full Static Analysis Results for Conventional Buoy with 31 m Side Spar Length and 10-year Current

Pipeline:	10"ID Riser, Wall thickness 26mm, 3" Coating
Buoy type:	**Side spar length = 11m**
Water Depth:	1500m
Current:	100-year
Content:	0.5Te/m³

			Flexible (no1)							Buoy			Max values for SCR					Mooring line		
Flexible length	Current Case	Vessel position	Tension at FPSO	Tension at buoy	Declination at FPSO	Declination at Buoy	Horizontal projection	MBR	Hmin	Position rel nominal	Buoy trim angle	Depth in Water	Tension at buoy	Horizontal projection	Declination at buoy	Max von Mises Top	Max von Mises Sag	Max Top Tension	Max Anchor Tension	Min Anchor Tension
[m]	[-]	[m]	[kN]	[kN]	[deg]	[deg]	[m]	[m]	[m]	[m]	[deg]	[m]	[kN]	[m]	[deg]	[MPa]	[MPa]	[kN]	[kN]	[kN]
380	Near	-30	838	332	19	43	241	78	36	-56	1.6	204	1397	462	11	275	303	1160	671	449
380	Near	0	855	360	21	49	254	90	30	-39	1.8	203	1385	494	11	275	293	1178	687	424
380	No current	-30	810	322	11	31	198	54	53	-13	1.7	201	1486	574	8	276	262	1153	661	321
380	No current	0	821	330	13	36	215	64	46	0	1.8	201	1514	602	9	276	259	1164	675	298
380	No current	30	834	343	15	42	231	76	40	14	1.9	200	1531	631	9	276	256	1184	692	272
380	Far	0	803	317	3	28	169	45	61	47	3.1	200	1606	728	7	278	247	1181	688	150
380	Far	30	812	326	5	32	188	55	54	57	3.6	200	1651	748	8	278	246	1191	699	131

C.1 - 7: Full Static Analysis Results for Conventional Buoy with 11 m Side Spar Length and 100-year Current

Pipeline:	10"ID Riser, Wall thickness 26mm, 3" Coating
Buoy type:	**Side spar length = 16m**
Water Depth:	1500m
Current:	100-year
Content:	0.5Te/m³

			Flexible (no1)							Buoy			Max values for SCR					Mooring line		
Flexible length	Current Case	Vessel position	Tension at FPSO	Tension at buoy	Declination at FPSO	Declination at Buoy	Horizontal projection	MBR	Hmin	Position rel nominal	Buoy trim angle	Depth in Water	Tension at buoy	Horizontal projection	Declination at buoy	Max von Mises Top	Max von Mises Sag	Max Top Tension	Max Anchor Tension	Min Anchor Tension
[m]	[-]	[m]	[kN]	[kN]	[deg]	[deg]	[m]	[m]	[m]	[m]	[deg]	[m]	[kN]	[m]	[deg]	[MPa]	[MPa]	[kN]	[kN]	[kN]
380	Near	-30	829	329	18	40	233	71	40	-53	0.1	203	1376	470	11	275	301	1238	747	725
380	Near	0	845	343	20	46	247	84	34	-38	0.3	202	1388	500	11	275	291	1252	761	704
380	No current	-30	807	316	10	29	191	50	55	-11	0.5	201	1505	581	8	276	261	1222	733	605
380	No current	0	816	326	12	34	210	61	49	0	0.6	200	1519	603	9	276	259	1236	744	586
380	No current	30	830	339	14	40	227	73	42	13	0.7	200	1535	630	9	276	256	1250	758	565
380	Far	0	802	316	3	27	166	44	61	44	1.2	200	1610	726	7	278	247	1245	753	447
380	Far	30	811	314	5	32	186	54	55	53	1.3	200	1644	745	8	278	246	1255	763	430

C.1 - 8: Full Static Analysis Results for Conventional Buoy with 16 m Side Spar Length and 100-year Current

Pipeline:	10"ID Riser, Wall thickness 26mm, 3" Coating
Buoy type:	Side spar length = 21 m
Water Depth:	1500m
Current:	100-year
Content:	0.5Te/m³

		Flexible (no1)							Buoy			Max values for SCR					Mooring line		
Flexible length	Current Case	Vessel position	Tension at FPSO	Tension at buoy	Declination at FPSO	Declination at Buoy	Horizontal projection	MBR	Hmin	Position rel nominal	Buoy trim angle	Depth in Water	Tension at buoy	Horizontal projection	Declination at buoy	Max von Mises Top	Max von Mises Sag	Max Top Tension	Max Anchor Tension	Min Anchor Tension
[m]	[-]	[m]	[kN]	[kN]	[deg]	[deg]	[m]	[m]	[m]	[m]	[deg]	[m]	[kN]	[m]	[deg]	[MPa]	[MPa]	[kN]	[kN]	[kN]
380	Near	-30	820	314	17	36	225	64	44	-51	-0.5	203	1408	478	11	275	298	1470	982	845
380		0	835	343	19	43	241	77	37	-37	-0.4	202	1415	502	11	275	290	1451	963	857
380	No current	-30	803	313	9	27	184	47	58	-10	-0.1	200	1508	588	8	276	261	1354	865	831
380		0	812	314	11	33	204	57	51	0	0.0	200	1490	609	9	276	259	1337	849	841
380		30	825	337	13	38	222	69	44	12	0.1	200	1535	630	9	276	256	1345	853	830
380	Far	0	801	302	3	26	162	42	62	41	0.4	199	1610	725	7	278	247	1338	846	717
380		30	810	313	5	31	184	52	56	50	0.5	199	1616	743	8	278	246	1343	854	701

C.1 - 9: Full Static Analysis Results for Conventional Buoy with 21 m Side Spar Length and 100-year Current

Pipeline:	10"ID Riser, Wall thickness 26mm, 3" Coating
Buoy type:	Side spar length = 26m
Water Depth:	1500m
Current:	100-year
Content:	0.5Te/m³

		Flexible (no1)							Buoy			Max values for SCR					Mooring line		
Flexible length	Current Case	Vessel position	Tension at FPSO	Tension at buoy	Declination at FPSO	Declination at Buoy	Horizontal projection	MBR	Hmin	Position rel nominal	Buoy trim angle	Depth in Water	Tension at buoy	Horizontal projection	Declination at buoy	Max von Mises Top	Max von Mises Sag	Max Top Tension	Max Anchor Tension	Min Anchor Tension
[m]	[-]	[m]	[kN]	[kN]	[deg]	[deg]	[m]	[m]	[m]	[m]	[deg]	[m]	[kN]	[m]	[deg]	[MPa]	[MPa]	[kN]	[kN]	[kN]
380	Near	-30	813	315	16	33	216	59	47	-48	-0.7	202	1412	481	11	275	296	1711	1220	961
380		0	827	333	18	40	234	71	40	-36	-0.6	201	1424	509	11	275	289	1695	1203	972
380	No current	-30	800	298	9	25	177	43	60	-9	-0.4	200	1511	590	8	276	260	1596	1105	949
380		0	809	310	11	31	198	54	53	0	-0.3	200	1522	609	9	276	258	1582	1091	957
380		30	821	326	13	37	217	66	46	11	-0.3	199	1535	630	9	276	256	1563	1074	968
380	Far	0	799	314	2	25	159	41	64	39	0.0	199	1633	723	7	278	247	1453	964	960
380		30	808	319	5	30	181	51	57	47	0.0	199	1644	736	8	278	246	1460	968	950

C.1 - 10: Full Static Analysis Results for Conventional Buoy with 26 m Side Spar Length and 100-year Current

Pipeline:	10"ID Riser, Wall thickness 26mm, 3" Coating
Buoy type:	Side spar length = 31m
Water Depth:	1500m
Current:	100-year
Content:	0.5Te/m³

			Flexible (no1)							Buoy			Max values for SCR					Mooring line		
Flexible length	Current Case	Vessel position	Tension at FPSO	Tension at buoy	Declination at FPSO	Declination at Buoy	Horizontal projection	MBR	Hmin	Position rel nominal	Buoy trim angle	Depth in Water	Tension at buoy	Horizontal projection	Declination at buoy	Max von Mises Top	Max von Mises Sag	Max Top Tension	Max Anchor Tension	Min Anchor Tension
[m]	[-]	[m]	[kN]	[kN]	[deg]	[deg]	[m]	[m]	[m]	[m]	[deg]	[m]	[kN]	[m]	[deg]	[MPa]	[MPa]	[kN]	[kN]	[kN]
380	Near	-30	808	312	16	30	208	54	51	-46	-0.9	201	1414	489	11	275	294	1938	1450	1086
380		0	820	329	18	37	227	66	43	-35	-0.8	201	1427	510	12	275	288	1927	1435	1096
380	No current	-30	797	309	8	24	171	40	62	-8	-0.6	200	1484	597	9	276	260	1828	1336	1076
380		0	806	307	10	29	192	51	55	0	-0.5	199	1494	610	9	276	258	1816	1324	1083
380		30	817	333	12	35	213	63	48	10	-0.5	199	1536	630	9	276	256	1801	1309	1092
380	Far	0	798	313	2	25	155	39	65	38	-0.3	199	1632	722	7	278	247	1693	1201	1084
380		30	806	314	4	30	178	49	58	45	-0.2	199	1613	735	7	278	246	1678	1189	1091

C.1 - 11: Full Static Analysis Results for Conventional Buoy with 31 m Side Spar Length and 100-year Current

Pipeline:	10"ID Riser, Wall thickness 26mm, 3" Coating
Water Depth:	1500m
Current:	-
Content:	0.5Te/m³

			Flexible (no1)							Buoy		Max values for SCR					Mooring line		
Flexible length	Current Case	Anchor position	Tension at FPSO	Tension at buoy	Declination at FPSO	Declination at Buoy	Horizontal projection	MBR	Hmin	Buoy trim angle	Depth in water	Tension at buoy	Horizontal projection	Declination at buoy	Max von Mises Top	Max von Mises Sag	Max Top Tension	Max Anchor Tension	Min Anchor Tension
[m]	[-]	[m]	[kN]	[kN]	[deg]	[deg]	[m]	[m]	[m]	[deg]	[m]	[kN]	[m]	[deg]	[MPa]	[MPa]	[kN]	[kN]	[kN]
380		1265	801	314	9	27	183	46	59	-0.4	199	1426	490	7	275	275	1425	933	806
380		1315	807	318	10	30	195	52	54	-0.2	200	1492	558	8	276	264	1374	885	825
380	No current	1350	812	314	11	33	204	57	51	0.0	200	1490	609	9	276	259	1337	849	841
380		1400	822	330	13	37	217	66	46	0.2	201	1541	680	10	276	252	1357	866	793
380		1450	836	338	15	42	231	76	40	0.5	201	1606	756	12	277	248	1386	894	733

C.1 - 12: Full Static Analysis Results for Riser Anchor Length Variation at Zero Vessel Offset and No Current – Conventional Buoy

Pipeline: 10"ID Riser, Wall thickness 26mm, 3" Coating
Buoy type: Conventional buoy, Cd=1.2
Water Depth: 1500m
Current: 10-year
Content: 0.5Te/m³

		Flexible (no1)								Buoy			Max values for SCR					Mooring line		
Flexible length	Current Case	Vessel position	Tension at FPSO	Tension at buoy	Declination at FPSO	Declination at Buoy	Horizontal projection	MBR	Hmin	Position rel nominal	Buoy trim angle	Depth in water	Tension at buoy	Horizontal projection	Declination at buoy	Max von Mises Top	Max von Mises Sag	Max Top Tension	Max Anchor Tension	Min Anchor Tension
[m]	[-]	[m]	[kN]	[kN]	[deg]	[deg]	[m]	[m]	[m]	[m]	[deg]	[m]	[kN]	[m]	[deg]	[MPa]	[MPa]	[kN]	[kN]	[kN]
380	Near	-50	809	311	15	30	205	53	51	-51.65	-0.48	203	1411	477	10	274.58	293.30	1463	975	834
380		0	830	332	18	41	234	73	40	-30.58	-0.31	201	1437	518	11	274.83	282.27	1437	946	852
380	No current	-50	798	308	8	24	170	40	62	-16.47	-0.15	201	1501	572	8	275.59	262.13	1363	875	826
380		0	812	314	11	33	204	57	51	0.00	-0.02	200	1490	609	9	275.84	258.53	1337	849	841
380		50	836	351	15	42	234	78	39	20.11	0.14	200	1546	649	10	276.16	254.86	1355	862	816
380	Far	0	803	304	4	27	170	45	61	33.51	0.31	199	1610	702	7	277.82	248.19	1336	844	740
380		50	820	326	8	36	205	63	49	49.20	0.45	199	1605	737	8	278.10	246.81	1350	860	711

C.1 - 13: Full Static Analysis Results for Riser System (with Content-filled flowlines) supported by Conventional Buoy with C$_d$ = 1.2, at Near, Zero, and Far Vessel Offsets, with 10-year Current

Pipeline: 10"ID Riser, Wall thickness 26mm, 3" Coating
Buoy type: Conventional buoy, Cd=1.2
Water Depth: 1500m
Current: 100-year
Content: 0.5Te/m³

		Flexible (no1)								Buoy			Max values for SCR					Mooring line		
Flexible length	Current Case	Vessel position	Tension at FPSO	Tension at buoy	Declination at FPSO	Declination at Buoy	Horizontal projection	MBR	Hmin	Position rel nominal	Buoy trim angle	Depth in water	Tension at buoy	Horizontal projection	Declination at buoy	Max von Mises Top	Max von Mises Sag	Max Top Tension	Max Anchor Tension	Min Anchor Tension
[m]	[-]	[m]	[kN]	[kN]	[deg]	[deg]	[m]	[m]	[m]	[m]	[deg]	[m]	[kN]	[m]	[deg]	[MPa]	[MPa]	[kN]	[kN]	[kN]
380	Near	-30	819	320	17	36	224	64	44	-49.75	-0.47	203	1409	479	11	274.65	297.65	1469	981	844
380		0	834	333	19	42	240	76	37	-36.07	-0.36	202	1423	503	11	274.80	289.59	1454	963	856
380	No current	-30	803	313	9	27	184	47	58	-10.28	-0.10	200	1508	588	8	275.68	260.70	1354	865	831
380		0	812	314	11	33	204	57	51	0.00	-0.02	200	1490	609	9	275.84	258.53	1337	849	841
380		30	825	337	13	38	222	69	44	11.59	0.07	200	1535	630	9	276.02	256.34	1345	853	830
380	Far	0	801	305	3	27	164	43	62	40.24	0.38	199	1632	724	7	278.26	246.98	1338	846	718
380		30	810	314	5	31	185	53	55	48.80	0.46	199	1644	737	8	278.42	246.31	1345	854	702

C.1 - 14: Full Static Analysis Results for Riser System (with Content-filled flowlines) supported by Conventional Buoy with C$_d$ = 1.2, at Near, Zero, and Far Vessel Offsets, with 100-year Current

Pipeline: 10"ID Riser, Wall thickness 26mm, 3" Coating
Buoy type: Conventional buoy, Cd=1.4
Water Depth: 1500m
Current: 10-year
Content: 0.5Te/m³

		Flexible (no1)							Buoy			Max values for SCR					Mooring line		
Flexible length	Current Case	Vessel position	Tension at FPSO	Tension at buoy	Declination at FPSO	Declination at Buoy	Horizontal projection	MBR	Hmin	Position rel nominal	Buoy trim angle	Depth in water	Tension at buoy	Horizontal projection	Declination at buoy	Max von Mises Top	Max von Mises Sag	Max Top Tension	Max Anchor Tension	Min Anchor Tension
[m]	[-]	[m]	[kN]	[kN]	[deg]	[deg]	[m]	[m]	[m]	[m]	[deg]	[m]	[kN]	[m]	[deg]	[MPa]	[MPa]	[kN]	[kN]	[kN]
380	Near	-50	810	311	15	31	206	54	50	-52.55	-0.48	202.79	1408	476	10	274.57	293.82	1463	975	835
380		0	831	337	18	41	235	74	39	-31.36	-0.30	201.39	1406	517	11	274.80	282.62	1437	946	853
380	No current	-50	798	308	8	24	170	40	62	-16.47	-0.15	200.63	1501	572	8	275.59	262.13	1363	875	826
380		0	812	314	11	33	204	57	51	0.00	-0.02	200.00	1490	609	9	275.84	258.53	1337	849	841
380		50	836	351	15	42	234	78	39	20.11	0.14	199.50	1546	649	10	276.16	254.86	1355	862	816
380	Far	0	802	317	4	27	169	44	61	34.50	0.31	199.43	1615	703	7	277.84	248.10	1336	844	739
380		50	820	332	8	36	204	62	49	50.08	0.45	199.46	1637	738	8	278.12	246.74	1350	860	710

C.1 - 15: Full Static Analysis Results for Riser System (with Content-filled flowlines) supported by Conventional Buoy with C_d = 1.4, at Near, Zero, and Far Vessel Offsets, with 10-year Current

Pipeline: 10"ID Riser, Wall thickness 26mm, 3" Coating
Buoy type: Conventional buoy, Cd=1.4
Water Depth: 1500m
Current: 100-year
Content: 0.5Te/m³

		Flexible (no1)							Buoy			Max values for SCR					Mooring line		
Flexible length	Current Case	Vessel position	Tension at FPSO	Tension at buoy	Declination at FPSO	Declination at Buoy	Horizontal projection	MBR	Hmin	Position rel nominal	Buoy trim angle	Depth in water	Tension at buoy	Horizontal projection	Declination at buoy	Max von Mises Top	Max von Mises Sag	Max Top Tension	Max Anchor Tension	Min Anchor Tension
[m]	[-]	[m]	[kN]	[kN]	[deg]	[deg]	[m]	[m]	[m]	[m]	[deg]	[m]	[kN]	[m]	[deg]	[MPa]	[MPa]	[kN]	[kN]	[kN]
380	Near	-30	820	314	17	36	225	64	44	-50.76	-0.47	202.66	1408	478	11	274.64	298.32	1470	982	845
380		0	835	343	19	43	241	77	37	-36.99	-0.35	201.73	1415	502	11	274.79	290.08	1451	963	857
380	No current	-30	803	313	9	27	184	47	58	-10.28	-0.10	200.37	1508	588	8	275.68	260.70	1354	865	831
380		0	812	314	11	33	204	57	51	0.00	-0.02	200.00	1490	609	9	275.84	258.53	1337	849	841
380		30	825	337	13	38	222	69	44	11.59	0.07	199.67	1535	630	9	276.02	256.34	1345	853	830
380	Far	0	801	302	3	26	162	42	62	41.45	0.39	199.45	1610	725	7	278.28	246.89	1338	846	717
380		30	810	313	5	31	184	52	56	49.93	0.47	199.49	1616	743	8	278.44	246.22	1343	854	701

C.1 - 16: Full Static Analysis Results for Riser System (with Content-filled flowlines) supported by Conventional Buoy with C_d = 1.4, at Near, Zero, and Far Vessel Offsets, with 100-year Current

Pipeline:	10"ID Riser, Wall thickness 26mm, 3" Coating
Buoy type:	Conventional buoy, Cd=1,6
Water Depth:	1500m
Current:	10-year
Content:	0.5Te/m³

Flexible (no1)										Buoy			Max values for SCR					Max Top Tension	Mooring line	
Flexible length	Current Case	Vessel position	Tension at FPSO	Tension at buoy	Declination at FPSO	Declination at Buoy	Horizontal projection	MBR	Hmin	Position rel nominal	Buoy trim angle	Depth in water	Tension at buoy	Horizontal projection	Declination at buoy	Max von Mises Top	Max von Mises Sag	Max Top Tension	Max Anchor Tension	Min Anchor Tension
[m]	[-]	[m]	[kN]	[kN]	[deg]	[deg]	[m]	[m]	[m]	[m]	[deg]	[m]	[kN]	[m]	[deg]	[MPa]	[MPa]	[kN]	[kN]	[kN]
380	Near	-50	811	312	15	31	207	54	50	-53.45	-0.48	203	1413	475	10	274.56	294.33	1467	976	835
380		0	832	331	18	41	236	74	39	-32.14	-0.30	201	1436	517	11	274.82	283.03	1438	947	854
380	No current	-50	798	308	8	24	170	40	62	-16.47	-0.15	201	1501	572	8	275.59	262.13	1363	875	826
380		0	812	314	11	33	204	57	51	0.00	-0.02	200	1490	609	9	275.84	258.53	1337	849	841
380		50	836	351	15	42	234	78	39	20.11	0.14	200	1546	649	10	276.16	254.86	1355	862	816
380	Far	0	802	316	4	27	168	44	61	35.49	0.31	199	1616	709	7	277.86	248.00	1336	843	737
380		50	819	331	8	35	203	62	50	50.96	0.46	199	1608	739	8	278.14	246.68	1352	860	709

C.1 - 17: Full Static Analysis Results for Riser System (with Content-filled flowlines) supported by Conventional Buoy with C_d = 1.6, at Near, Zero, and Far Vessel Offsets, with 10-year Current

Pipeline:	10"ID Riser, Wall thickness 26mm, 3" Coating
Buoy type:	Conventional buoy, Cd=1.6
Water Depth:	1500m
Current:	100-year
Content:	0.5Te/m³

Flexible (no1)										Buoyancy			Max values for SCR					Max Top Tension	Mooring line	
Flexible length	Current Case	Vessel position	Tension at FPSO	Tension at buoy	Declination at FPSO	Declination at Buoy	Horizontal projection	MBR	Hmin	Position rel nominal	Buoy trim angle	Depth in water	Tension at buoy	Horizontal projection	Declination at buoy	Max von Mises Top	Max von Mises Sag	Max Top Tension	Max Anchor Tension	Min Anchor Tension
[m]	[-]	[m]	[kN]	[kN]	[deg]	[deg]	[m]	[m]	[m]	[m]	[deg]	[m]	[kN]	[m]	[deg]	[MPa]	[MPa]	[kN]	[kN]	[kN]
380	Near	-30	821	315	17	37	226	65	43	-51.76	-0.47	203	1407	472	11	274.63	298.98	1473	982	846
380		0	836	335	19	43	242	78	36	-37.89	-0.35	202	1419	501	11	274.78	290.58	1455	964	858
380	No current	-30	803	313	9	27	184	47	58	-10.28	-0.10	200	1508	588	8	275.68	260.70	1354	865	831
380		0	812	314	11	33	204	57	51	0.00	-0.02	200	1490	609	9	275.84	258.53	1337	849	841
380		30	825	337	13	38	222	69	44	11.59	0.07	200	1535	630	9	276.02	256.34	1345	853	830
380	Far	0	800	315	3	26	161	42	63	42.65	0.40	199	1635	726	7	278.30	246.79	1338	846	715
380		30	809	323	5	31	183	52	56	51.07	0.47	199	1647	744	8	278.46	246.14	1346	854	699

C.1 - 18: Full Static Analysis Results for Riser System (with Content-filled flowlines) supported by Conventional Buoy with C_d = 1.6, at Near, Zero, and Far Vessel Offsets, with 100-year Current

Pipeline:	10"ID Riser, Wall thickness 26mm, 3" Coating
Buoy type:	Conventional buoy, Cd=1.2
Water Depth:	1500m
Current:	10-year
Content:	0.0Te/m³

			Flexible (no1)							Buoy			Max values for SCR					Mooring line		
Flexible length	Current Case	Vessel position	Tension at FPSO	Tension at buoy	Declination at FPSO	Declination at Buoy	Horizontal projection	MBR	Hmin	Position rel nominal	Buoy trim angle	Depth in water	Tension at buoy	Horizontal projection	Declination at buoy	Max von Mises Top	Max von Mises Sag	Max Top Tension	Max Anchor Tension	Min Anchor Tension
[m]	[-]	[m]	[kN]	[kN]	[deg]	[deg]	[m]	[m]	[m]	[m]	[deg]	[m]	[kN]	[m]	[deg]	[MPa]	[MPa]	[kN]	[kN]	[kN]
380	Near	-50	729	268	14	25	192	45	56	-51.38	-2.09	201	1060	501	12	49.89	220.41	1899	1407	774
380		0	745	296	17	36	224	64	45	-33.11	-1.92	200	1047	539	12	50.31	201.85	1876	1387	787
380	No current	-50	722	265	7	20	155	34	67	-13.98	-1.66	200	1139	613	9	52.90	147.01	1808	1316	764
380		0	733	280	10	29	191	50	56	0.00	-1.55	199	1152	637	9	53.57	140.46	1790	1298	775
380		50	752	313	14	39	223	70	44	17.39	-1.42	199	1166	674	10	54.43	133.12	1767	1275	792
380	Far	0	726	286	3	24	155	39	65	35.43	-1.25	199	1238	747	7	63.29	117.02	1692	1200	776
380		50	741	303	6	33	192	56	53	48.74	-1.16	199	1253	775	8	63.99	115.14	1672	1180	789

C.1 - 19: Full Static Analysis Results for Riser System (with Empty flowlines) supported by Conventional Buoy with C_d = 1.2, at Near, Zero, and Far Vessel Offsets, with 10-year Current

Pipeline:	10"ID Riser, Wall thickness 26mm, 3" Coating
Buoy type:	Conventional buoy, Cd=1.2
Water Depth:	1500m
Current:	100-year
Content:	0.0Te/m³

			Flexible (no1)							Buoy			Max values for SCR					Mooring line		
Flexible length	Current Case	Vessel position	Tension at FPSO	Tension at buoy	Declination at FPSO	Declination at Buoy	Horizontal projection	MBR	Hmin	Position rel nominal	Buoy trim angle	Depth in water	Tension at buoy	Horizontal projection	Declination at buoy	Max von Mises Top	Max von Mises Sag	Max Top Tension	Max Anchor Tension	Min Anchor Tension
[m]	[-]	[m]	[kN]	[kN]	[deg]	[deg]	[m]	[m]	[m]	[m]	[deg]	[m]	[kN]	[m]	[deg]	[MPa]	[MPa]	[kN]	[kN]	[kN]
380	Near	-30	736	286	16	31	212	55	49	-51.12	-2.11	201	1052	496	13	50.61	233.92	1907	1416	782
380		0	748	297	18	38	230	67	42	-39.16	-1.99	201	1061	518	13	50.86	220.12	1895	1403	792
380	No current	-30	726	283	8	23	170	40	63	-8.75	-1.62	199	1140	623	9	53.15	144.48	1798	1309	768
380		0	733	280	10	29	191	50	56	0.00	-1.55	199	1152	637	9	53.57	140.46	1790	1298	775
380		30	743	293	12	35	211	61	49	9.98	-1.47	199	1136	662	10	54.06	136.13	1777	1285	784
380	Far	0	726	285	1	24	148	37	66	42.45	-1.20	199	1226	769	7	65.27	114.80	1669	1180	778
380		30	733	292	3	29	171	47	59	49.67	-1.15	199	1244	786	7	65.65	113.89	1658	1169	785

C.1 - 20: Full Static Analysis Results for Riser System (with Empty flowlines) supported by Conventional Buoy with C_d = 1.2, at Near, Zero, and Far Vessel Offsets, with 100-year Current

Pipeline: 10"ID Riser, Wall thickness 26mm, 3" Coating
Buoy type: Conventional buoy, Cd=1.4
Water Depth: 1500m
Current: 10-year
Content: 0.0Te/m³

			Flexible (no1)							Buoy			Max values for SCR					Mooring line		
Flexible length	Current Case	Vessel position	Tension at FPSO	Tension at buoy	Declination at FPSO	Declination at Buoy	Horizontal projection	MBR	Hmin	Position rel nominal	Buoy trim angle	Depth in water	Tension at buoy	Horizontal projection	Declination at buoy	Max von Mises Top	Max von Mises Sag	Max Top Tension	Max Anchor Tension	Min Anchor Tension
[m]	[-]	[m]	[kN]	[kN]	[deg]	[deg]	[m]	[m]	[m]	[m]	[deg]	[m]	[kN]	[m]	[deg]	[MPa]	[MPa]	[kN]	[kN]	[kN]
380	Near	-50	729	269	14	26	193	46	56	-52.36	-2.09	201	1059	500	12	49.86	221.48	1899	1408	774
380		0	745	291	17	36	225	65	44	-33.98	-1.92	200	1074	538	12	50.29	202.68	1876	1388	788
380	No current	-50	722	265	7	20	155	34	67	-13.98	-1.66	200	1139	613	9	52.90	147.01	1808	1316	764
380		0	733	280	10	29	191	50	56	0.00	-1.55	199	1152	637	9	53.57	140.46	1790	1298	775
380		50	752	313	14	39	223	70	44	17.39	-1.42	199	1166	674	10	54.43	133.12	1767	1275	792
380	Far	0	726	286	3	24	154	39	65	36.47	-1.25	199	1239	748	7	63.35	116.87	1691	1199	776
380		50	740	298	6	33	191	56	53	49.68	-1.16	199	1254	776	8	64.04	115.01	1671	1179	789

C.1 - 21: Full Static Analysis Results for Riser System (with Empty flowlines) supported by Conventional Buoy with C_d = 1.4, at Near, Zero, and Far Vessel Offsets, with 10-year Current

Pipeline: 10"ID Riser, Wall thickness 26mm, 3" Coating
Buoy type: Conventional buoy, Cd=1.4
Water Depth: 1500m
Current: 100-year
Content: 0.0Te/m³

			Flexible (no1)							Buoy			Max values for SCR					Mooring line		
Flexible length	Current Case	Vessel position	Tension at FPSO	Tension at buoy	Declination at FPSO	Declination at Buoy	Horizontal projection	MBR	Hmin	Position rel nominal	Buoy trim angle	Depth in water	Tension at buoy	Horizontal projection	Declination at buoy	Max von Mises Top	Max von Mises Sag	Max Top Tension	Max Anchor Tension	Min Anchor Tension
[m]	[-]	[m]	[kN]	[kN]	[deg]	[deg]	[m]	[m]	[m]	[m]	[deg]	[m]	[kN]	[m]	[deg]	[MPa]	[MPa]	[kN]	[kN]	[kN]
380	Near	-30	737	286	16	31	213	56	49	-52.22	-2.11	201	1051	495	13	50.58	235.08	1907	1416	783
380		0	749	294	18	38	231	68	42	-40.18	-1.99	201	1048	517	13	50.83	221.26	1892	1403	793
380	No current	-30	726	283	8	23	170	40	63	-8.75	-1.62	199	1140	623	9	53.15	144.48	1798	1309	768
380		0	733	280	10	29	191	50	56	0.00	-1.55	199	1152	637	9	53.57	140.46	1790	1298	775
380		30	743	293	12	35	211	61	49	9.98	-1.47	199	1136	662	10	54.06	136.13	1777	1285	784
380	Far	0	725	286	1	24	147	37	66	43.72	-1.20	199	1227	770	7	65.34	114.65	1671	1179	778
380		30	733	287	3	28	170	46	60	50.87	-1.15	199	1235	787	7	65.71	113.74	1660	1168	785

C.1 - 22: Full Static Analysis Results for Riser System (with Empty flowlines) supported by Conventional Buoy with C_d = 1.4, at Near, Zero, and Far Vessel Offsets, with 100-year Current

Pipeline:	10"ID Riser, Wall thickness 26mm, 3" Coating
Buoy type:	Conventional buoy, Cd=1.6
Water Depth:	1500m
Current:	10-year
Content:	0.0Te/m³

			Flexible (no1)							Buoy			Max values for SCR					Mooring line		
Flexible length	Current Case	Vessel position	Tension at FPSO	Tension at buoy	Declination at FPSO	Declination at Buoy	Horizontal projection	MBR	Hmin	Position rel nominal	Buoy trim angle	Depth in water	Tension at buoyancy	Horizontal projection	Declination at buoy	Max von Mises Top	Max von Mises Sag	Max Top Tension	Max Anchor Tension	Min Anchor Tension
[m]	[-]	[m]	[kN]	[kN]	[deg]	[deg]	[m]	[m]	[m]	[m]	[deg]	[m]	[kN]	[m]	[deg]	[MPa]	[MPa]	[kN]	[kN]	[kN]
380	Near	-50	730	269	14	26	194	46	56	-53.34	-2.09	201	1058	499	12	49.84	222.38	1899	1408	775
380		0	746	297	17	37	226	66	44	-34.84	-1.92	200	1071	532	12	50.27	203.50	1876	1388	789
380	No current	-50	722	265	7	20	155	34	67	-13.98	-1.66	200	1139	613	9	52.90	147.01	1808	1316	764
380		0	733	280	10	29	191	50	56	0.00	-1.55	199	1152	637	9	53.57	140.46	1790	1298	775
380		50	752	313	14	39	223	70	44	17.39	-1.42	199	1166	674	10	54.43	133.12	1767	1275	792
380	Far	0	726	286	2	24	153	38	65	37.51	-1.25	199	1240	754	7	63.40	116.71	1690	1198	776
380		50	740	297	6	32	190	55	54	50.63	-1.16	199	1243	782	8	64.09	114.88	1667	1178	789

C.1 - 23: Full Static Analysis Results for Riser System (with Empty flowlines) supported by Conventional Buoy with C_d = 1.6, at Near, Zero, and Far Vessel Offsets, with 10-year Current

Pipeline:	10"ID Riser, Wall thickness 26mm, 3" Coating
Buoy type:	Conventional buoy, Cd=1.6
Water Depth:	1500m
Current:	100-year
Content:	0.0Te/m³

			Flexible (no1)							Buoy			Max values for SCR					Mooring line		
Flexible length	Current Case	Vessel position	Tension at FPSO	Tension at buoy	Declination at FPSO	Declination at Buoy	Horizontal projection	MBR	Hmin	Position rel nominal	Buoy trim angle	Depth in water	Tension at buoy	Horizontal projection	Declination at buoy	Max von Mises Top	Max von Mises Sag	Max Top Tension	Max Anchor Tension	Min Anchor Tension
[m]	[-]	[m]	[kN]	[kN]	[deg]	[deg]	[m]	[m]	[m]	[m]	[deg]	[m]	[kN]	[m]	[deg]	[MPa]	[MPa]	[kN]	[kN]	[kN]
380	Near	-30	738	286	17	32	214	56	48	-53.32	-2.11	201	1050	494	13	50.56	236.38	1907	1416	784
380		0	750	295	19	38	232	69	41	-41.18	-1.99	201	1036	516	13	50.81	222.23	1895	1404	794
380	No current	-30	726	283	8	23	170	40	63	-8.75	-1.62	199	1140	623	9	53.15	144.48	1798	1309	768
380		0	733	280	10	29	191	50	56	0.00	-1.55	199	1152	637	9	53.57	140.46	1790	1298	775
380		30	743	293	12	35	211	61	49	9.98	-1.47	199	1136	662	10	54.06	136.13	1777	1285	784
380	Far	0	725	271	1	23	146	36	67	44.99	-1.20	199	1250	777	7	65.41	114.48	1667	1178	778
380		30	732	293	3	28	169	46	60	52.08	-1.15	199	1263	789	7	65.77	113.60	1659	1167	785

C.1 - 24: Full Static Analysis Results for Riser System (with Empty flowlines) supported by Conventional Buoy with C_d = 1.6, at Near, Zero, and Far Vessel Offsets, with 100-year Current

Pipeline: 10"ID Riser, Wall thickness 26mm, 3" Coating
Buoy type: Conventional buoy, Cd=1.2
Water Depth: 1500m
Current: 10-year
Content: 1.025Te/m³

			Flexible (no1)							Buoy			Max values for SCR					Mooring line		
Flexible length	Current Case	Vessel position	Tension at FPSO	Tension at buoy	Declination at FPSO	Declination at Buoy	Horizontal projection	MBR	Hmin	Position rel nominal	Buoy trim angle	Depth in water	Tension at buoy	Horizontal projection	Declination at buoy	Max von Mises Top	Max von Mises Sag	Max Top Tension	Max Anchor Tension	Min Anchor Tension
[m]	[-]	[m]	[kN]	[kN]	[deg]	[deg]	[m]	[m]	[m]	[m]	[deg]	[m]	[kN]	[m]	[deg]	[MPa]	[MPa]	[kN]	[kN]	[kN]
380	Near	-50	897	346	16	35	218	62	45	-51.87	1.47	204	1772	459	9	79.07	226.74	1388	897	528
380		0	923	374	19	45	244	82	35	-27.84	1.61	203	1801	503	10	80.25	200.67	1411	920	488
380	No current	-50	881	340	9	28	185	47	57	-19.24	1.52	202	1843	542	8	83.93	162.98	1384	892	419
380		0	899	359	13	37	216	65	46	0.00	1.64	201	1873	581	8	85.35	150.79	1399	911	382
380		50	928	390	16	46	243	87	35	22.99	1.79	200	1933	624	9	87.11	138.22	1430	938	337
380	Far	0	884	338	6	30	185	51	56	31.47	1.94	200	2000	662	7	93.51	120.80	1407	915	264
380		50	906	365	10	39	216	70	45	49.84	2.23	200	2011	701	8	94.99	114.61	1425	936	225

C.1 - 25: Full Static Analysis Results for Riser System (with Flooded flowlines) supported by Conventional Buoy with C_d = 1.2, at Near, Zero, and Far Vessel Offsets, with 10-year Current

Pipeline: 10"ID Riser, Wall thickness 26mm, 3" Coating
Buoy type: Conventional buoy, Cd=1.2
Water Depth: 1500m
Current: 100-year
Content: 1.025Te/m³

			Flexible (no1)							Buoyancy			Max values for SCR					Mooring line		
Flexible length	Current Case	Vessel position	Tension at FPSO	Tension at buoyancy	Declination at FPSO	Declination at Buoy	Horizontal projection	MBR	Hmin	Position rel nominal	Buoy trim angle	Depth in water	Tension at buoyancy	Horizontal projection	Declination at buoyancy	Max von Mises Top	Max von Mises Sag	Max Top Tension	Max Anchor Tension	Min Anchor Tension
[m]	[-]	[m]	[kN]	[kN]	[deg]	[deg]	[m]	[m]	[m]	[m]	[deg]	[m]	[kN]	[m]	[deg]	[MPa]	[MPa]	[kN]	[kN]	[kN]
380	Near	-30	910	357	18	41	234	73	39	-48.21	1.52	204	1769	458	10	79.39	231.16	1399	908	531
380		0	928	378	20	47	249	86	33	-32.75	1.61	203	1776	489	10	80.14	213.12	1414	923	506
380	No current	-30	887	336	11	31	198	54	53	-11.96	1.56	202	1884	554	8	84.46	158.21	1387	899	405
380		0	899	352	13	37	216	65	46	0.00	1.64	201	1902	581	8	85.35	150.79	1399	911	382
380		30	915	375	15	42	233	77	39	13.31	1.72	201	1891	604	9	86.36	143.28	1415	926	356
380	Far	0	883	348	5	29	178	49	58	37.91	2.10	200	2018	679	7	95.18	116.63	1409	917	241
380		30	894	350	7	34	198	60	51	48.03	2.29	200	2037	704	8	95.99	113.45	1420	928	219

C.1 - 26: Full Static Analysis Results for Riser System (with Flooded flowlines) supported by Conventional Buoy with C_d = 1.2, at Near, Zero, and Far Vessel Offsets, with 100-year Current

Pipeline: 10"ID Riser, Wall thickness 26mm, 3" Coating
Buoy type: Conventional buoy, Cd=1.4
Water Depth: 1500m
Current: 10-year
Content: 1.025Te/m³

			Flexible (no1)							Buoy			Max values for SCR					Mooring line		
Flexible length	Current Case	Vessel position	Tension at FPSO	Tension at buoy	Declination at FPSO	Declination at Buoy	Horizontal projection	MBR	Hmin	Position rel nominal	Buoy trim angle	Depth in water	Tension at buoy	Horizontal projection	Declination at buoy	Max von Mises Top	Max von Mises Sag	Max Top Tension	Max Anchor Tension	Min Anchor Tension
[m]	[-]	[m]	[kN]	[kN]	[deg]	[deg]	[m]	[m]	[m]	[m]	[deg]	[m]	[kN]	[m]	[deg]	[MPa]	[MPa]	[kN]	[kN]	[kN]
380	Near	-50	898	347	16	35	219	62	45	-52.68	1.47	204	1782	454	9	79.03	227.65	1388	898	529
380		0	924	374	19	45	245	83	35	-28.53	1.62	203	1814	503	10	80.21	201.32	1411	921	488
380	No current	-50	881	340	9	28	185	47	57	-19.24	1.52	202	1843	542	8	83.93	162.98	1384	892	419
380		0	899	359	13	37	216	65	46	0.00	1.64	201	1873	581	8	85.35	150.79	1399	911	382
380		50	928	390	16	46	243	87	35	22.99	1.79	200	1933	624	9	87.11	138.22	1430	938	337
380	Far	0	884	338	6	30	184	51	56	32.40	1.95	200	2002	668	7	93.58	120.47	1404	915	262
380		50	906	364	10	39	216	69	45	50.65	2.24	200	2033	701	8	95.06	114.36	1428	936	224

C.1 - 27: Full Static Analysis Results for Riser System (with Flooded flowlines) supported by Conventional Buoy with C$_d$ = 1.4, at Near, Zero, and Far Vessel Offsets, with 10-year Current

Pipeline: 10"ID Riser, Wall thickness 26mm, 3" Coating
Buoy type: Conventional buoy, Cd=1.4
Water Depth: 1500m
Current: 100-year
Content: 1.025Te/m³

			Flexible (no1)							Buoy			Max values for SCR					Mooring line		
Flexible length	Current Case	Vessel position	Tension at FPSO	Tension at buoy	Declination at FPSO	Declination at Buoy	Horizontal projection	MBR	Hmin	Position rel nominal	Buoy trim angle	Depth in water	Tension at buoy	Horizontal projection	Declination at buoy	Max von Mises Top	Max von Mises Sag	Max Top Tension	Max Anchor Tension	Min Anchor Tension
[m]	[-]	[m]	[kN]	[kN]	[deg]	[deg]	[m]	[m]	[m]	[m]	[deg]	[m]	[kN]	[m]	[deg]	[MPa]	[MPa]	[kN]	[kN]	[kN]
380	Near	-30	912	355	18	41	235	73	38	-49.10	1.52	204	1756	457	10	79.34	232.21	1400	909	532
380		0	930	379	20	47	250	87	32	-33.56	1.62	203	1798	488	10	80.10	214.12	1412	925	507
380	No current	-30	887	336	11	31	198	54	53	-11.96	1.56	202	1884	554	8	84.46	158.21	1387	899	405
380		0	899	352	13	37	216	65	46	0.00	1.64	201	1902	581	8	85.35	150.79	1399	911	382
380		30	915	375	15	42	233	77	39	13.31	1.72	201	1891	604	9	86.36	143.28	1415	926	356
380	Far	0	882	348	5	29	177	49	58	39.06	2.12	200	2022	685	7	95.27	116.26	1409	917	239
380		30	893	359	7	34	197	59	52	49.09	2.31	200	2034	705	8	96.08	113.13	1420	928	217

C.1 - 28: Full Static Analysis Results for Riser System (with Flooded flowlines) supported by Conventional Buoy with C$_d$ = 1.4, at Near, Zero, and Far Vessel Offsets, with 100-year Current

Pipeline: 10"ID Riser, Wall thickness 26mm, 3" Coating
Buoy type: Conventional buoy, Cd=1.6
Water Depth: 1500m
Current: 10-year
Content: 1.025Te/m³

			Flexible (no1)							Buoyancy			Max values for SCR					Mooring line		
Flexible length	Current Case	Vessel position	Tension at FPSO	Tension at buoyancy	Declination at FPSO	Declination at Buoy	Horizontal projection	MBR	Hmin	Position rel nominal	Buoy trim angle	Depth in water	Tension at buoyancy	Horizontal projection	Declination at buoyancy	Max von Mises Top	Max von Mises Sag	Max Top Tension	Max Anchor Tension	Min Anchor Tension
[m]	[-]	[m]	[kN]	[kN]	[deg]	[deg]	[m]	[m]	[m]	[m]	[deg]	[m]	[kN]	[m]	[deg]	[MPa]	[MPa]	[kN]	[kN]	[kN]
380	Near	-50	899	349	16	36	220	63	44	-53.50	1.47	205	1781	453	9	78.99	228.58	1389	898	530
380		0	925	376	19	46	245	84	34	-29.22	1.62	203	1813	502	10	80.16	201.96	1413	921	489
380	No current	-50	881	340	9	28	185	47	57	-19.24	1.52	202	1843	542	8	83.93	162.98	1384	892	419
380		0	899	359	13	37	216	65	46	0.00	1.64	201	1873	581	8	85.35	150.79	1399	911	382
380		50	928	390	16	46	243	87	35	22.99	1.79	200	1933	624	9	87.11	138.22	1430	938	337
380	Far	0	883	340	6	30	183	50	57	33.33	1.96	200	1973	669	7	93.66	120.13	1407	915	261
380		50	905	363	10	39	215	69	46	51.47	2.25	200	2034	707	8	95.12	114.10	1428	936	222

C.1 - 29: Full Static Analysis Results for Riser System (with Flooded flowlines) supported by Conventional Buoy with C_d = 1.6, at Near, Zero, and Far Vessel Offsets, with 10-year Current

Pipeline: 10"ID Riser, Wall thickness 26mm, 3" Coating
Buoy type: Conventional buoy, Cd=1.6
Water Depth: 1500m
Current: 100-year
Content: 1.025Te/m³

			Flexible (no1)							Buoy			Max values for SCR					Mooring line		
Flexible length	Current Case	Vessel position	Tension at FPSO	Tension at buoy	Declination at FPSO	Declination at Buoy	Horizontal projection	MBR	Hmin	Position rel nominal	Buoy trim angle	Depth in water	Tension at buoy	Horizontal projection	Declination at buoy	Max von Mises Top	Max von Mises Sag	Max Top Tension	Max Anchor Tension	Min Anchor Tension
[m]	[-]	[m]	[kN]	[kN]	[deg]	[deg]	[m]	[m]	[m]	[m]	[deg]	[m]	[kN]	[m]	[deg]	[MPa]	[MPa]	[kN]	[kN]	[kN]
380	Near	-30	913	356	18	42	236	74	38	-50.00	1.52	204	1777	456	10	79.30	233.43	1401	910	533
380		0	931	380	20	48	251	88	32	-34.36	1.62	203	1797	487	10	80.06	215.04	1416	926	508
380	No current	-30	887	336	11	31	198	54	53	-11.96	1.56	202	1884	554	8	84.46	158.21	1387	899	405
380		0	899	352	13	37	216	65	46	0.00	1.64	201	1902	581	8	85.35	150.79	1399	911	382
380		30	915	375	15	42	233	77	39	13.31	1.72	201	1891	604	9	86.36	143.28	1415	926	356
380	Far	0	881	349	4	29	176	48	59	40.20	2.13	200	2024	686	7	95.36	115.89	1409	917	237
380		30	892	348	7	34	196	58	52	50.16	2.32	200	2041	706	8	96.17	112.81	1420	928	215

C.1 - 30: Full Static Analysis Results for Riser System (with Flooded flowlines) supported by Conventional Buoy with C_d = 1.6, at Near, Zero, and Far Vessel Offsets, with 100-year Current

Pipeline: 10"ID Riser, Wall thickness 26mm, 3" Coating
Water Depth: 1500m
Current: -
Content: 0.5Te/m³

			Flexible (no1)							Buoy		Max values for SCR					Mooring line		
Flexible length	Current Case	Main spar offset	Tension at FPSO	Tension at buoy	Declination at FPSO	Declination at Buoy	Horizontal projection	MBR	Hmin	Buoy trim angle	Depth in water	Tension at buoy	Horizontal projection	Declination at buoy	Max von Mises Top	Max von Mises Sag	Max Top Tension	Max Anchor Tension	Min Anchor Tension
[m]	[-]	[m]	[kN]	[kN]	[deg]	[deg]	[m]	[m]	[m]	[deg]	[m]	[kN]	[m]	[deg]	[MPa]	[MPa]	[kN]	[kN]	[kN]
380		-5.0	811	298	11	32	203	57	52	-0.3	198	1506	602	9	276	259	1194	751	693
380		**-4.0**	**811**	**298**	**11**	**32**	**203**	**57**	**52**	**0.0**	**198**	**1506**	**602**	**9**	**276**	**259**	**1165**	**723**	**722**
380	No current	-3.0	811	298	11	32	204	57	51	0.3	198	1506	602	9	276	259	1193	751	694
380		-2.0	811	298	11	32	204	57	51	0.6	198	1505	601	9	276	259	1222	779	666
380		-1.0	811	299	11	33	204	57	51	0.9	198	1505	601	9	276	259	1251	808	638
380		0.0	811	299	11	33	205	58	51	1.3	198	1505	601	9	276	259	1279	836	609
380		1.0	812	299	11	33	205	58	51	1.6	198	1504	595	9	276	259	1308	865	581

C.1 - 31: Full Static Analysis Results for Main Spar Offset Variation of H-shaped Buoy, at Zero Vessel Offset and No Current

Pipeline: 10"ID Riser, Wall thickness 26mm, 3" Coating
Water Depth: 1500m
Current: -
Content: 0.5Te/m³

			Flexible (no1)							Buoy		Max values for SCR					Mooring line		
Flexible length	Current Case	Anchor position	Tension at FPSO	Tension at buoy	Declination at FPSO	Declination at Buoy	Horizontal projection	MBR	Hmin	Buoy trim angle	Depth in water	Tension at buoy	Horizontal projection	Declination at buoy	Max von Mises Top	Max von Mises Sag	Max Top Tension	Max Anchor Tension	Min Anchor Tension
[m]	[-]	[m]	[kN]	[kN]	[deg]	[deg]	[m]	[m]	[m]	[deg]	[m]	[kN]	[m]	[deg]	[MPa]	[MPa]	[kN]	[kN]	[kN]
380		1270	803	291	10	28	190	49	57	0.0	198	1468	530	7	275	268	1179	737	736
380	No current	**1320**	811	298	11	32	203	57	52	0.0	198	1506	602	**9**	276	259	1165	723	722
380		1350	817	303	12	35	212	62	48	0.0	199	1531	644	10	276	255	1156	714	713
380		1400	830	314	14	40	226	72	42	0.0	199	1577	714	11	276	250	1141	699	699
380		1450	848	330	16	46	241	84	35	0.0	200	1628	795	13	277	247	1127	685	683

C.1 - 32: Full Static Analysis Results for Riser Anchor Length Variation at Zero Vessel Offset and No Current – H-shaped Buoy

Pipeline: 10"ID Riser, Wall thickness 26mm, 3" Coating
Buoy type: H-buoy, Cd=1.2
Water Depth: 1500m
Current: 10-year
Content: 0.5Te/m³

			Flexible (no1)							Buoy			Max values for SCR					Mooring line		
Flexible length	Current Case	Vessel position	Tension at FPSO	Tension at buoy	Declination at FPSO	Declination at Buoy	Horizontal projection	MBR	Hmin	Position rel nominal	Buoy trim angle	Depth in water	Tension at buoy	Horizontal projection	Declination at buoy	Max von Mises Top	Max von Mises Sag	Max Top Tension	Max Anchor Tension	Min Anchor Tension
[m]	[-]	[m]	[kN]	[kN]	[deg]	[deg]	[m]	[m]	[m]	[m]	[deg]	[m]	[kN]	[m]	[deg]	[MPa]	[MPa]	[kN]	[kN]	[kN]
380	Near	-50	810	288	15	31	209	55	50	-55.15	0.1	201	1397	467	10	274.27	297.09	1233	791	777
380		0	830	312	18	41	236	74	39	-32.75	0.1	200	1420	509	11	274.53	284.66	1229	786	769
380	No current	-50	797	282	8	24	171	41	62	-17.35	0.0	199	1485	565	8	275.31	263.08	1173	730	728
380		0	811	298	11	32	203	57	52	0.00	0.0	198	1506	602	9	275.58	259.13	1165	723	722
380		50	833	322	15	42	233	77	40	20.90	0.0	198	1532	643	10	275.92	255.21	1160	717	715
380	Far	0	800	290	4	26	167	43	62	36.42	-0.1	197	1603	703	7	277.58	248.22	1119	675	660
380		50	816	306	8	35	201	60	51	52.49	-0.1	197	1626	734	8	277.87	246.81	1111	668	655

C.1 - 33: Full Static Analysis Results for Riser System (with Content-filled flowlines) supported by H-shaped Buoy with C$_d$ = 1.2, at Near, Zero, and Far Vessel Offsets, with 10-year Current

Pipeline: 10"ID Riser, Wall thickness 26mm, 3" Coating
Buoy type: H-buoy, Cd=1.2
Water Depth: 1500m
Current: 100-year
Content: 0.5Te/m³

			Flexible (no1)							Buoy			Max values for SCR					Mooring line		
Flexible length	Current Case	Vessel position	Tension at FPSO	Tension at buoy	Declination at FPSO	Declination at Buoy	Horizontal projection	MBR	Hmin	Position rel nominal	Buoy trim angle	Depth in water	Tension at buoy	Horizontal projection	Declination at buoy	Max von Mises Top	Max von Mises Sag	Max Top Tension	Max Anchor Tension	Min Anchor Tension
[m]	[-]	[m]	[kN]	[kN]	[deg]	[deg]	[m]	[m]	[m]	[m]	[deg]	[m]	[kN]	[m]	[deg]	[MPa]	[MPa]	[kN]	[kN]	[kN]
380	Near	-30	821	298	18	37	227	66	43	-53.08	0.1	201	1390	464	11	274.20	301.61	1243	801	783
380		0	835	316	19	43	242	78	37	-38.56	0.1	200	1405	494	11	274.36	292.40	1241	799	778
380	No current	-30	802	288	9	27	184	47	58	-10.80	0.0	199	1493	581	8	275.28	261.39	1170	727	726
380		0	811	298	11	32	203	57	52	0.00	0.0	198	1506	602	9	275.45	259.01	1165	723	722
380		30	823	311	13	38	221	68	45	12.08	0.0	198	1521	624	9	275.64	256.65	1162	719	718
380	Far	0	799	288	2	26	160	41	64	43.77	-0.1	197	1623	720	7	277.89	246.84	1110	667	649
380		30	807	297	5	30	181	51	57	52.53	-0.1	198	1635	739	8	278.05	246.15	1105	662	645

C.1 - 34: Full Static Analysis Results for Riser System (with Content-filled flowlines) supported by H-shaped Buoy with C$_d$ = 1.2, at Near, Zero, and Far Vessel Offsets, with 100-year Current

Pipeline: 10"ID Riser, Wall thickness 26mm, 3" Coating
Buoy type: H-buoy, Cd=1.4
Water Depth: 1500m
Current: 10-year
Content: 0.5Te/m³

			Flexible (no1)							Buoy			Max values for SCR					Mooring line		
Flexible length	Current Case	Vessel position	Tension at FPSO	Tension at buoy	Declination at FPSO	Declination at Buoy	Horizontal projection	MBR	Hmin	Position rel nominal	Buoy trim angle	Depth in water	Tension at buoy	Horizontal projection	Declination at buoy	Max von Mises Top	Max von Mises Sag	Max Top Tension	Max Anchor Tension	Min Anchor Tension
[m]	[-]	[m]	[kN]	[kN]	[deg]	[deg]	[m]	[m]	[m]	[m]	[deg]	[m]	[kN]	[m]	[deg]	[MPa]	[MPa]	[kN]	[kN]	[kN]
380	Near	-50	811	288	15	32	210	56	49	-56.28	0.1	201.43	1396	466	10	274.25	297.82	1234	793	777
380	Near	0	832	313	18	41	237	75	39	-33.73	0.1	199.77	1419	508	11	274.52	285.15	1230	788	769
380	No current	-50	797	282	8	24	171	41	62	-17.35	0.0	198.91	1485	565	8	275.31	263.08	1173	730	728
380	No current	0	811	298	11	32	203	57	52	0.00	0.0	198.15	1506	602	9	275.58	259.13	1165	723	722
380	No current	50	833	322	15	42	233	77	40	20.90	0.0	197.54	1532	643	10	275.92	255.21	1160	717	715
380	Far	0	800	289	4	26	166	43	62	37.69	-0.1	197.47	1605	704	8	277.60	248.11	1118	675	659
380	Far	50	816	306	8	34	200	60	51	53.63	-0.1	197.47	1627	740	8	277.89	246.71	1111	668	653

C.1 - 35: Full Static Analysis Results for Riser System (with Content-filled flowlines) supported by H-shaped Buoy with C_d = 1.4, at Near, Zero, and Far Vessel Offsets, with 10-year Current

Pipeline: 10"ID Riser, Wall thickness 26mm, 3" Coating
Buoy type: H-buoy, Cd=1.4
Water Depth: 1500m
Current: 100-year
Content: 0.5Te/m³

			Flexible (no1)							Buoy			Max values for SCR					Mooring line		
Flexible length	Current Case	Vessel position	Tension at FPSO	Tension at buoy	Declination at FPSO	Declination at Buoy	Horizontal projection	MBR	Hmin	Position rel nominal	Buoy trim angle	Depth in water	Tension at buoy	Horizontal projection	Declination at buoy	Max von Mises Top	Max von Mises Sag	Max Top Tension	Max Anchor Tension	Min Anchor Tension
[m]	[-]	[m]	[kN]	[kN]	[deg]	[deg]	[m]	[m]	[m]	[m]	[deg]	[m]	[kN]	[m]	[deg]	[MPa]	[MPa]	[kN]	[kN]	[kN]
380	Near	-30	822	299	18	37	228	67	43	-54.33	0.1	201	1389	463	11	274.32	302.58	1245	803	783
380	Near	0	837	317	20	43	243	79	36	-39.70	0.1	200	1404	492	11	274.48	293.19	1243	801	778
380	No current	-30	802	288	9	27	184	47	58	-10.80	0.0	199	1493	581	8	275.42	261.51	1170	727	726
380	No current	0	811	298	11	32	203	57	52	0.00	0.0	198	1506	602	9	275.58	259.13	1165	723	722
380	No current	30	823	311	13	38	221	68	45	12.08	0.0	198	1521	624	9	275.78	256.78	1162	719	718
380	Far	0	798	288	2	25	158	41	64	45.33	-0.1	197	1625	727	7	278.05	246.84	1109	666	647
380	Far	30	807	296	4	30	179	50	58	54.00	-0.1	198	1637	746	8	278.21	246.17	1105	662	644

C.1 - 36: Full Static Analysis Results for Riser System (with Content-filled flowlines) supported by H-shaped Buoy with C_d = 1.4, at Near, Zero, and Far Vessel Offsets, with 100-year Current

Pipeline: 10"ID Riser, Wall thickness 26mm, 3" Coating
Buoy type: H-buoy, Cd=1.6
Water Depth: 1500m
Current: 10-year
Content: 0.5Te/m³

			Flexible (no1)							Buoy			Max values for SCR					Mooring line		
Flexible length	Current Case	Vessel position	Tension at FPSO	Tension at buoy	Declination at FPSO	Declination at Buoy	Horizontal projection	MBR	Hmin	Position rel nominal	Buoy trim angle	Depth in water	Tension at buoy	Horizontal projection	Declination at buoy	Max von Mises Top	Max von Mises Sag	Max Top Tension	Max Anchor Tension	Min Anchor Tension
[m]	[-]	[m]	[kN]	[kN]	[deg]	[deg]	[m]	[m]	[m]	[m]	[deg]	[m]	[kN]	[m]	[deg]	[MPa]	[MPa]	[kN]	[kN]	[kN]
380	Near	-50	812	289	15	32	211	56	49	-57.41	0.1	202	1394	460	10	274.24	298.54	1236	794	778
380		0	833	314	18	42	238	76	38	-34.70	0.1	200	1418	507	11	274.50	285.63	1231	789	770
380	No current	-50	797	282	8	24	171	41	62	-17.35	0.0	199	1485	565	8	275.31	263.08	1173	730	728
380		0	811	298	11	32	203	57	52	0.00	0.0	198	1506	602	9	275.58	259.13	1165	723	722
380		50	833	322	15	42	233	77	40	20.90	0.0	198	1532	643	10	275.92	255.21	1160	717	715
380	Far	0	799	289	4	26	164	42	63	38.97	-0.1	197	1607	706	8	277.62	247.98	1118	675	658
380		50	815	305	7	34	199	59	52	54.77	-0.1	197	1629	741	8	277.92	246.62	1111	668	652

C.1 - 37: Full Static Analysis Results for Riser System (with Content-filled flowlines) supported by H-shaped Buoy with C_d = 1.6, at Near, Zero, and Far Vessel Offsets, with 10-year Current

Pipeline: 10"ID Riser, Wall thickness 26mm, 3" Coating
Buoy type: H-buoy, Cd=1.6
Water Depth: 1500m
Current: 100-year
Content: 0.5Te/m³

			Flexible (no1)							Buoy			Max values for SCR					Mooring line		
Flexible length	Current Case	Vessel position	Tension at FPSO	Tension at buoy	Declination at FPSO	Declination at Buoy	Horizontal projection	MBR	Hmin	Position rel nominal	Buoy trim angle	Depth in water	Tension at buoy	Horizontal projection	Declination at buoy	Max von Mises Top	Max von Mises Sag	Max Top Tension	Max Anchor Tension	Min Anchor Tension
[m]	[-]	[m]	[kN]	[kN]	[deg]	[deg]	[m]	[m]	[m]	[m]	[deg]	[m]	[kN]	[m]	[deg]	[MPa]	[MPa]	[kN]	[kN]	[kN]
380	Near	-30	823	300	18	38	229	68	42	-55.57	0.1	201	1388	462	11	274.17	303.23	1247	805	783
380		0	838	318	20	44	244	80	36	-40.83	0.1	200	1403	491	11	274.33	293.77	1245	803	778
380	No current	-30	802	288	9	27	184	47	58	-10.80	0.0	199	1493	581	8	275.28	261.39	1170	727	726
380		0	811	298	11	32	203	57	52	0.00	0.0	198	1506	602	9	275.45	259.01	1165	723	722
380		30	823	311	13	38	221	68	45	12.08	0.0	198	1521	624	9	275.64	256.65	1162	719	718
380	Far	0	798	287	2	25	157	40	65	46.90	-0.1	197	1627	729	7	277.95	246.59	1109	666	645
380		30	806	296	4	30	178	49	58	55.47	-0.1	198	1639	747	8	278.11	245.93	1105	662	642

C.1 - 38: Full Static Analysis Results for Riser System (with Content-filled flowlines) supported by H-shaped Buoy with C_d = 1.6, at Near, Zero, and Far Vessel Offsets, with 100-year Current

Pipeline: 10"ID Riser, Wall thickness 26mm, 3" Coating
Buoy type: H-buoy, Cd=1.2
Water Depth: 1500m
Current: 10-year
Content: 0.0Te/m³

			Flexible (no1)							Buoy			Max values for SCR					Mooring line		
Flexible length	Current Case	Vessel position	Tension at FPSO	Tension at buoy	Declination at FPSO	Declination at Buoy	Horizontal projection	MBR	Hmin	Position rel nominal	Buoy trim angle	Depth in water	Tension at buoy	Horizontal projection	Declination at buoy	Max von Mises Top	Max von Mises Sag	Max Top Tension	Max Anchor Tension	Min Anchor Tension
[m]	[-]	[m]	[kN]	[kN]	[deg]	[deg]	[m]	[m]	[m]	[m]	[deg]	[m]	[kN]	[m]	[deg]	[MPa]	[MPa]	[kN]	[kN]	[kN]
380	Near	-50	728	256	14	26	195	47	56	-55.20	0.2	200	1045	491	12	49.42	226.93	1431	989	946
380		0	743	275	17	36	225	65	45	-35.78	0.3	198	1060	525	12	49.87	206.39	1429	987	941
380	No current	-50	720	254	7	20	154	34	68	-14.66	0.2	198	1127	601	9	52.64	148.52	1373	931	902
380		0	730	266	10	28	189	49	57	0.00	0.2	197	1141	636	9	53.35	141.45	1370	927	898
380		50	748	284	13	38	221	68	45	18.02	0.2	197	1158	669	10	54.25	133.67	1368	925	893
380	Far	0	723	260	2	23	151	37	67	38.73	0.1	197	1231	749	7	62.98	116.86	1314	871	854
380		50	736	273	6	31	187	53	56	52.28	0.1	197	1246	778	8	63.70	114.95	1311	868	850

C.1 - 39: Full Static Analysis Results for Riser System (with Empty flowlines) supported by H-shaped Buoy with C_d = 1.2, at Near, Zero, and Far Vessel Offsets, with 10-year Current

Pipeline: 10"ID Riser, Wall thickness 26mm, 3" Coating
Buoy type: H-buoy, Cd=1.2
Water Depth: 1500m
Current: 100-year
Content: 0.0Te/m³

			Flexible (no1)							Buoy			Max values for SCR					Mooring line		
Flexible length	Current Case	Vessel position	Tension at FPSO	Tension at buoy	Declination at FPSO	Declination at Buoy	Horizontal projection	MBR	Hmin	Position rel nominal	Buoy trim angle	Depth in water	Tension at buoy	Horizontal projection	Declination at buoy	Max von Mises Top	Max von Mises Sag	Max Top Tension	Max Anchor Tension	Min Anchor Tension
[m]	[-]	[m]	[kN]	[kN]	[deg]	[deg]	[m]	[m]	[m]	[m]	[deg]	[m]	[kN]	[m]	[deg]	[MPa]	[MPa]	[kN]	[kN]	[kN]
380	Near	-30	736	264	17	32	214	56	49	-54.95	0.3	200	1036	481	13	50.03	241.04	1442	1000	953
380		0	747	277	18	38	232	69	42	-42.25	0.3	199	1046	509	13	50.32	225.66	1441	999	950
380	No current	-30	723	258	8	23	169	40	64	-9.16	0.2	197	1132	617	9	52.91	145.77	1372	929	900
380		0	730	266	10	28	189	49	57	0.00	0.2	197	1141	636	9	53.35	141.45	1370	927	898
380		30	739	276	12	34	209	60	50	10.37	0.2	197	1151	656	10	53.86	136.84	1369	926	895
380	Far	0	722	259	1	23	143	35	68	46.43	0.1	197	1249	772	7	64.94	114.58	1304	861	846
380		30	729	265	3	27	166	44	62	53.77	0.1	197	1257	789	8	65.33	113.66	1302	859	844

C.1 - 40: Full Static Analysis Results for Riser System (with Empty flowlines) supported by H-shaped Buoy with C_d = 1.2, at Near, Zero, and Far Vessel Offsets, with 100-year Current

Pipeline:	10"ID Riser, Wall thickness 26mm, 3" Coating
Buoy type:	H-buoy, Cd=1.4
Water Depth:	1500m
Current:	10-year
Content:	0.0Te/m³

			Flexible (no1)							Buoy			Max values for SCR					Mooring line		
Flexible length	Current Case	Vessel position	Tension at FPSO	Tension at buoy	Declination at FPSO	Declination at Buoy	Horizontal projection	MBR	Hmin	Position rel nominal	Buoy trim angle	Depth in water	Tension at buoy	Horizontal projection	Declination at buoy	Max von Mises Top	Max von Mises Sag	Max Top Tension	Max Anchor Tension	Min Anchor Tension
[m]	[-]	[m]	[kN]	[kN]	[deg]	[deg]	[m]	[m]	[m]	[m]	[deg]	[m]	[kN]	[m]	[deg]	[MPa]	[MPa]	[kN]	[kN]	[kN]
380	Near	-50	729	257	14	26	196	47	56	-56.44	0.3	200	1044	485	12	49.39	228.40	1433	991	946
380		0	744	275	17	36	226	66	44	-36.88	0.3	199	1059	524	12	49.84	207.45	1431	988	941
380	No current	-50	720	254	7	20	154	34	68	-14.66	0.2	198	1127	601	9	52.64	148.52	1373	931	902
380		0	730	266	10	28	189	49	57	0.00	0.2	197	1141	636	9	53.35	141.45	1370	927	898
380		50	748	284	13	38	221	68	45	18.02	0.2	197	1158	669	10	54.25	133.67	1368	925	893
380	Far	0	723	259	2	23	149	37	67	40.08	0.1	197	1232	751	7	63.05	116.67	1313	870	854
380		50	735	272	6	31	186	53	56	53.51	0.1	197	1247	779	8	63.77	114.79	1310	867	850

C.1 - 41: Full Static Analysis Results for Riser System (with Empty flowlines) supported by H-shaped Buoy with C_d = 1.4, at Near, Zero, and Far Vessel Offsets, with 10-year Current

Pipeline:	10"ID Riser, Wall thickness 26mm, 3" Coating
Buoy type:	H-buoy, Cd=1.4
Water Depth:	1500m
Current:	100-year
Content:	0.0Te/m³

			Flexible (no1)							Buoy			Max values for SCR					Mooring line		
Flexible length	Current Case	Vessel position	Tension at FPSO	Tension at buoy	Declination at FPSO	Declination at Buoy	Horizontal projection	MBR	Hmin	Position rel nominal	Buoy trim angle	Depth in water	Tension at buoy	Horizontal projection	Declination at buoy	Max von Mises Top	Max von Mises Sag	Max Top Tension	Max Anchor Tension	Min Anchor Tension
[m]	[-]	[m]	[kN]	[kN]	[deg]	[deg]	[m]	[m]	[m]	[m]	[deg]	[m]	[kN]	[m]	[deg]	[MPa]	[MPa]	[kN]	[kN]	[kN]
380	Near	-30	736	264	17	32	216	57	49	-56.35	0.3	200	1035	480	13	50.00	242.91	1443	1001	953
380		0	748	278	19	38	233	70	42	-43.54	0.3	199	1045	508	13	50.29	227.24	1443	1000	950
380	No current	-30	723	258	8	23	169	40	64	-9.16	0.2	197	1132	617	9	52.91	145.77	1372	929	900
380		0	730	266	10	28	189	49	57	0.00	0.2	197	1141	636	9	53.35	141.45	1370	927	898
380		30	739	276	12	34	209	60	50	10.37	0.2	197	1151	656	10	53.86	136.84	1369	926	895
380	Far	0	722	258	0	22	141	35	69	48.08	0.1	197	1251	774	7	65.03	114.38	1302	859	846
380		30	728	265	2	27	164	44	62	55.34	0.1	197	1259	791	8	65.41	113.47	1300	857	844

C.1 - 42: Full Static Analysis Results for Riser System (with Empty flowlines) supported by H-shaped Buoy with C_d = 1.4, at Near, Zero, and Far Vessel Offsets, with 100-year Current

Pipeline: 10"ID Riser, Wall thickness 26mm, 3" Coating
Buoy type: H-buoy, Cd=1.6
Water Depth: 1500m
Current: 10-year
Content: 0.0Te/m³

Flexible length	Current Case	Vessel position	Tension at FPSO	Tension at buoy	Declination at FPSO	Declination at Buoy	Horizontal projection	MBR	Hmin	Position rel nominal	Buoy trim angle	Depth in water	Tension at buoy	Horizontal projection	Declination at buoy	Max von Mises Top	Max von Mises Sag	Max Top Tension	Max Anchor Tension	Min Anchor Tension
[m]	[-]	[m]	[kN]	[kN]	[deg]	[deg]	[m]	[m]	[m]	[m]	[deg]	[m]	[kN]	[m]	[deg]	[MPa]	[MPa]	[kN]	[kN]	[kN]
380	Near	-50	729	257	14	27	197	48	55	-57.68	0.3	200	1043	484	12	49.36	229.86	1434	992	947
380		0	745	276	17	37	227	67	44	-37.97	0.3	199	1058	523	12	49.82	208.53	1432	989	942
380	No current	-50	720	254	7	20	154	34	68	-14.66	0.2	198	1127	601	9	52.64	148.52	1373	931	902
380		0	730	266	10	28	189	49	57	0.00	0.2	197	1141	636	9	53.35	141.45	1370	927	898
380		50	748	284	13	38	221	68	45	18.02	0.2	197	1158	669	10	54.25	133.67	1368	925	893
380	Far	0	722	259	2	23	148	36	68	41.43	0.1	197	1234	757	8	63.12	116.47	1312	869	854
380		50	735	271	5	31	185	52	56	54.74	0.1	197	1248	785	8	63.84	114.62	1308	865	850

C.1 - 43: Full Static Analysis Results for Riser System (with Empty flowlines) supported by H-shaped Buoy with C_d = 1.6, at Near, Zero, and Far Vessel Offsets, with 10-year Current

Pipeline: 10"ID Riser, Wall thickness 26mm, 3" Coating
Buoy type: H-buoy, Cd=1.6
Water Depth: 1500m
Current: 100-year
Content: 0.0Te/m³

Flexible length	Current Case	Vessel position	Tension at FPSO	Tension at buoy	Declination at FPSO	Declination at Buoy	Horizontal projection	MBR	Hmin	Position rel nominal	Buoy trim angle	Depth in water	Tension at buoy	Horizontal projection	Declination at buoy	Max von Mises Top	Max von Mises Sag	Max Top Tension	Max Anchor Tension	Min Anchor Tension
[m]	[-]	[m]	[kN]	[kN]	[deg]	[deg]	[m]	[m]	[m]	[m]	[deg]	[m]	[kN]	[m]	[deg]	[MPa]	[MPa]	[kN]	[kN]	[kN]
380	Near	-30	737	265	17	33	217	58	48	-57.73	0.3	200	1034	479	13	49.97	244.59	1445	1003	953
380		0	749	279	19	39	234	71	41	-44.81	0.3	199	1044	501	13	50.26	228.78	1444	1002	950
380	No current	-30	723	258	8	23	169	40	64	-9.16	0.2	197	1132	617	9	52.91	145.77	1372	929	900
380		0	730	266	10	28	189	49	57	0.00	0.2	197	1141	636	9	53.35	141.45	1370	927	898
380		30	739	276	12	34	209	60	50	10.37	0.2	197	1151	656	10	53.86	136.84	1369	926	895
380	Far	0	722	258	0	22	140	34	69	49.73	0.1	197	1252	780	7	65.11	114.16	1301	858	846
380		30	728	264	2	27	163	43	63	56.91	0.1	197	1260	793	8	65.50	113.29	1299	856	843

C.1 - 44: Full Static Analysis Results for Riser System (with Empty flowlines) supported by H-shaped Buoy with C_d = 1.6, at Near, Zero, and Far Vessel Offsets, with 100-year Current

Pipeline:	10"ID Riser, Wall thickness 26mm, 3" Coating
Buoy type:	H-buoy, Cd=1.2
Water Depth:	1500m
Current:	10-year
Content:	1.025Te/m³

			Flexible (no1)							Buoy			Max values for SCR					Mooring line		
Flexible length	Current Case	Vessel position	Tension at FPSO	Tension at buoy	Declination at FPSO	Declination at Buoy	Horizontal projection	MBR	Hmin	Position rel nominal	Buoy trim angle	Depth in water	Tension at buoy	Horizontal projection	Declination at buoy	Max von Mises Top	Max von Mises Sag	Max Top Tension	Max Anchor Tension	Min Anchor Tension
[m]	[-]	[m]	[kN]	[kN]	[deg]	[deg]	[m]	[m]	[m]	[m]	[deg]	[m]	[kN]	[m]	[deg]	[MPa]	[MPa]	[kN]	[kN]	[kN]
380	Near	-50	901	324	16	37	222	64	44	-55.02	-0.1	203	1761	444	9	78.28	234.48	1043	602	588
380		0	926	355	19	46	246	84	34	-29.48	-0.1	201	1795	495	10	79.54	205.27	1032	590	580
380	No current	-50	882	314	9	28	187	48	56	-20.33	-0.2	200	1855	534	7	83.26	165.92	995	552	520
380		0	899	335	13	37	217	65	46	0.00	-0.2	199	1884	574	8	84.76	152.64	984	542	511
380		50	928	366	16	46	243	86	35	23.94	-0.2	198	1921	623	9	86.61	139.20	973	530	502
380	Far	0	883	322	6	30	183	50	57	33.84	-0.3	198	1987	663	7	93.00	121.04	934	491	444
380		50	904	344	10	38	214	68	46	52.72	-0.3	198	2019	701	8	94.55	114.59	923	480	435

C.1 - 45: Full Static Analysis Results for Riser System (with Flooded flowlines) supported by H-shaped Buoy with C$_d$ = 1.2, at Near, Zero, and Far Vessel Offsets, with 10-year Current

Pipeline:	10"ID Riser, Wall thickness 26mm, 3" Coating
Buoy type:	H-buoy, Cd=1.2
Water Depth:	1500m
Current:	100-year
Content:	1.025Te/m³

			Flexible (no1)							Buoy			Max values for SCR					Mooring line		
Flexible length	Current Case	Vessel position	Tension at FPSO	Tension at buoy	Declination at FPSO	Declination at Buoy	Horizontal projection	MBR	Hmin	Position rel nominal	Buoy trim angle	Depth in water	Tension at buoy	Horizontal projection	Declination at buoy	Max von Mises Top	Max von Mises Sag	Max Top Tension	Max Anchor Tension	Min Anchor Tension
[m]	[-]	[m]	[kN]	[kN]	[deg]	[deg]	[m]	[m]	[m]	[m]	[deg]	[m]	[kN]	[m]	[deg]	[MPa]	[MPa]	[kN]	[kN]	[kN]
380	Near	-30	915	339	19	42	238	75	37	-50.99	-0.1	203	1758	448	10	78.61	238.62	1048	607	598
380		0	933	360	21	48	251	88	31	-34.62	0.0	201	1779	479	10	79.41	218.66	1041	600	593
380	No current	-30	888	321	11	31	199	55	52	-12.60	-0.2	200	1866	546	8	83.83	160.73	991	548	516
380		0	899	335	13	37	217	65	46	0.00	-0.2	199	1884	574	8	84.76	152.64	984	542	511
380		30	915	352	15	42	233	77	40	13.90	-0.2	199	1905	603	9	85.83	144.58	977	535	506
380	Far	0	881	321	4	29	176	48	59	40.78	-0.3	198	2008	679	7	94.69	116.67	925	482	431
380		30	892	332	7	34	196	58	52	51.16	-0.3	198	2025	700	8	95.55	113.36	918	475	426

C.1 - 46: Full Static Analysis Results for Riser System (with Flooded flowlines) supported by H-shaped Buoy with C$_d$ = 1.2, at Near, Zero, and Far Vessel Offsets, with 100-year Current

Pipeline:	10"ID Riser, Wall thickness 26mm, 3" Coating
Buoy type:	**H-buoy, Cd=1.4**
Water Depth:	1500m
Current:	10-year
Content:	1.025Te/m³

			Flexible (no1)							Buoy			Max values for SCR					Mooring line		
Flexible length	Current Case	Vessel position	Tension at FPSO	Tension at buoy	Declination at FPSO	Declination at Buoy	Horizontal projection	MBR	Hmin	Position rel nominal	Buoy trim angle	Depth in water	Tension at buoy	Horizontal projection	Declination at buoy	Max von Mises Top	Max von Mises Sag	Max Top Tension	Max Anchor Tension	Min Anchor Tension
[m]	[-]	[m]	[kN]	[kN]	[deg]	[deg]	[m]	[m]	[m]	[m]	[deg]	[m]	[kN]	[m]	[deg]	[MPa]	[MPa]	[kN]	[kN]	[kN]
380	Near	-50	902	325	16	37	223	65	43	-56.03	-0.1	203	1760	443	9	78.24	235.73	1043	602	589
380		0	928	357	19	46	247	85	33	-30.34	-0.1	201	1793	494	10	79.50	206.10	1033	591	581
380	No current	-50	882	314	9	28	187	48	56	-20.33	-0.2	200	1855	534	7	83.26	165.92	995	552	520
380		0	899	335	13	37	217	65	46	0.00	-0.2	199	1884	574	8	84.76	152.64	984	542	511
380		50	928	366	16	46	243	86	35	23.94	-0.2	198	1921	623	9	86.61	139.20	973	530	502
380	Far	0	883	322	6	30	182	50	57	35.02	-0.3	198	1989	664	7	93.10	120.61	934	491	442
380		50	903	343	9	38	213	68	46	53.75	-0.3	198	2020	702	8	94.64	114.26	923	480	433

C.1 - 47: Full Static Analysis Results for Riser System (with Flooded flowlines) supported by H-shaped Buoy with C_d = 1.4, at Near, Zero, and Far Vessel Offsets, with 10-year Current

Pipeline:	10"ID Riser, Wall thickness 26mm, 3" Coating
Buoy type:	**H-buoy, Cd=1.4**
Water Depth:	1500m
Current:	100-year
Content:	1.025Te/m³

			Flexible (no1)							Buoy			Max values for SCR					Mooring line		
Flexible length	Current Case	Vessel position	Tension at FPSO	Tension at buoy	Declination at FPSO	Declination at Buoy	Horizontal projection	MBR	Hmin	Position rel nominal	Buoy trim angle	Depth in water	Tension at buoy	Horizontal projection	Declination at buoy	Max von Mises Top	Max von Mises Sag	Max Top Tension	Max Anchor Tension	Min Anchor Tension
[m]	[-]	[m]	[kN]	[kN]	[deg]	[deg]	[m]	[m]	[m]	[m]	[deg]	[m]	[kN]	[m]	[deg]	[MPa]	[MPa]	[kN]	[kN]	[kN]
380	Near	-30	917	340	19	43	239	76	37	-52.09	-0.1	203	1757	447	10	78.56	240.05	1048	607	599
380		0	935	362	21	48	252	89	31	-35.61	0.0	202	1778	478	10	79.36	219.76	1042	600	595
380	No current	-30	888	321	11	31	199	55	52	-12.60	-0.2	200	1866	546	8	83.83	160.73	991	548	516
380		0	899	335	13	37	217	65	46	0.00	-0.2	199	1884	574	8	84.76	152.64	984	542	511
380		30	915	352	15	42	233	77	40	13.90	-0.2	199	1905	603	9	85.83	144.58	977	535	506
380	Far	0	881	320	4	29	174	47	59	42.25	-0.3	198	2010	681	7	94.81	116.19	924	481	429
380		30	891	331	6	33	194	57	53	52.53	-0.3	198	2028	706	8	95.66	112.94	918	475	424

C.1 - 48: Full Static Analysis Results for Riser System (with Flooded flowlines) supported by H-shaped Buoy with C_d = 1.4, at Near, Zero, and Far Vessel Offsets, with 100-year Current

Pipeline: 10"ID Riser, Wall thickness 26mm, 3" Coating
Buoy type: H-buoy, Cd=1.6
Water Depth: 1500m
Current: 10-year
Content: 1.025Te/m³

			Flexible (no1)							Buoy			Max values for SCR					Mooring line		
Flexible length	Current Case	Vessel position	Tension at FPSO	Tension at buoy	Declination at FPSO	Declination at Buoy	Horizontal projection	MBR	Hmin	Position rel nominal	Buoy trim angle	Depth in water	Tension at buoy	Horizontal projection	Declination at buoy	Max von Mises Top	Max von Mises Sag	Max Top Tension	Max Anchor Tension	Min Anchor Tension
[m]	[-]	[m]	[kN]	[kN]	[deg]	[deg]	[m]	[m]	[m]	[m]	[deg]	[m]	[kN]	[m]	[deg]	[MPa]	[MPa]	[kN]	[kN]	[kN]
380	Near	-50	903	325	16	37	224	66	43	-57.03	-0.1	203	1759	442	9	78.19	236.97	1044	603	591
380		0	929	358	19	47	248	86	33	-31.19	-0.1	201	1792	488	10	79.46	206.94	1033	591	583
380	No current	-50	882	314	9	28	187	48	56	-20.33	-0.2	200	1855	534	7	83.26	165.92	995	552	520
380		0	899	335	13	37	217	65	46	0.00	-0.2	199	1884	574	8	84.76	152.64	984	542	511
380		50	928	366	16	46	243	86	35	23.94	-0.2	198	1921	623	9	86.61	139.20	973	530	502
380	Far	0	882	321	6	29	180	49	58	36.22	-0.3	198	1991	665	7	93.19	120.19	933	490	441
380		50	902	342	9	38	212	67	47	54.80	-0.3	198	2022	703	8	94.73	113.93	922	479	432

C.1 - 49: Full Static Analysis Results for Riser System (with Flooded flowlines) supported by H-shaped Buoy with C_d = 1.6, at Near, Zero, and Far Vessel Offsets, with 10-year Current

Pipeline: 10"ID Riser, Wall thickness 26mm, 3" Coating
Buoy type: H-buoy, Cd=1.6
Water Depth: 1500m
Current: 100-year
Content: 1.025Te/m³

			Flexible (no1)							Buoy			Max values for SCR					Mooring line		
Flexible length	Current Case	Vessel position	Tension at FPSO	Tension at buoy	Declination at FPSO	Declination at Buoy	Horizontal projection	MBR	Hmin	Position rel nominal	Buoy trim angle	Depth in water	Tension at buoy	Horizontal projection	Declination at buoy	Max von Mises Top	Max von Mises Sag	Max Top Tension	Max Anchor Tension	Min Anchor Tension
[m]	[-]	[m]	[kN]	[kN]	[deg]	[deg]	[m]	[m]	[m]	[m]	[deg]	[m]	[kN]	[m]	[deg]	[MPa]	[MPa]	[kN]	[kN]	[kN]
380	Near	-30	918	341	19	43	240	77	36	-53.19	0.0	203	1755	446	10	78.54	241.46	1049	607	601
380		0	937	364	21	49	253	91	30	-36.59	0.0	202	1777	477	10	79.35	220.85	1042	600	597
380	No current	-30	888	321	11	31	199	55	52	-12.60	-0.2	200	1866	546	8	83.84	160.74	991	548	516
380		0	899	335	13	37	217	65	46	0.00	-0.2	199	1884	574	8	84.78	152.65	984	542	511
380		30	915	352	15	42	233	77	40	13.90	-0.2	199	1905	603	9	85.84	144.59	977	535	506
380	Far	0	880	319	4	28	173	47	60	43.72	-0.3	198	2013	687	7	94.95	115.73	923	480	427
380		30	890	330	6	33	193	57	53	53.89	-0.3	198	2030	707	8	95.79	112.54	917	474	422

C.1 - 50: Full Static Analysis Results for Riser System (with Flooded flowlines) supported by H-shaped Buoy with C_d = 1.6, at Near, Zero, and Far Vessel Offsets, with 100-year Current

C.2 Full Dynamic Analysis Results

Load Case	Vessel Offset (m)	Current Direction (deg)	Wave	Wave Direction	Max Tension (kN)		Top Angle (deg)		Max Von Mises Stress (MPa)	
					Top	Sagbend	Max	Min	Top	Sagbend
1	-50	0	100 year wave	0	1449	453	10,9	8,8	275,49	302,85
3	50	180		180	1658	703	8,9	7,5	278,60	247,32

C.2 - 1: Full Dynamic Analysis Results for SCRs with 10-yr Current + 100-yr Wave – Base Case Conventional Buoy

Load Case	Minimum Radius (m)	Minimum Tension (kN)	Maximum Tension (kN)		Angle at Vessel (deg)		Angle at Buoy (deg)	
			Vessel	Buoy	Min	Max	Min	Max
1	40	19	1159	440	5,3	28,5	20,1	34,1
3	56	84	1122	476	0,0	15,3	32,5	44,8

C.2 - 2: Full Dynamic Analysis Results for Flexible Jumpers with 10-yr Current + 100-yr Wave – Base Case Conventional Buoy

Load Case	Vessel Offset (m)	Current Direction (deg)	Wave	Wave Direction	Max Tension (kN)		Top Angle (deg)		Max Von Mises Stress (MPa)	
					Top	Sagbend	Max	Min	Top	Sagbend
4	-30	0	10 year wave	0	1436	445	11,6	9,7	275,61	306,48
6	30	180		180	1668	709	8,3	7,1	278,84	246,65

C.2 - 3: Full Dynamic Analysis Results for SCRs with 100-yr Current + 10-yr Wave – Base Case Conventional Buoy

Load Case	Minimum Radius (m)	Minimum Tension (kN)	Maximum Tension (kN)		Angle at Vessel (deg)		Angle at Buoy (deg)	
			Vessel	Buoy	Min	Max	Min	Max
4	46	38	1147	460	9,9	28,1	24,1	40,3
6	48	77	1065	409	0,0	10,3	29,5	38,1

C.2 - 4: Full Dynamic Analysis Results for Flexible Jumpers with 100-yr Current + 10-yr Wave – Base Case Conventional Buoy

Load Case	Vessel Offset (m)	Current Direction (deg)	Wave	Wave Direction	Max Tension (kN)		Top Angle (deg)		Max Von Mises Stress (MPa)	
					Top	Sagbend	Max	Min	Top	Sagbend
1	-50	0	100 year wave	0	1438	447	10,8	8,6	275,44	305,96
3	50	180		180	1662	703	8,9	7,5	278,56	247,34

C.2 - 5: Full Dynamic Analysis Results for SCRs with 10-yr Current + 100-yr Wave – Flooded Conventional Buoy

Load Case	Minimum Radius (m)	Minimum Tension (kN)	Maximum Tension (kN)		Angle at Vessel (deg)		Angle at Buoy (deg)	
			Vessel	Buoy	Min	Max	Min	Max
1	41	16	1167	454	5,6	28,8	20,6	36,3
3	56	84	1122	475	0,0	15,2	32,4	44,6

C.2 - 6: Full Dynamic Analysis Results for Flexible Jumpers with 10-yr Current + 100-yr Wave – Flooded Conventional Buoy

Load Case	Vessel Offset (m)	Current Direction (deg)	Wave	Wave Direction	Max Tension (kN)		Top Angle (deg)		Max Von Mises Stress (MPa)	
					Top	Sagbend	Max	Min	Top	Sagbend
4	-30	0	10 year wave	0	1428	440	11,5	9,5	275,60	309,66
6	30	180		180	1668	708	8,3	7,1	278,79	246,67

C.2 - 7: Full Dynamic Analysis Results for SCRs with 100-yr Current + 10-yr Wave – Flooded Conventional Buoy

Load Case	Minimum Radius (m)	Minimum Tension (kN)	Maximum Tension (kN)		Angle at Vessel (deg)		Angle at Buoy (deg)	
			Vessel	Buoy	Min	Max	Min	Max
4	46	35	1156	476	10,3	28,4	24,5	42,5
6	47	77	1065	408	0,0	10,2	29,4	37,9

C.2 - 8: Full Dynamic Analysis Results for Flexible Jumpers with 100-yr Current + 10-yr Wave – Flooded Conventional Buoy

Load Case	Vessel Offset (m)	Current Direction (deg)	Wave	Wave Direction	Max Tension (kN)		Top Angle (deg)		Max Von Mises Stress (MPa)	
					Top	Sagbend	Max	Min	Top	Sagbend
1	-50	0	100 year wave	0	1453	447	10,8	8,4	275,43	311,38
3	50	180		180	1691	719	9,1	7,6	278,71	248,36

C.2 - 9: Full Dynamic Analysis Results for SCRs with 10-yr Current + 100-yr Wave – H-shaped Buoy

Load Case	Minimum Radius (m)	Minimum Tension (kN)	Maximum Tension (kN)		Angle at Vessel (deg)		Angle at Buoy (deg)	
			Vessel	Buoy	Min	Max	Min	Max
1	43	19	1163	414	5,6	28,7	21,7	35,5
3	54	82	1115	431	0,0	14,8	31,6	43,0

C.2 - 10: Full Dynamic Analysis Results for Flexible Jumpers with 10-yr Current + 100-yr Wave – H-shaped Buoy

Load Case	Vessel Offset (m)	Current Direction (deg)	Wave	Wave Direction	Max Tension (kN)		Top Angle (deg)		Max Von Mises Stress (MPa)	
					Top	Sagbend	Max	Min	Top	Sagbend
4	-30	0	100 year wave	0	1442	440	11,4	9,3	275,60	315,64
6	30	180		180	1683	718	8,5	7,3	278,89	247,11

C.2 - 11: Full Dynamic Analysis Results for SCRs with 100-yr Current + 10-yr Wave – H-shaped Buoy

Load Case	Minimum Radius (m)	Minimum Tension (kN)	Maximum Tension (kN)		Angle at Vessel (deg)		Angle at Buoy (deg)	
			Vessel	Buoy	Min	Max	Min	Max
4	48	26	1152	436	10,2	28,4	25,9	41,6
6	46	73	1060	372	0,0	10,0	28,5	36,5

C.2 - 12: Full Dynamic Analysis Results for Flexible Jumpers with 100-yr Current + 10-yr Wave – H-shaped Buoy